

GRI-93-0022

QUANTIFYING RESERVOIR HETEROGENEITY THROUGH OUTCROP
CHARACTERIZATION: 1. ARCHITECTURE, LITHOLOGY, AND PERMEABILITY DISTRIBUTION
OF A LANDWARD-STEPPING FLUVIAL-DELTAIC SEQUENCE, FERRON SANDSTONE
(CRETACEOUS), CENTRAL UTAH

TOPICAL REPORT

(November 1, 1989–November 30, 1992)

Prepared by

R. Stephen Fisher, Mark D. Barton, and Noel Tyler

Bureau of Economic Geology

W. L. Fisher, Director

The University of Texas at Austin

Austin, Texas 78713-7508

for

GAS RESEARCH INSTITUTE

Contract No. 5089-260-1902

GRI Project Manager, Anthony W. Gorody

June 1993

DISCLAIMER

LEGAL NOTICE This report was prepared by the Bureau of Economic Geology as an account of work sponsored by the Gas Research Institute (GRI). Neither GRI, members of GRI, nor any person acting on behalf of either:

- a. Makes any warranty or representation, expressed or implied, with respect to the accuracy, completeness, or usefulness of the information contained in this report, or that the use of any apparatus, method, or process disclosed in this report may not infringe privately owned rights; or
- b. Assumes any liability with respect to the use of, or for damages resulting from the use of, any information, apparatus, method, or process disclosed in this report.

REPORT DOCUMENTATION PAGE	1. REPORT NO. GRI-93/0022	2.	3. Recipient's Accession No.
4. Title and Subtitle Quantifying Reservoir Heterogeneity through Outcrop Characterization: 1. Architecture, Lithology, and Permeability Distribution of a Landward-Stepping Fluvial-Deltaic Sequence, the Ferron Sandstone (Cretaceous), Central Utah		5. Report Date June 1993	
7. Author(s) R. Stephen Fisher, Mark D. Barton, and Noel Tyler		6.	
9. Performing Organization Name and Address Bureau of Economic Geology The University of Texas at Austin University Station, Box X Austin, Texas 78713-7508		8. Performing Organization Rept. No.	
12. Sponsoring Organization Name and Address Gas Research Institute 8600 West Bryn Mawr Avenue Chicago, IL 60631 Project Manager: Anthony W. Gorody		10. Project/Task/Work Unit No.	
		11. Contract(C) or Grant(G) No. (C) 5089-260-1902 (G)	
		13. Type of Report & Period Covered Topical Report 11/01/89-11/30/92	
15. Supplementary Notes		14.	
16. Abstract (Limit: 200 words) The internal architecture of natural gas reservoirs fundamentally controls production efficiency and the volume of gas unrecovered at abandonment. To better understand reservoir complexity, we investigated relations between sandstone architecture and permeability structure of landward-stepping (wave-modified) Ferron deltaic sandstones exposed in central Utah. Deltaic sandstones extend 4 mi along sediment-transport direction in the landward-stepping Ferron genetic sequence GS 5. Most sand was deposited in transgressive, delta-front, and distributary-channel facies. Distributary channels constitute the principal reservoir facies because mean permeability in distributary-channel sandstones is approximately twice that of delta-front and transgressive sandstones, and because distributary-channel sandstones are well developed. Channel architecture, bounding-surface character, and permeability distribution change systematically from landward to seaward position in the system. Near the landward limit, mean permeability is 300 md, mud occurs as clasts along channel-flank bounding surfaces, and permeability systematically decreases upward. Near the seaward extent of the system, mean permeability is 750 md, mud is segregated into discrete strata-bounding sand bodies, and vertical permeability trends are uniformly high. Statistical analysis shows that lithofacies are the fundamental sandstone architectural units. Similar lithofacies have similar permeability character, regardless of position in the facies tract. Variable preservation of lithofacies controls permeability distribution throughout the channel system. Semivariogram analysis shows that vertical and horizontal permeability correlation distances correspond to distances between bounding surfaces and to sand-body dimensions. Diagenetic overprint is minor, owing to low burial temperatures.			
17. Document Analysis a. Descriptors Ferron Sandstone, fluvial-deltaic reservoirs, permeability distribution, reservoir analog, sandstone architecture, Utah			
b. Identifiers/Open-Ended Terms permeability analysis on outcrop reservoir analogs, sandstone architecture in landward-stepping depositional setting, sequence stratigraphy controls on sandstone permeability			
c. COSATI Field/Group			
18. Availability Statement Release Unlimited	19. Security Class (This Report) Unclassified	21. No. of Pages 150	
	20. Security Class (This Page) Unclassified	22. Price	

RESEARCH SUMMARY

- Title** Quantifying Reservoir Heterogeneity through Outcrop Characterization: 1. Architecture, Lithology, and Permeability Distribution of a Landward-Stepping Fluvial-Deltaic Sequence, the Ferron Sandstone (Cretaceous), Central Utah
- Contractor** Bureau of Economic Geology, The University of Texas at Austin, GRI Contract No. 5089-260-1902, entitled "Quantification of flow unit and bounding element properties and geometries, Ferron Sandstone, Utah: Implications for heterogeneity in Gulf Coast Tertiary deltaic reservoirs."
- Principal Investigators** Noel Tyler, Mark A. Miller, Ken E. Gray
- Objectives** Natural gas recovery from shaley sandstone reservoirs is limited by complex internal architectures. The goal of this work is to improve our knowledge of sandstone architecture and the barriers that control gas migration in analogous reservoirs. This will enable us to develop more realistic three-dimensional reservoir models that can be used to test various infill drilling scenarios and optimize incremental gas reserve growth from mature sandstone reservoirs.
- This research has three primary objectives: (1) to determine the factors controlling the size, shape, internal architecture, and permeability character of flow units and the associated baffles and barriers of a sandstone reservoir; (2) to transform information gained from specific measurements to a realistic three-dimensional reservoir model; and (3) to establish general principles for outcrop studies of reservoir analogs that can be used by other researchers and field operators.
- Outcrop characterization, including permeability measurement, is an effective approach for developing detailed, quantitative descriptions of reservoir architecture. We selected the superbly exposed Ferron Sandstone (Cretaceous, central Utah) because it represents a reservoir class that accounts for 64 percent of total production from Texas Gulf Coast reservoirs, because of depositional and diagenetic settings similar to those of Gulf Coast deltaic reservoirs, and because the geologic setting of the Ferron had been previously established.
- This report summarizes our work on a landward-stepping sequence within the Ferron; these results are applicable to wave-modified deltaic reservoirs. A companion report presents results of our work on a seaward-stepping deltaic sequence of the Ferron; those conclusions are applicable to river-dominated deltaic reservoirs. These two reports provide a means to compare and predict the characteristics of fluvially dominated and wave-modified deltaic sandstone reservoirs.
- Technical Perspective** Reservoir architecture, the internal fabric and structure of reservoirs, fundamentally governs migration paths during natural gas production. Reservoir architecture is determined by the depositional and diagenetic processes that form the reservoir. Therefore, if we better understand the origin and history of the reservoir, gas migration paths and production efficiency become predictable. With greater understanding of the reservoir fabric and its inherent control on gas migration paths, we can more efficiently target remaining, conventionally recoverable hydrocarbons that are prevented from migrating to the wellbore by intrareservoir seals or bounding surfaces. Furthermore, advanced recovery strategies that account for the internal compartmentalization of the reservoir can be designed and implemented.

The predictability of reservoir and seal properties and geometries is therefore the crux of this research. We chose to focus on fluvial-deltaic sandstones for this study because they account for 64 percent of total production from Texas Gulf Coast reservoirs.

The projected long-term benefits of the study are twofold. First, increased understanding of internal architecture and improved methods for quantification of heterogeneity will facilitate developing strategies to reduce risk in the extended development of fluvial-deltaic gas reservoirs. Second, targeting incremental gas resources in mature reservoirs will lead to extended recovery of a low-cost, low-risk resource.

Technical Approach

We selected the Ferron Sandstone outcrop for study because it is well exposed, the sequence stratigraphic setting is established, and the various Ferron genetic sequences were deposited in fluvially dominated to wave-modified deltaic settings. We designed the project to test the fundamental hypothesis that depositional and diagenetic processes operate within a sequence stratigraphic framework to produce a predictable arrangement of flow units and seals.

Specific outcrops were selected for investigation on the basis of position in the facies tract, quality of exposure, and cross-sectional orientation relative to sediment transport direction. We first photographed cliff faces with a medium format camera and mapped major sand-body and bounding-surface geometries on photomosaics. We then established positions for vertical transects at 50- to 100-ft spacings, described the vertical sections, and measured permeability at 12-, 6-, or 4-inch intervals. At selected sites we measured permeability on nested two-dimensional grids to establish vertical and horizontal correlation distances. Horizontal permeability transects and lateral correlation of vertical permeability profiles provide a second measure of lateral permeability continuity. We determined field-scale relations of sandstone architecture and permeability by geologic mapping between the outcrop locations. We used various statistical and geostatistical methods to identify permeability groups, distribution types, and correlation distances.

In conjunction with the field permeability characterization, we collected representative samples of probable flow unit, baffle, and barrier strata for petrographic and petrophysical measurements. Until flow modeling under effective reservoir conditions can be performed, we consider sand bodies that have air permeability values greater than about 5 md and that lack continuous internal low-permeability strata to be flow units. Laterally continuous low-permeability (<5 md) strata are considered flow barriers or baffles.

The detrital and authigenic composition of Ferron sandstones was determined by standard thin-section petrography, scanning electron microscopy assisted by energy dispersive analysis, electron microprobe analysis, and X-ray diffraction for clay mineral identification. Petrophysical measurements were conducted at the Earth Science Engineering Laboratory and evaluated at the Center for Petroleum and Geosystems Engineering. Those results are presented separately.

Results

Most of the sand in the landward-stepping genetic sequence resides in distributary-channel, delta-front, and transgressive facies. Distributary-channel sandstones are the primary reservoir facies because (1) they have higher mean permeability than delta-front and transgressive sandstones, (2) distributary-channel deposits erosionally remove much of the underlying delta front, and (3) distributary-channel deposits contain most of the preserved sand.

We recognize three different types of distributary channels that reflect early, middle, and late deposition within the sequence. The early stage of channel-belt evolution records channel incision into delta-front and shoreface deposits; the middle stage is characterized by lateral migration; and the late stage records aggradation. Early-stage channels are thin and narrow in the landward portion of the facies tract, becoming thicker and much wider near the seaward limit of the facies tract. Middle-stage channel deposits have approximately the same width-to-thickness ratio from landward to seaward extent of the facies tract. Late-stage channel deposits are both wide and thick; however, they are isolated from each other by overbank and delta-plain mudstones and shales, and occur only near the landward limit of the facies tract. Macroforms in middle-stage distributary-channel sandstones, the volumetrically most important type in Ferron GS 5, are the product of lateral accretion, are laterally stacked within channel belts, and are poorly connected internally. Mean permeability increases seaward in the channel complex, reflecting systematic changes in channel type and lithofacies proportions.

Macroform stacking patterns and preservation potential are the primary controls of permeability in the Ferron Sandstone. A strong and predictable relation exists between permeability, macroform type, and lithofacies type. Our results show that lithofacies and macroforms are the fundamental architectural building blocks for both sandstones and sandstone reservoir models. Constructing reservoir models as an assemblage of lithofacies grouped into macroforms, each with its characteristic permeability distribution type and attendant bounding surfaces, would provide improved reservoir models and consequently more accurate results from simulation experiments.

Permeability relations within lithofacies and macroforms are consistent throughout the facies tract. However, syndepositional erosion and truncation of earlier deposits significantly modifies both preservation of lithofacies and macroforms and the resulting permeability structure. Permeability characteristics and structure are scale dependent. Changes in the variance, distribution type, and correlation structure closely reflect geologic scales of heterogeneity. Statistical tests show that stratal types or lithofacies display the highest degree of permeability stationarity. Permeability variation and patterns at higher levels of stratal organization reflect variation in the proportion and arrangement of lithofacies or stratal types. Permeability characteristics are transferable between localities within the facies tract but not between sequences. Thus, in a comparable field situation, reservoir properties must be calibrated to rock type for each genetic sequence.

Diagenetic overprint is mild because the Ferron Sandstone was never heated significantly during burial. Consequently, both detrital and diagenetic mineralogy correlate well with depositional facies. Detrital mineralogy, particularly the abundance of rock fragments, correlates predictably with permeability variations from landward to seaward positions in the depositional system. Rock fragments in the Ferron are ductile grains that fill pore space and reduce porosity and permeability during burial compaction. The abundance of rock fragments reflects the amount of physical abrasion prior to final deposition. Rock fragment content decreases seaward within the distributary-channel facies, and rock fragments are less abundant in delta-front and transgressive sandstones. Quartz, kaolinite, and carbonate are the most abundant authigenic phases; however, total cement volume rarely exceeds 6 percent.

A good correlation in permeability characteristics exists between the outcrop and nearby shallow core samples. These results confirm that surface weathering has not severely altered outcrop permeability characteristics and that Ferron

outcrops are suitable reservoir analogs for investigating permeability patterns. The distribution of distributary-channel types, degree of internal sandstone organization, segregation of mud from sand within and between channel macroforms, sandstone mineralogy, and permeability structure of landward-stepping distributary-channel sandstones differ significantly from that of seaward-stepping sandstones. Therefore, landward-stepping systems can be distinguished from seaward-stepping systems on the basis of well logs and other conventional exploration tools.

Using field-scale maps of the Ferron GS 5 sandstone as a model for infill drilling shows that only about 41 percent of the total potential reservoir rock would be contacted, even at 160-acre well spacing. Landward-stepping fluvial-deltaic sandstone reservoirs are therefore excellent candidates for geologically directed infill drilling that is guided by exploration techniques such as three-dimensional seismic surveys.

CONTENTS

RESEARCH SUMMARY	vii
INTRODUCTION	1
Purpose	1
Projected Benefits to Natural Gas Consumers	2
Objectives	3
Approach	4
Applicability of Outcrop Results to Reservoir Studies.....	5
OUTCROP ANALOG: THE FERRON SANDSTONE, CENTRAL UTAH	7
Selection Criteria	7
Geologic Setting of the Ferron Sandstone	9
METHODS	14
Architectural Analysis of Landward-Stepping Deltaic Sandstones	14
Field Permeability Measurements	15
Sampling for Petrographic and Petrophysical Analyses.....	16
Petrologic Investigations	20
Petrophysical Measurements.....	21
FERRON GS 5 SANDSTONE ARCHITECTURE	21
Delta-Front Lithofacies	24
Bioturbated Lithofacies	24
Hummocky Cross-Stratified Lithofacies	25
Swaley Cross-Stratified Lithofacies	26
Trough Cross-Stratified Lithofacies.....	26
Delta-Front Facies	27
Lower Delta-Front Facies.....	27
Upper/Middle Delta-Front Facies	27
Foreshore Facies.....	28

Distributary-Channel Complex Lithofacies	28
Ripple-Laminated/Cross-Stratified Lithofacies	29
Low-Angle Stratified Lithofacies	29
Trough Cross-Stratified Lithofacies	30
Contorted Bedding Lithofacies	30
Lag Deposit Lithofacies	31
Fine-Grained Sediment Lithofacies	31
Distributary-Channel Complex Facies	32
Early-Stage Distributary-Channel Facies	32
Middle-Stage Distributary-Channel Facies	33
Late-Stage Distributary-Channel Facies	33
Abandoned Channel Fill Facies	34
Crevasse Splay Facies	34
Bounding Elements	35
PETROGRAPHY, DIAGENESIS, AND PERMEABILITY	35
Mineralogy of Ferron Sandstones	35
Framework Grains	37
Intergranular Material	38
Ferron GS 5 Sandstones at Muddy Creek	39
Sandstone Types	39
Intergranular Composition	39
Ferron Sandstones from UURI Cores	43
Sandstone Types	43
Intergranular Composition	45
Ferron Sandstones at Picture Flats	45
Sandstone Types	45
Intergranular Composition	47

Ferron Sandstones at Cedar Ridge	47
Sandstone Types	47
Intergranular Composition	49
Sandstone Texture and Petrophysical Properties	49
PERMEABILITY CHARACTERISTICS OF LITHOFACIES AND FACIES.....	49
Factors Controlling Mean Permeability	55
Geologic Controls on Permeability Variation	61
Permeability Distribution	62
Stationarity of Permeability Measures	65
Petrology-Permeability Relations	72
Comparison of Outcrop and Subsurface Permeability.....	77
Spatial Permeability Variation.....	81
Permeability Anisotropy	86
PERMEABILITY RELATIONS AND SANDSTONE ARCHITECTURE	89
Muddy Creek Canyon	90
Sandstone Architecture	90
Delta-Front Sandstones	90
Distributary-Channel and Associated Deposits	91
Early-Stage Distributary Channels.....	91
Middle-Stage Distributary Channels	91
Late-Stage Distributary Channels	93
Permeability Characteristics	93
Picture Flats Canyon.....	95
Sandstone Architecture	95
Permeability Character.....	100
Cedar Ridge Canyon.....	101
Cedar Ridge Distributary-Channel Architecture	101

Cedar Ridge Distributary-Channel Permeability Characteristics	102
Cedar Ridge Distal Delta-Front Architecture	102
Cedar Ridge Distal Delta-Front Permeability Characteristics	104
Regional Architecture and Permeability Relations.....	106
Delta-Front Sandstones	106
Distributary-Channel Sandstones	108
Regional Variations in Distributary-Channel Lithofacies Proportions, Macroform Types, and Sandstone Architecture	115
IMPLICATIONS FOR INFILL DRILLING	118
SUMMARY AND CONCLUSIONS.....	124
ACKNOWLEDGMENTS	128
REFERENCES	129

Figures

1. Location map of the Ferron Sandstone outcrop in Castle Valley, central Utah.....	8
2. Cross section of Cretaceous strata in central Utah	10
3. Cross section of the Ferron Sandstone in central Utah	13
4. Comparison of permeability determined by the field minipermeameter and by conventional core-plug measurement. Measurements were taken at each end of the core plug and averaged to obtain the minipermeameter permeability value	17
5. Arrangement of architectural elements along depositional dip in Ferron GS 5.....	23
6. Framework grain composition of sandstones from Muddy Creek	40
7. Framework grain composition of sandstones from UURI core	44
8. Framework grain composition of sandstones from Picture Flats.....	46
9. Framework grain composition of sandstones from Cedar Ridge.....	48
10. Cumulative percent plot of permeability comparing distributary-channel and delta-front deposits.....	56
11. Cumulative percent plot of permeability comparing lithofacies types from distributary- channel facies	57

12.	Plot of permeability versus grain size for the distributary-channel facies showing mean permeability, range, and number of analyses for each grain size	59
13.	Cumulative percent plot of permeability comparing stratal types from delta-front deposits.....	60
14.	Scale-dependent permeability characteristics of stratal elements	64
15.	Cumulative percent plot of permeability for distributary-channel deposits from South Muddy Creek, Picture Flats, and Cedar Ridge	67
16.	Cumulative probability plot of permeability for stratal types from distributary-channel facies at South Muddy Creek	68
17.	Cumulative probability plot of permeability comparing stratal types from distributary-channel facies at Picture Flats	69
18.	Cumulative probability plot of permeability comparing stratal types from distributary-channel facies at Cedar Ridge Canyon	70
19.	Framework grain composition of distributary-channel sandstones from Muddy Creek	74
20.	Framework grain composition of distributary-channel sandstones from Picture Flats	75
21.	Framework grain composition of distributary-channel sandstones from Cedar Ridge	76
22.	Cumulative probability plot of permeability for stratal types within distributary-channel facies from UURI Well No. 2	79
23.	Comparison of permeability profiles between outcrop and UURI Well No. 2.....	80
24.	Horizontal and vertical variograms for contorted lithofacies, distributary-channel facies	83
25.	Horizontal and vertical variograms for low-angle strata, distributary-channel facies	84
26.	Horizontal and vertical variograms for trough cross-strata, distributary-channel facies	85
27.	Horizontal and vertical variograms for bioturbated lithofacies, delta-front facies	87
28.	Horizontal and vertical variograms for swaley cross-strata, delta-front facies	88
29.	Permeability profiles and distributary-channel architecture from South Muddy Creek.....	94
30.	Horizontal variogram from distributary-channel facies from South Muddy Creek.....	96
31.	Vertical variogram within distributary-channel facies from South Muddy Creek.....	97
32.	Permeability profiles and distributary-channel architecture from Picture Flats	98
33.	Permeability profiles and distributary-channel architecture from Cedar Ridge.....	103
34.	Permeability profiles and delta-front architecture from Cedar Ridge	105

35. Regional cross section along depositional dip displaying permeability profiles and delta-front architecture	107
36. Comparison of channel dimensions for early-, middle-, and late-stage distributary channels at Muddy Creek, Picture Flats, and Cedar Ridge outcrops	110
37. Comparison of early-stage distributary-channel dimensions at Muddy Creek, Picture Flats, and Cedar Ridge.....	111
38. Comparison of middle-stage distributary-channel dimensions at Muddy Creek and Picture Flats	112
39. Comparison of early-, middle-, and late-stage distributary-channel dimensions at Muddy Creek	113
40. Comparison of distributary-channel dimensions at Picture Flats	114
41. Comparison of vertical lithofacies proportion curves within GS 5 from South Muddy Creek, Picture Flats, and Cedar Ridge	116
42. Comparison of stratal diversity within distributary-channel facies between South Muddy Creek, Picture Flats, and Cedar Ridge	117
43. Map of distributary-channel and interdistributary strata in Ferron GS 5 from the landward extent near Muddy Creek to the seaward limit near Cedar Ridge	119
44. Map of distributary-channel and interdistributary strata in Ferron GS 5 from the landward extent near Muddy Creek to the seaward limit near Cedar Ridge showing effects of conventional infill drilling at 640-acre spacing.....	121
45. Map of distributary-channel and interdistributary strata in Ferron GS 5 from the landward extent near Muddy Creek to the seaward limit near Cedar Ridge showing effects of conventional infill drilling at 320-acre spacing	122
46. Map of distributary-channel and interdistributary strata in Ferron GS 5 from the landward extent near Muddy Creek to the seaward limit near Cedar Ridge showing effects of conventional infill drilling at 160-acre spacing.....	123

Tables

1. Hierarchical sampling plan to provide material for outcrop characterization, petrographic examination, and petrophysical analyses.....	18
2. Hierarchy of bounding elements and surfaces in Ferron GS 5 fluvial-deltaic sandstones.....	36
3. Summary of petrographic data for major constituents in Ferron GS 5 and GS 4 sandstones.....	41
4. Descriptions of samples collected for petrophysical property measurements	50

5. Results of grain-size distribution analysis of sandstone blocks collected for petrophysical measurements.....	52
6. Results of ESEL petrophysical analyses	53
7. Permeability characteristics of stratal types	66

INTRODUCTION

Purpose

Natural gas reservoirs typically display a complex internal architecture that fundamentally controls gas flow paths, gas recovery efficiency, and ultimately the volume of natural gas left in a reservoir at abandonment. Improved efficiency in natural gas recovery, particularly in mature reservoirs, requires a more sophisticated understanding of reservoir anatomy and the spatial distribution of the properties that affect gas flow. The improved knowledge of reservoir architecture that results will allow geologists and engineers to develop and test advanced infill drilling strategies to increase natural gas recovery from established fields.

Reservoir complexity results from geologic, chemical, and physical processes that vary over time and space and operate over a wide range of scales during reservoir creation and hydrocarbon migration. Therefore, reservoir architecture, and hence the paths of fluid migration, can be better predicted as we improve our understanding of how reservoirs are created. Production attributes of gas reservoirs are controlled by the depositional, diagenetic, and tectonic processes that determine the petrophysical properties of the reservoir rock. Petrophysical character in turn defines the efficiency with which hydrocarbons in a reservoir compartment migrate to the wellbore. Petrophysical heterogeneity within reservoir units can potentially retard or divert flow to the well. Of potentially greater importance to natural gas recovery are the low-permeability strata between major reservoir units that obstruct or prohibit gas flow. Such bounding elements may be efficient intrareservoir stratigraphic traps that cause substantial volumes of recoverable gas to remain in reservoirs at abandonment at current levels of technology. With improved understanding of how reservoir fabric develops and controls natural gas flow paths, we can more efficiently target remaining, conventionally recoverable hydrocarbons that are prevented from migrating to the wellbore by intrareservoir seals or bounding surfaces. Furthermore, advanced recovery strategies that account for reservoir compartmentation can be designed, tested in computer simulations, and implemented.

This research investigates how sandstone architecture controls permeability structure in a superbly exposed and cored delta and distributary-channel complex, the Cretaceous Ferron Sandstone of central Utah. We chose this outcrop because it provides access to sandstones deposited in a wide range of fluvial-deltaic depositional environments. Fluvial-deltaic reservoirs of the Tertiary Wilcox and Frio Formations, Texas Gulf Coast, have produced 38.2 trillion cubic feet (Tcf) of nonassociated natural gas. Therefore, finding ways to increase recovery efficiency from these reservoirs would constitute a low-cost, low-risk source of additional energy resources. In this report we focus on a single retrogradational deltaic unit that was deposited as a landward-stepping genetic sequence and is analogous to Tertiary wave-modified deltaic reservoirs of the Texas Gulf Coast. A companion report focuses on a seaward-stepping Ferron genetic sequence that represents the progradational component of this delta system and is analogous to Tertiary fluvially dominated reservoirs of the Texas Gulf Coast.

Projected Benefits to Natural Gas Consumers

Our ultimate goal is to translate this understanding of outcrop architecture to more realistic models that can be applied to specific reservoirs, appropriately conditioned by data specific to each reservoir. These models can then be used to test the effects of various reservoir development schemes on the ultimate recovery of natural gas in mature fields in various depositional, tectonic, and sequence stratigraphic settings; to test hypotheses concerning the most efficient methods for recovery of incremental gas reserves in heterogeneous, compartmented sandstones; and to efficiently perform risk analysis for reserve growth estimates. We selected fluvial-deltaic sandstones for this study because gas reservoirs deposited in such environments account for a significant amount of total natural gas production from the Texas Gulf Coast and because fluvial-deltaic reservoirs are the focus of current industry efforts to achieve natural gas reserve growth.

Objectives

A major goal of reservoir characterization is to determine the properties and spatial arrangement of flow units (strata through which gas will readily pass) and barriers or baffles (strata that prevent, retard, or deflect gas flow). Because accurate subsurface reservoir description is usually limited by insufficient knowledge of rock-property distributions between wells, there has been a tendency either to stochastically model interwell reservoir architecture or to assume homogeneity. However, we suggest that reservoir heterogeneity is predictable if we understand the depositional and diagenetic processes that produce flow units, baffles, and barriers sufficiently well.

Because it is virtually impossible to determine the detailed spatial distribution of petrophysical properties in the subsurface, outcrop studies are increasingly being used to provide data on sand-body geometry, positions and continuity of bounding elements between major sand bodies, the internal architecture of sandstones, and the distribution of permeability values within and between strata. This project is designed to (1) document and quantify the geometric and petrophysical attributes and production behavior of flow units and their associated flow baffles on the outcrop, (2) quantify directional attributes and properties of flow barriers bounding flow units on the outcrop, (3) transport outcrop architecture and petrophysical relations to a three-dimensional reservoir model, and (4) use the reservoir model to determine predictability of locations and volumes of unrecovered gas potentially remaining in analogous reservoirs after drilling at conventional well spacing.

This research is designed to determine the controls of sedimentary architecture and diagenesis on permeability structure in a superbly exposed and cored delta/distributary-channel complex, and how this permeability structure would affect gas mobility in a sandstone reservoir. We seek to develop methods to quantify styles and scales of sandstone reservoir heterogeneity by combining outcrop studies, petrographic and petrophysical analyses, and geostatistical analysis. In this research we test the hypotheses that we can (1) characterize reservoir heterogeneity through outcrop studies of geologic and permeability attributes and petrophysical property measurements, (2) establish

discrete permeability groups on the basis of depositional systems, facies and lithofacies relations, and cementation patterns, and (3) develop a realistic reservoir model that captures the three-dimensional distribution of flow baffles and barriers in a sandstone reservoir. Our goals are to develop better methods for predicting the spatial distribution of flow units and intrareservoir barriers to gas flow in fluvial-deltaic sandstones and to demonstrate that deterministic models for sandstone gas reservoirs can be developed from outcrop studies.

Approach

Our approach was to select a sandstone outcrop that is geologically analogous to Tertiary Gulf Coast natural gas reservoirs, to establish the depositional architecture and diagenetic modification of fluvial-deltaic sandstones within the context of a well-defined sequence stratigraphic framework, and to determine how these factors affect the spatial distribution of permeability and reservoir properties. Specific goals in the outcrop characterization of heterogeneity are to (1) identify potentially important lithofacies and bounding surfaces, (2) characterize permeability patterns within the lithofacies framework and across bounding surfaces, (3) determine the geometry, interconnectedness, and arrangements of lithofacies internal to discrete, mappable sand bodies and their relationship to permeability patterns, and (4) determine geometry and interconnectedness among discrete, mappable bodies.

Petrographic studies augment the field characterizations by resolving the relative importance of depositional and diagenetic processes on porosity, permeability, and petrophysical properties. Our petrologic investigations were designed to determine the mineralogical and textural parameters that characterize flow units, barriers, and baffles, and to relate these features to depositional processes and burial history to develop criteria for predicting reservoir heterogeneity and compartmentation. The principal objectives of this work are to (1) determine the relations among depositional processes, detrital and authigenic mineralogy, primary and secondary porosity, and permeability that affect reservoir properties of flow units, (2) determine the type, distribution, and

origin of detrital and authigenic minerals that characterize bounding surfaces, flow barriers, and baffles within and between flow units, (3) deduce the diagenetic history of the outcrop sandstone so that similarities and differences between the outcrop reservoir analog and Tertiary sandstone gas reservoirs of the Texas Gulf Coast can be evaluated, and (4) provide data to guide and constrain the transforms that will allow us to extrapolate from outcrop geologic characterization studies to effective reservoir properties.

Petrophysical studies conducted at The University of Texas Earth Sciences and Engineering Laboratories (ESEL) complement the outcrop and petrographic studies by measuring static and dynamic rock properties under reservoir conditions. We conducted petrophysical property measurements of predominant facies, stratal types, and bounding elements between major sand bodies so that field minipermeameter data could be related to the properties that control reservoir behavior. Analyses performed at ESEL include properties related to one- and two-phase flow (porosity, air and brine permeability, relative permeability, formation factor, and saturation exponent) and static and dynamic mechanical properties (Young's modulus, Poisson's ratio, P- and S-wave velocity). Finding ways to transform outcrop, petrographic, and petrophysical data to effective reservoir properties is the ultimate objective of such investigations.

Applicability of Outcrop Results to Reservoir Studies

Reservoir characterization from outcrop studies allows the continuous sampling necessary for a more detailed reservoir description than is available from subsurface data alone. However, developing quantitative models of reservoir heterogeneity on the basis of outcrop studies requires that the permeability structure of outcrop rocks adequately reflect the permeability structure of analogous reservoir rocks in the subsurface. That is, the spatial trends in permeability variation, although not necessarily the absolute permeability values, must be portable from outcrop to subsurface. Outcrop observations may not be portable to the subsurface if the rock surfaces have

been significantly altered by surface weathering. These potential effects must be critically evaluated before outcrop data can be incorporated in reservoir models.

Several studies have demonstrated the portability of outcrop observations to the subsurface (Stalkup and Ebanks, 1986; Goggin, 1988; Kittredge, 1988; Chandler and others, 1989). In general, the mean of the permeability measurements is not portable. However, distribution type, coefficient of variation, and correlation measures are portable between outcrop and subsurface. Stalkup and Ebanks (1986), in a study of the Cretaceous Ferron Sandstone of central Utah, compared outcrop to subsurface rocks of the same stratigraphic interval in a nearby well and found that permeability contrast among lithofacies is greater in the subsurface than in the outcrops. They attributed this to the effects of surface weathering. However, they also found that the vertical arrangement of statistically different permeability groups is preserved in both core and outcrop, indicating the portability of outcrop data to equivalent subsurface strata.

Recent studies show that sedimentary facies exert an important control on permeability distribution in clastic rocks (Weber, 1982; Stalkup and Ebanks, 1986; Jones and others, 1987; Dreyer and others, 1990). The most influential variables influencing permeability are grain size, grain sorting, mineralogy, fabric, and degree of cementation (Dreyer and others, 1990). On the basis of results of these earlier studies, we relate permeability measurements at the outcrop to quantification of these same variables. Permeability variation on the outcrop can then be compared with rock-property variation to establish discrete permeability populations for specific depositional systems and settings. This information provides the basis for assigning values and distributions of petrophysical properties to reservoir models of sandstones from similar depositional systems and settings on outcrop.

Diagenetic effects on reservoir properties are less studied than primary depositional characteristics such as facies and bedding type. Early cementation and porosity occlusion resulting from compaction of ductile grains generally occur along primary depositional features such as bedding planes and bounding surfaces (van Veen, 1977; Weber, 1982, 1986). However, the effects of deep, late cementation and secondary porosity development and the relations between facies,

diagenesis, and permeability distribution are still poorly understood. Our study includes detailed petrographic analyses because we wish to investigate relations between depositional heterogeneity, cement mineralogy, and porosity preservation and the distribution of reservoir properties; to evaluate the role of diagenesis and weathering on the permeability and petrophysical properties of outcrop samples; and to provide data for comparing the mineralogy of the Ferron reservoir analog with the mineralogy of natural gas sandstone reservoirs.

OUTCROP ANALOG: THE FERRON SANDSTONE, CENTRAL UTAH

Selection Criteria

Four fundamental criteria guided our selection of an outcrop for this reservoir-analog investigation. First, the candidate sandstone must have been deposited in a fluvial-deltaic setting so that our results could be extrapolated to natural gas reservoirs in the Texas Gulf Coast that were deposited in similar environments. Second, burial depths, temperatures, and diagenetic modifications of the outcrop sandstone must be similar to those of Tertiary Gulf Coast reservoirs. Major differences in original mineralogy, maximum burial temperatures, or tectonic activity could reduce the petrophysical similarities between outcrop and reservoir and thus make it difficult to apply information gained at the outcrop to subsurface formations. Third, there must be sufficient access for the field investigations. Outcrop exposures along and across the entire facies tract are needed for complete characterization. Finally, the regional stratigraphic and geologic setting of the candidate formation must be already known; the time constraints of this project did not permit us to complete both regional and detailed investigations.

The Ferron Sandstone of central Utah proved ideal for this study. The Ferron Sandstone is a Cretaceous (Turonian) fluvial-deltaic system that displays a complete systems tract from fluvial through deltaic, coastal plain, and marine facies. It outcrops along the eastern margin of Castle Valley in east-central Utah (fig. 1), between the Wasatch Plateau to the west and the San Rafael Swell to the east. Along the eastern margin of Castle Valley, the Ferron Sandstone forms a

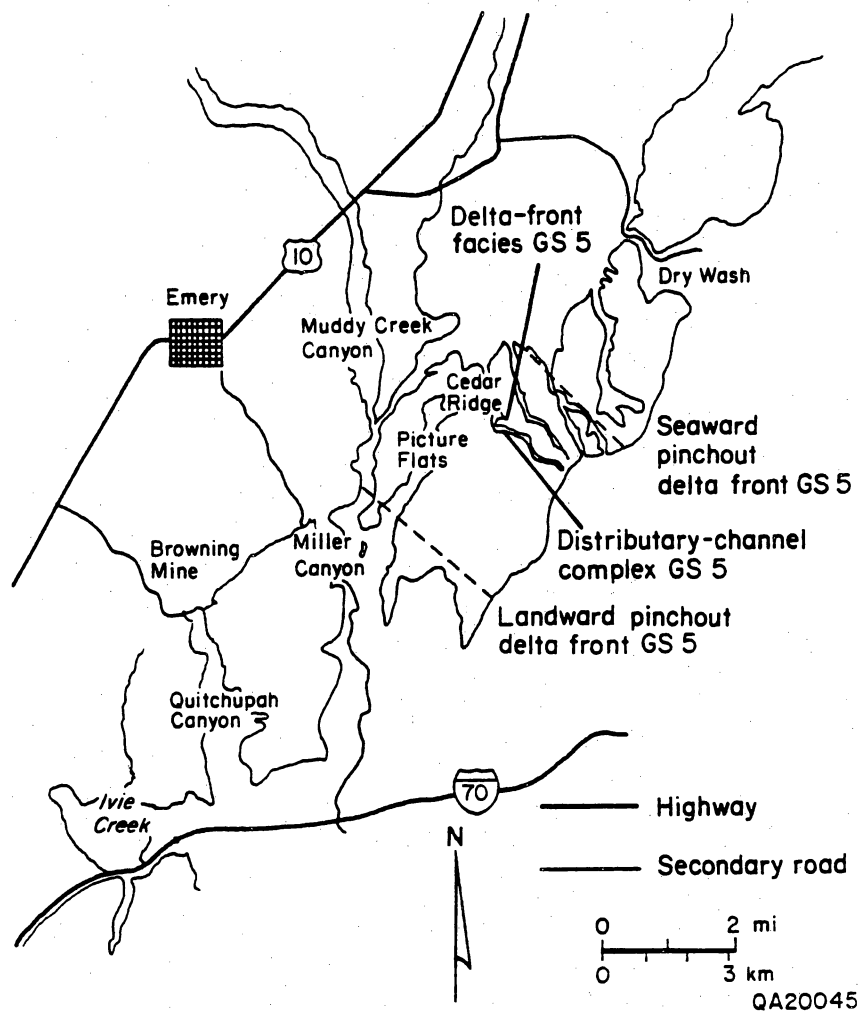


Figure 1. Location map of the Ferron Sandstone outcrop in Castle Valley, central Utah.

succession of northwestward-dipping, northeast-trending ridges. Paleocurrent analysis of symmetrical ripple crests in Ferron marine sandstones indicates that the Ferron ridges are oriented subparallel to the northeasterly progradation of the upper Turonian shoreline.

Three-dimensional exposures of the Ferron Sandstone exist where small canyons dissect the western limb of the San Rafael Swell. Sparse vegetation and structural simplicity allow continuous examination and sampling of outcrops both parallel and perpendicular to the direction of sediment transport. Because Ferron exposures represent an exhumed fluvial-deltaic reservoir, relationships gleaned from this study provide the basis for relating fluid-flow pathways to stratigraphic architecture. The advantage of this approach is the ability to deterministically characterize smaller scale elements (facies architecture, reservoir compartments) of intermediate-scale features (genetic sequences) to understand and predict similar elements and relations in larger scale and more poorly constrained stratigraphic systems (depositional sequences).

Geologic Setting of the Ferron Sandstone

Mid-Cretaceous strata in central Utah, and particularly the Ferron Sandstone, have been extensively studied. The strata are subdivided into lithostratigraphic units that include, in ascending stratigraphic order, the lower Tununk Shale, Coon Spring Sandstone bed, upper Tununk Shale, Ferron Sandstone, and Blue Gate Shale Members of the Mancos Shale (fig. 2). The tectonic history of Cretaceous strata in central Utah is complex and relatively poorly known in the Castle Valley area. Available evidence summarized by Almendinger and others (1983) and Lawton (1985) indicates that initial subsidence was fairly rapid. Burial depth of the Ferron Sandstone can be estimated from the thickness of overlying strata. Measured sections along the Wasatch Plateau approximately 20 mi northwest of the study area and along the Wasatch Plateau escarpment east of Castle Valley show that 5,350 to 13,850 ft (thickness not adjusted for burial compaction) of predominantly sandstone and shale overlie the Ferron (Hintze, 1988). Simply taking the average thickness of each formation

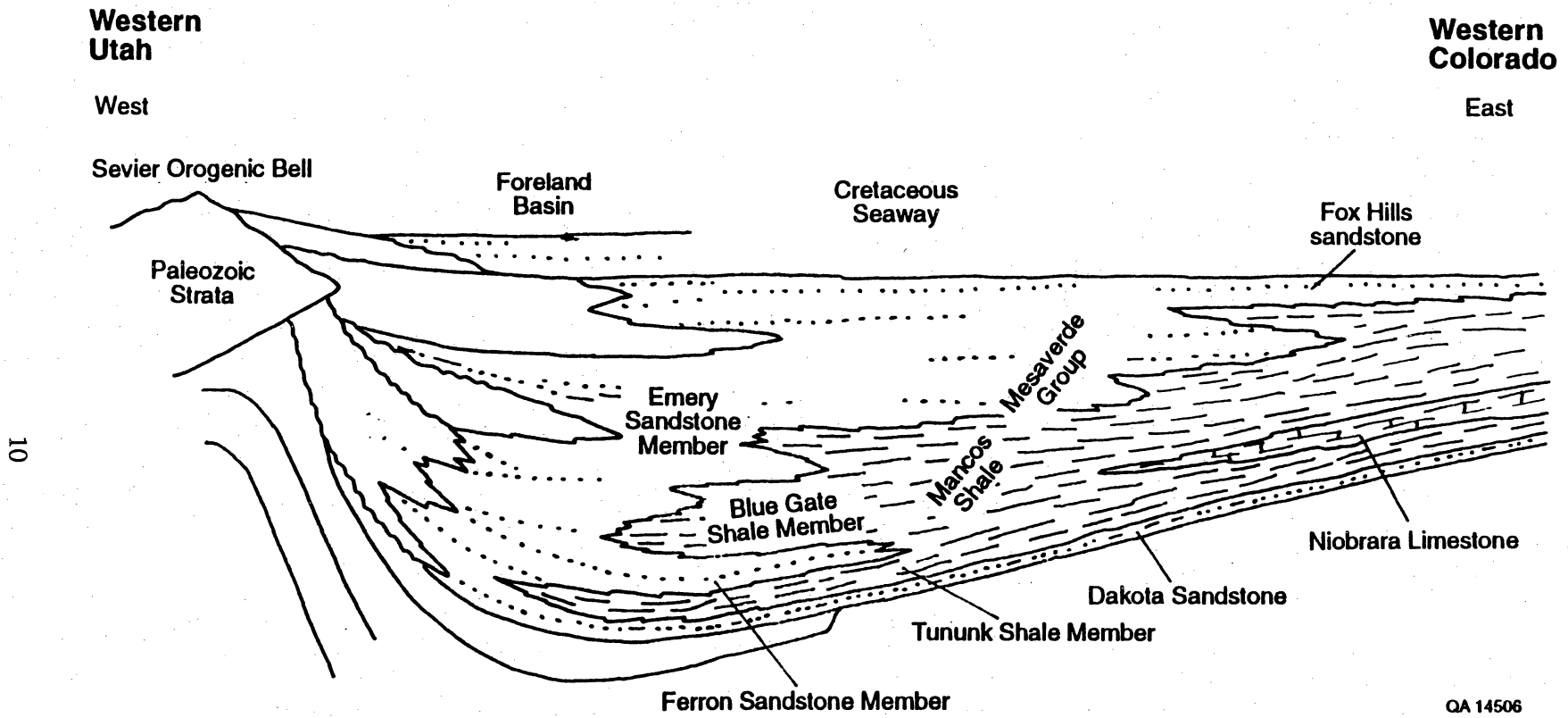


Figure 2. Cross section of Cretaceous strata in central Utah (after Armstrong, 1968).

above the Ferron Sandstone at the nearest measured section yields a best estimate of 9,200 ft for the Ferron burial depth.

Maximum burial temperatures are somewhat better constrained than burial depths. Doelling (1972) reported that Ferron coals in the Emery coal field rank as high volatile C bituminous, having an average of 7.4 percent moisture content and 44.8 percent fixed carbon. Nadeau and Reynolds (1981) investigated the diagenetic history of the Mancos Shale in the southern Rocky Mountain and Colorado Plateau areas by determining the percent illite in mixed-layered illite/smectite. In central Utah their data show that the Mancos Shale contains unordered illite/smectite with 60 percent or less illite in the illite/smectite. We analyzed one sample of Ferron coal for vitrinite reflectance and found a mean value of $R_o = 0.47$ (20 measurements ranged from 0.42 to 0.50). Collectively these data suggest that the Ferron Sandstone sustained maximum burial temperatures of about 65° to 80°C.

The Ferron Sandstone Member comprises two clastic wedges characterized by distinct interbedded sandstone and mudstone successions, which early workers separated into discrete depositional systems (Katich, 1954; Davis, 1954; Hale and Van De Graaf, 1964; Hale, 1972). The lower depositional system, informally called the Vernal delta by Hale and Van De Graaf (1964), is an older and thinner northerly derived clastic wedge that contains the ammonite *P. hyatti* and is called the Hyatti sequence. The southerly derived, westward-thickening, coal-bearing upper depositional system is called the Ferron sequence. Landward-stepping sandstones of the Ferron sequence are the subject of this study.

The Ferron sequence has been informally called the Last Chance delta by Hale (1972). Katich (1954) documented a north-northeast transport direction for the Last Chance delta, whereas Cotter (1975) interpreted this depositional system as a high constructive lobate delta. The most comprehensive work was presented in a series of papers by Ryer (1981a, b; 1982, 1983), who used surface and subsurface data to document six depositional environments (offshore marine, prodelta, delta-front, delta-plain, alluvial-plain and transgressive deposits) in a fluvial-dominated deltaic system.

Ryer (1981a) subdivided the upper Ferron interval into seven discrete delta lobes (genetic sequences [GS] 1 through 7) that progress from seaward-stepping (GS 1 and 2) sandstones at the base, to vertically stacked (GS 3 and 4) deposits in the middle, and to landward-stepping depositional geometries (GS 5, 6, and 7) at the top of the Ferron (fig. 3). Each unit consists of a regressive-transgressive cycle that is bounded by time-significant marine flooding surfaces. The change from seaward-stepping to vertically stacked to landward-stepping sandstones reflects a significant change in tectonic and depositional conditions during a time of continuous sea-level rise. Early in Ferron deposition, both relief from source terrain to base level and transport energy were high, and sediments were carried vigorously to the place of ultimate deposition, producing the seaward-stepping Ferron sequences GS 1 and GS 2. In these genetic sequences, sediment-transport energy exceeded the energy of marine processes, and sandstone geometries reflect primarily fluvial processes. Over time, source-area relief and transport energy decreased and the net effects of sea-level rise and sediment transport approximately balanced, resulting in a series of vertically stacked sandstones (Ferron GS 3 and GS 4). The geometries of these deposits reflect approximately equal influences of fluvial transport and marine reworking processes. Finally, as relief and transport energy waned, the net effect of rising sea level became stronger than sediment transport energy, and the landward-stepping Ferron GS 5, GS 6, and GS 7 units were deposited. Sand-body geometries of these genetic sequences reflect wave- and storm-related sediment redistribution processes.

Recently Gardner (1992, 1993) extended Ryer's work to a detailed analysis of Ferron Sandstone sequence stratigraphy. Sequence stratigraphy is a conceptual framework that places stratigraphic studies within a chronostratigraphic context. A sequence is defined as "a relatively conformable, genetically related succession of strata bounded by unconformities or their correlative conformities" (Mitchum, 1977). Summarizing the concepts of sequence stratigraphy is beyond the scope of this report; excellent reviews are provided by Van Wagoner and others (1990), Brown and others (1990), and references cited therein. The significance of a sequence stratigraphic framework to outcrop characterization and reservoir-analog studies is that sequence stratigraphy provides a conceptual framework for predicting sandstone stacking patterns, sand-body geometry, sediment-volume

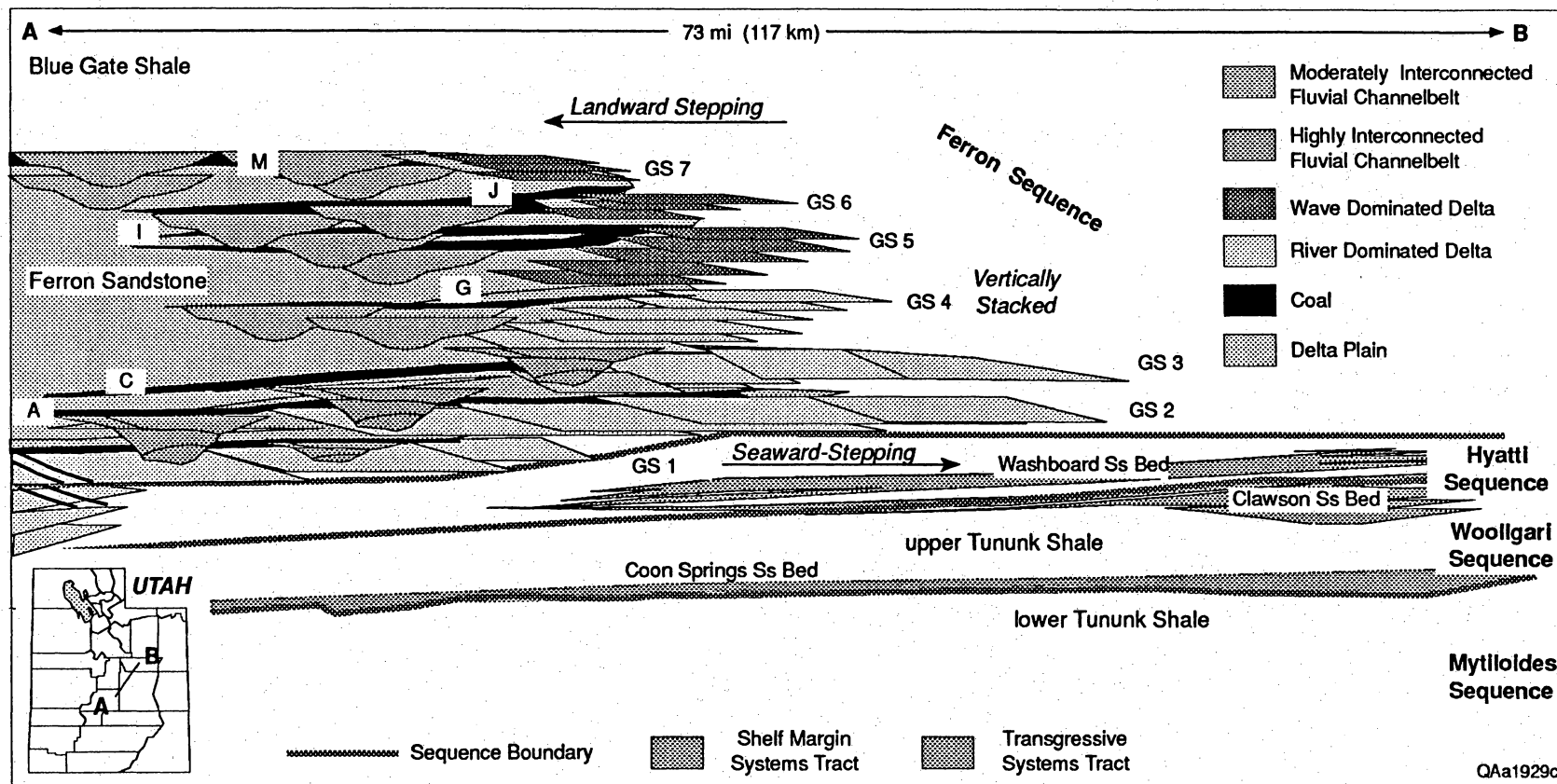


Figure 3. Cross section of the Ferron Sandstone in central Utah (after Ryer, 1981a).

distributions, location of sediment accumulation, and sediment-preservation potential within and between genetic sequences.

Gardner (1992, 1993) showed that systematic and predictable changes in facies arrangement and internal characteristics are related to stratigraphic position within the Ferron system. This well-documented geological framework of the Ferron Sandstone allowed us to quickly select strata that appear to represent the styles and scales of heterogeneity that exemplify Gulf Coast deltaic gas reservoirs. For detailed examination we chose Ferron GS 5 as an example of a landward-stepping (wave-modified) depositional sequence and GS 2 as an example of a seaward-stepping (fluvially dominated) unit. This report summarizes our investigation of Ferron GS 5; results of Ferron GS 2 characterization are reported separately.

METHODS

Architectural Analysis of Landward-Stepping Deltaic Sandstones

After initial field reconnaissance of outcrops along canyon walls that are oriented either parallel or perpendicular to depositional dip, we selected sites for detailed geologic investigations and permeability measurements on the basis of sandstone architecture displayed, quality of the exposure, accessibility, and safety. Because Ferron GS 5 is a landward-stepping unit, the entire facies tract is compressed; total length from landward to seaward extent of the Ferron GS 5 deltaic sandstones is only approximately 4 mi. Reconnaissance studies indicated that the influence of marine processes increased markedly from proximal to distal position in the facies tract, even over relatively short distances. We wanted to investigate how this increased influence of marine processes and marine reworking of the delta platform resulted in markedly different sand-body geometries as a function of position in the facies tract and whether these different geometries correlate with mineralogical or petrophysical differences. Therefore, we chose to concentrate our efforts at three locations: (1) Muddy Creek canyon, which is near the landward (proximal, or updip) pinch-out of Ferron GS 5 deltaic facies, (2) Picture Flats canyon, which is approximately 1.5 mi

seaward from Muddy Creek and occupies an intermediate position in the facies tract, and (3) Cedar Ridge, approximately 1.5 mi seaward from Picture Flats and near the seaward (distal, or downdip) pinch-out of Ferron GS 5 (fig. 1).

At each field study site, we established locations for detailed vertical sections at 50-, 100-, or 200-ft spacings, depending on the dimensions of the sand bodies. Along each vertical section we recorded rock type, facies, bedding type, grain size, lithological discontinuities, and sedimentary structures. We measured paleocurrent directions of various directional features to determine the direction of sediment transport; we used this information to select outcrop facies parallel and perpendicular to local sediment-transport directions for detailed study. In addition to logging these vertical sections, we photographed canyon walls using a medium format (6 × 7 cm) camera, compiled photomosaics of the outcrop, mapped the distribution and interrelations of component architectural elements between vertical sections and in areas beyond outcrop windows, and measured sand-body dimensions. These data were then summarized on logs of the measured sections and were combined to produce outcrop cross sections.

Field Permeability Measurements

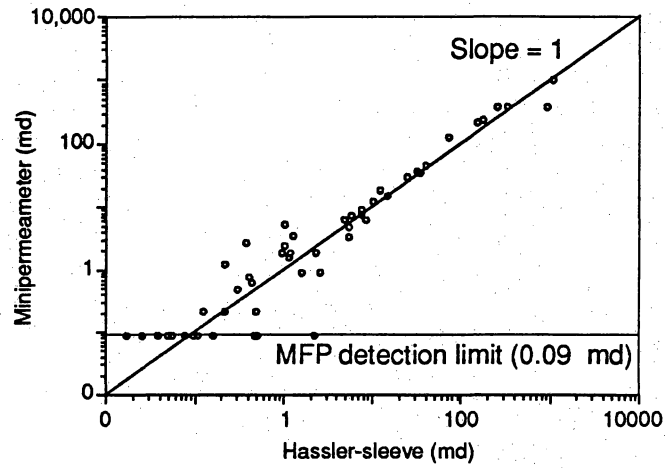
We used a portable field minipermeameter to measure air permeability along each of the measured vertical sections and within grids established on the outcrop face. The minipermeameter is a gas-flow measuring system that is ideal for quickly making a large number of permeability determinations on the outcrop with minimal sample preparation. Effects of outcrop weathering were minimized by choosing relatively fresh surfaces and then chipping away the weathered surface of the rock. Numerous studies have demonstrated the accuracy of the minipermeameter measurements in comparison with conventional measures of permeability (Weber, 1982; Goggin, 1988; Kittredge, 1988). In general, good correspondence between minipermeameter and conventional measurements is reported over the range of approximately one to several thousand millidarcys. The minipermeameter we used has a detection range of about 0.1 md and accurately

measures permeability as high as about 3,000 md. Permeabilities below about 3 md tend to be slightly overestimated; however, application of a tip sealant such as petroleum jelly eliminates instrument bias. Comparison of measured and accepted permeability values for 60 specimens over the range of 0.01 to 1,000 md showed agreement to be within 5 percent (fig. 4). Repeated permeability measurements collected from a single sample point show that precision is within 5 percent over the range of one to several hundred millidarcys. These measures of accuracy and precision allow us to confidently compare our permeability data with the results of other studies. However, our primary goal was not to precisely measure extremely low or high permeability values at the outcrop. We used the field permeability measurements to establish the range of permeability values of the various major sandstone (flow) units and low-permeability bounding elements (potential baffles or barriers), the range of permeability contrast between high- and low-permeability strata, the correlation distances of permeability values, and vertical permeability trends. We collected samples for laboratory measurements in cases where highly precise and accurate data were required.

In addition to measuring permeability along each vertical transect, we constructed sample grids to examine the detailed spatial variability of permeability within and between lithofacies. This task was designed to determine how far permeability data could be extrapolated in a reservoir model. The sampling grids were located on vertical exposures to minimize the effects of surface weathering and to ensure that profiles were truly vertical and orthogonal.

Sampling for Petrographic and Petrophysical Analyses

To meet the needs of all the researchers and to optimize the amount of information derived from Ferron sandstones by the Bureau of Economic Geology (BEG), the Earth Sciences and Engineering Laboratory (ESEL), and The University of Texas Center for Petroleum and Geosystems Engineering (CPGE), we collected samples according to a three-tier, hierarchical sampling plan (table 1). The first level of investigation comprises field mapping of lithological facies and genetic



QA20052c

Figure 4. Comparison of permeability determined by the field minipermeameter and by conventional core-plug measurement. Measurements were taken at each end of the core plug and averaged to obtain the minipermeameter permeability value.

Table 1. Hierarchical sampling plan to provide material for outcrop characterization, petrographic examination, and petrophysical analyses.

Analysis technique	Sample set	Number of samples
Field minipermeameter	Genetic sequence Lithofacies Macroforms Facies Flow units Flow baffles Flow barriers Selected reservoir analogs	$N \times 10^5$
Petrographic composition	Genetic sequence Lithofacies Macroforms Facies Flow units Flow baffles Flow barriers Selected reservoir analogs	$N \times 10^2$
Petrophysical properties*	Flow units Flow baffles Selected reservoir analogs	$N \times 10^1$

*Sample selection based on minipermeameter data and field relations.

associations within depositional systems, measuring and describing vertical outcrop sections at multiple locations along the fluvial-deltaic facies tract, and measuring permeability at 0.5-ft or 1-ft intervals on each vertical section. Because we have several tens of thousands of permeability measurements, far more than the number of samples that could be analyzed for petrographic compositions or petrophysical properties, we used information derived from the outcrop characterization and field minipermeameter measurements to guide sample selection for levels two and three of the study.

Petrographic analyses of sandstones that we judged would function as flow units, baffles, or barriers under reservoir conditions was the second level of investigation. This study is designed to answer such basic questions as (1) what are the relative effects of depositional and diagenetic processes on sandstone composition and permeability, and (2) to what extent are the distribution and petrophysical properties of flow barriers and baffles controlled by zones of preferential cementation or porosity generation. We selected samples for petrographic examination largely on the basis of facies relations and measured permeability values.

The third level consists of samples selected for petrophysical-property measurement at ESEL and used in outcrop-reservoir transform investigations by CPGE. On the basis of outcrop characterization, we attempted to select samples for petrophysical analysis that will provide three specimens for each principal flow unit, barrier, and baffle: one having representative permeability, one having permeability approximately two standard deviations greater than the typical value, and one having permeability about two standard deviations less than the typical value. We also sought samples that, on the basis of facies and bedding type, we thought would have anisotropic petrophysical properties. This suite of samples provides the most useful information regarding relations between sandstone architecture, petrophysical properties, reservoir characteristics, and gas mobility. Initially we collected block samples that we shipped back to ESEL, where cylinders were removed for testing. Later in the investigation we purchased a field coring drill that allowed us to remove 2 1/8-inch cylinders directly from the outcrop. This drill enabled us to be more selective of sampling sites and provided more control on the orientation of the samples relative to bedding.

Petrologic Investigations

We collected samples for the petrologic investigations directly from the outcrop by using a portable coring drill to obtain cylinders 1 inch in diameter and 3 to 6 inches long. Standard petrographic examination included quantifying framework grain and cement mineralogy, porosity, and intergranular volume by conventional thin-section petrography, examining pore properties by scanning electron microscopy, and identifying clay and carbonate mineralogy by X-ray diffraction. For the subset of samples used in the petrophysical property study, we determined the percent sand, silt, and clay, and the grain-size distribution within the sand-size fraction to complement the petrophysical measurements.

Core plugs collected along measured vertical transects in Muddy Creek, Picture Flats, and Cedar Ridge canyons provide most of the material for petrographic analysis; block samples collected for petrophysical testing make up the remainder of the data base. We collected representative samples of volumetrically significant sandstone bodies (presumed analogs of reservoir flow units), as well as low-permeability silty or muddy sandstones and siltstones that might act as flow barriers or baffles under reservoir conditions. Thick shale layers that have permeability values below the detection limit of our field minipermeameter and would probably be barriers to gas flow were omitted from the petrographic analyses.

For each sample we recorded geologic attributes such as facies, bedding type, field estimates of grain size and sorting, and position on the transect. This characterization of sandstone type and position on the outcrop allowed us to place petrographic information within a broader geologic context. In most cases we also measured air permeability of the core plugs using the field minipermeameter so that we could relate permeability to petrography and ultimately to petrophysical properties.

We first made thin sections of all samples and scanned them under a petrographic microscope. Thin sections were stained with sodium cobaltinitrite to help distinguish between plagioclase and potassium feldspar. Samples that contained carbonate minerals were also stained with potassium

ferricyanide and alizarin red-S to differentiate between calcite, Fe-calcite, dolomite, and ankerite. Two hundred to 300 points per slide were identified and tabulated to determine rock composition and thin-section porosity. Grain size and sorting were estimated by comparing thin sections with standard charts. For a selected subset of samples we used X-ray diffraction, scanning electron microscope (SEM) examination assisted by energy dispersive X-ray spectroscopy (EDS), and electron microprobe analysis to identify the mineralogical and chemical composition of sandstone grains, matrix, and cements.

Petrophysical Measurements

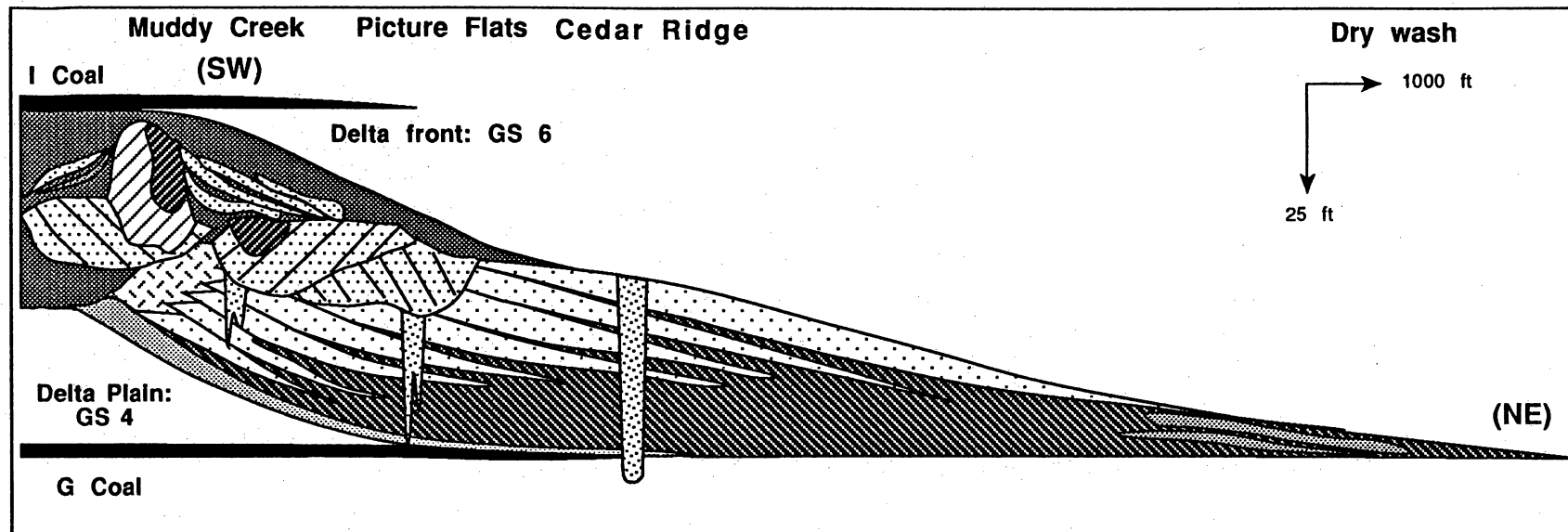
Laboratory measurements conducted at ESEL provide single-phase and two-phase flow data, conductivity and resistivity determinations, and velocity data. Analyses were performed on two 1/8-inch diameter cylinders approximately 4 inches long. Laboratory measurement techniques and preliminary results were reported previously (Fisher and others, 1992) and are the subject of a companion report (Miller and others, in preparation). In this report we present only the results of the petrophysical measurements and describe the samples analyzed.

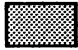
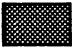
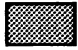








FERRON GS 5 SANDSTONE ARCHITECTURE

Ferron GS 5 deltaic facies consist mainly of basal transgressive, delta-front, and shoreface sandstones that are erosionally overlain by distributary-channel and associated deposits. Field efforts concentrated on mapping and measuring the geometry of these sandstones and the low-permeability bounding units surrounding and encasing them so that natural-gas reservoir models can be constructed with accurate dimensions and geometries of flow units and bounding elements. Reservoir modeling of the Ferron outcrop reservoir analog is beyond the scope of the present study but is planned for future work. Until flow modeling can be performed, we consider sandstones having permeability greater than about 5 md to be flow units and strata with lower permeability to be potential baffles or barriers to flow under effective reservoir conditions.

In quantifying Ferron sandstone architecture, we first describe lithofacies and bounding surfaces within individual sand bodies and facies. General information regarding depositional systems and sedimentary-basin analysis can be found in standard textbooks such as those by Davis (1983) and Miall (1990). Lithofacies are distinguished by common associations of sedimentary structures, grain size, and mineralogy. As discussed in the following sections, these parameters largely control permeability unless overprinted by diagenetic modification. Furthermore, variable preservation of lithofacies controls the large-scale permeability distribution of major sand bodies. For these reasons we consider lithofacies to be the fundamental building blocks that are arranged by geologic processes to construct the framework of flow units and barriers in natural-gas reservoirs. Lithofacies are organized by depositional processes into common associations or facies. Discrete facies display a characteristic arrangement of lithofacies and bounding surfaces and provide a process-based model for predicting the arrangement and distribution of major reservoir elements.

A variety of facies from shallow marine through coastal plain occurs in GS 5 (fig. 5). The basal transgressive interval is intensely bioturbated, directly overlies a sharp to erosional surface, and forms an areally extensive but locally discontinuous sandstone. This transgressive facies records the maximum flooding surface that marks the base of deltaic GS 5. Overlying the transgressive sandstones is an upward-coarsening sequence of interbedded mudstones, siltstones, and fine-grained hummocky to swaley cross-stratified sandstones. The preserved thickness of this unit depends on the amount of erosion by overlying distributary channels. Delta-front facies record deltaic progradation in a wave- to storm-dominated shallow marine setting. The overlying distributary-channel complex contains a wide range of internal and external variability. Three stages of channel occur in the distributary system: (1) early-stage, heterolithic channels that are deeply incised into the delta front, (2) middle-stage, laterally expansive, heterogeneous channels, and (3) late-stage, thick, homogeneous channels closely associated with crevasse splay and abandoned channel fill facies. The GS 5 sequence is capped by convoluted, highly bioturbated mudstones and extensive coal deposits that record delta abandonment and flooding.



- | | | | |
|---|------------------------|---|-----------------------------------|
|  | Transgressive |  | Delta plain |
|  | Slump deposits |  | Crevasse splay |
|  | Lower shoreface |  | Abandoned channel fill |
|  | Upper/middle shoreface |  | Late-stage distributary channel |
|  | Foreshore |  | Middle-stage distributary channel |
| | |  | Early-stage distributary channel |

QAa1202c

Figure 5. Arrangement of architectural elements along depositional dip in Ferron GS 5.

In the following sections we describe the geometry, facies, and lithofacies of Ferron GS 5 delta-front and distributary-channel sandstones and the associated internal low-permeability strata. These elements are equivalent to reservoir compartments, baffles, and barriers. We provide detailed descriptions of lithofacies, facies, and macroforms because these features are recognizable in core and well logs and thus assist exploration geologists in placing a reservoir in the proper sequence stratigraphic framework.

Delta-Front Lithofacies

Shallow marine strata of deltaic GS 5 consist of lower to upper shoreface associations. They are characterized by a 15- to 40-ft-thick upward-coarsening, bed-thickening sequence consisting of interbedded sandstone and laminated to bioturbated mudstone. Areally, the delta-front facies forms a strike-aligned deposit elongated north-west to south-east. Along depositional strike, where the delta-front facies has not been eroded by overlying distributary channels, lateral variation in depositional characteristics is minimal; lithofacies arrangement and thickness remain extremely constant and continuity of individual sand bodies is very high. Along depositional dip the cross-sectional geometry of individual sand bodies is characterized by a broadly lenticular shape that gradually thins at the seaward extent and abruptly thickens at the landward pinch-out. Laterally, the upper shoreface succession is gradually replaced by the lower shoreface succession in a seaward direction. Internally, the interval is composed of a series of offlapping, seaward-dipping subunits that range from several feet to tens of feet thick.

Bioturbated Lithofacies

Bioturbation has homogenized some intervals, creating poor sorting and introducing clay and silt. Burrowed intervals are apparent and have in places erased all original sedimentary structures. Such obliteration of original depositional stratification reflects the absence of processes such as wave or tidal effects that can physically rework sediments. Bioturbated strata occur as extensive intervals

within the transgressive and lower delta-front facies and in minor amounts capping hummocky and swaley cross-stratified beds.

Hummocky Cross-Stratified Lithofacies

Hummocky cross-stratification (HCS) consists of low-angle, gently undulating laminations with wavelengths typically 3 to 15 ft and heights from swale to adjacent hummock of several inches to a foot. In three dimensions the hummocks form low relief symmetrical domes capped by wave ripples. Within the hummocky sequences there is rarely any other stratification type. Preservation of these structures suggests that once the HCS is formed, it is not reworked by other tidal, longshore, or wind-generated currents. Harms and others (1975) suggested that the long, low undulating hummocky cross-stratification was produced by storm waves, below fair-weather wave base. Hamblin and Walker (1979) extended this interpretation to suggest that resuspended sand, entrained in storm-generated density currents and deposited seaward, was subsequently reworked by storm waves into HCS to the depth of storm wave base. The sharp-base sandstones represent the sudden influx of sand into a normally muddy environment, and, being below fair-weather wave base, there was no subsequent reworking of the storm-emplaced sand. In places, the HCS sandstones have become amalgamated by the erosion or nondeposition of interbedded mudstones. The amalgamation suggests slightly shallower water where smaller and more frequent storms were able to generate waves that could rework sediments. During the waning of the storm waves, small symmetric ripples were made on the upper surfaces of some HCS beds. The absence of other stratal types indicates that there was no reworking after storm emplacement (that is, below fair-weather wave base). The gradual passage from interbedded HCS and bioturbated mudstones to amalgamated HCS can be interpreted as a generally shallowing trend.

Swaley Cross-Stratified Lithofacies

Swaley cross-stratification (SCS) consists of a series of superimposed concave-upward shallow scours about 3 to 12 ft wide and 0.5 to 2 ft deep (Allen and Underhill, 1989). Stratification is gently curved, following the basal erosive surface of the swale. Dips along edges of the swale rarely exceed 10°, and the swales have the same geometry regardless of orientation. In a vertical sequence SCS (if present) always directly overlies HCS. In layers, SCS and HCS may occur together. Walker (1981) suggested that SCS is a storm-dominated structure formed in water shallower than the HCS and possibly above fair-weather wave base.

Trough Cross-Stratified Lithofacies

This stratification type occurs almost exclusively within the foreshore facies near the landward pinch-out of the delta-front facies. Deposits consist of clean, well-sorted, fine- to medium-grained sandstones that display multiple low-angle truncation surfaces. Inverse grading of laminae is observed with fine-grained sand and heavy minerals concentrated in discrete laminae and merging upward into a medium-grained, quartz-rich layer (Clifton, 1969). Occasionally, an interval of trough cross-stratified sandstone erosionally overlies these deposits. Cross bedsets vary in thickness from 0.5 to 3 ft, with an accumulated thickness of 10 to 15 ft. Dip directions are variable but are generally to the southwest (landward direction). The upper portion of this unit is bioturbated and contains abundant wood fragments and log impressions or is alternatively capped by parallel laminated sandstone that has similar characteristics. This facies is interpreted as a storm-generated washover channel within a wave-dominated foreshore environment. Carbonaceous shales and bioturbated siltstones overlie this unit.

Delta-Front Facies

Lower Delta-Front Facies

The lower shoreface sequence is dominated by sandstone beds that reflect storm-generated, waning-flow sequences of erosive-based cosets of hummocky cross-strata capped by wave ripples. This interval gradationally overlies the transgressive facies and consists of interbedded sharp-based sandstones and bioturbated mudstones. Total unit thickness can be as much as 30 ft; individual sandstones average 4 to 8 inches near the base of the unit, thickening to about 40 to 80 inches at the top. The dominant structure of the sandstones is HCS. The upper surfaces of the hummocks commonly show small-scale symmetrical ripples. The HCS beds become amalgamated upward within this unit to form sand bodies up to several meters thick. There is little variation in thickness of internal character along strike over a distance of several miles. In a downdip direction, the unit progressively thickens and thins from its landward to seaward pinch-outs.

Upper/Middle Delta-Front Facies

The upper shoreface contains a high percentage of amalgamated low-angle hummocky stratification, swaley cross-strata, and minor amounts of multidirectional trough cross-stratification. The multidirectional trough cross-stratification is the product of storm-surge ebb currents (Hayes, 1967) and storm-generated, wind-forced currents that attain upper-lower flow regime. The upward change from hummocky to swaley cross-strata reflects an increased frequency of episodic, high-energy storm events that obliterate fair-weather deposits, with increased truncation surfaces resulting in the absence of antiformal hummocks and sandstone amalgamation (Dott and Bourgeois, 1982). Internally, thin, extensively deposited mudstones divide the upper delta front into a series of offlapping subunits. Individual subunits consist of amalgamated hummocky to swaley cross-strata overlain by a thin veneer of wave-ripple-stratified sandstones that display a sharp to erosional basal contact and a sharp to bioturbated upper contact. These deposits are often overlain

by silty shales thought to represent brief episodes of deltaic abandonment and marine influx. Burrowing is attributed to the reworking of the upper portions of bars and interbar areas as abandonment and flooding proceeds.

Foreshore Facies

Foreshore deposits are characterized by wedged-shaped swash lamination and trough crossbedding that consist of clean, well-sorted, fine- to medium-grained sands. The foreshore deposits are restricted to the upper 10 to 20 ft of the delta-front succession near the landward pinch-out. Cross bedsets vary in thickness from 0.5 to 3 ft and often overlie a well-defined erosion surface. Dip directions are variable but generally to the southwest (landward direction). The upper portion of this unit is capped by fine-grained, parallel laminated sandstone that is moderately bioturbated and contains abundant wood fragments and log impressions. This facies is interpreted as a storm-generated washover channel within a wave-dominated foreshore environment. Carbonaceous shales and bioturbated siltstones overlie this unit.

Distributary-Channel Complex Lithofacies

Ferron GS 5 distributary channels form belts that are as much as 60 ft thick and 2,000 ft wide. Each channel belt consists of multiple-channel sand bodies. Individual channel sand bodies are 3 to 30 ft thick and tens to hundreds of feet wide. In profile they consist of an erosive-based upward-fining sequence (Allen, 1965) that produces a compound bar form called a macroform (Jackson, 1976; Friend, 1983; Miall, 1985). Several classes of distributary macroforms describe the temporal and spatial changes in the Ferron distributary system. Macroform variability largely results from differences in channel morphology, position in the channel, and channel stage (Gardner, 1991). We recognize several stages of channel sedimentation that reflect cycles of base-level fall and rise and differential subsidence in the distributary system. Each stage is characterized by a distinctive internal and external geometry and associated deposits. The distribution of channel types records

progressive back-filling within the distributary system during a single cycle of base-level rise. The complex internal architecture is attributed to higher in-channel sedimentation as a result of greater differential subsidence, greater preservation, and compartmentation of individual macroforms (Penland and others, 1988). In a more slowly subsiding channel, the sand would be periodically eroded by exceptionally high magnitude floods, and less complex sand bodies would be preserved.

Ripple-Laminated/Cross-Stratified Lithofacies

These deposits are very fine grained to fine-grained and thinly laminated. In some cases the entire ripple form is preserved (ripple-laminated sandstones) and may contain small amounts of clay drapes or wisps. Ripple sets are thin, rarely more than 1 inch thick, with sets occurring in packets as much as 8 ft thick. Ripple-stratified sandstones represent the final traction-flow event in a waning-flow sequence. As a result, deposits are usually restricted to the top portions of bars and channels, which are typically overlain by a layer of silt or clay. Preservation of this facies is moderate to poor because of erosion by overlying sequences.

Low-Angle Stratified Lithofacies

Low-angle stratification consists of strata within sets that are straight to slightly concave. Inclinations of strata are low, usually less than 10° , and maximum dips are downcurrent. Where strata approach the lower boundary of the set, they tend to turn up slightly and are concordant. Individual sets range from several inches to several feet in thickness, with accumulated thicknesses on the order of several feet to tens of feet. Deposition is by low-velocity currents, as indicated by fine-grain size, long length of thin strata, and low angles of inclination. Lithofacies may grade laterally into trough cross-stratification in channel deposits and upward into ripple or convolute stratification. This lithofacies records downcurrent migration of point and longitudinal bars.

Trough Cross-Stratified Lithofacies

This lithofacies consists of scooped-shaped sets of cross-strata. In transverse section, the strata within a set are concave upward and conform to the lower erosion surface. Individual sets are packed together with partial erosion by adjacent and overlying sets. In longitudinal view the sets are tabular or wedge shaped; strata are slightly concave upward and inclined downstream. Grain size within this lithofacies is variable, ranging from fine to very coarse. Individual sets range from 0.33 ft to several feet in thickness, with an accumulated thickness of 30 ft. These deposits are interpreted to form by moderate-velocity currents in the lower flow regime that were sufficient to produce dunes. They occur as a common lithofacies in the lower portion of most channel and bar deposits.

Contorted Bedding Lithofacies

This lithofacies is composed of trough, low-angle inclined, and ripple cross-stratified sediments that have suffered syndepositional deformation. Both small- and large-scale structures exist. Chaotic, vertical, and overturned bedding or laminae are found in sequences that are typically 1 to 10 ft thick but can be as much as 15 ft locally.

This type of soft-sediment deformation can result from several situations. In some crossbeds, oversteepening to overturning of the upper part of the cross-laminae with folds overturned in the downcurrent direction can be observed. This phenomenon may be due to plastic deformation of the bed at the time of deposition due to shear stress exerted by the current (Allen and Banks, 1972). Second, the basal portions of sand bodies directly overlying fine-grained sediments commonly display deformation structures presumably due to the loading of denser layers over less dense layers. This feature has been observed in crevasse splay deposited in topographically low interchannel areas. Third, the upper portions of sand bodies are commonly extensively deformed where they are directly overlain by thick laterally continuous mudstones. In these cases, partial liquefaction of the sediment results from excess pore pressure due to the low permeability of the overlying mudstone.

This prevents loss of pore fluids during compaction. Of the three types observed, the last is volumetrically the most important and extensive.

Lag Deposit Lithofacies

Lag deposit lithology is variable, but typically consists of a thick, 0.25- to 4-ft, poorly sorted and organized, fine-grained to granule, sand-matrix-supported clay/coal clast conglomerate. Lag composition is attributed to repeated erosion of fine-grained channel margin and interchannel deposits. This lithofacies occurs along channel-base bounding and reactivation surfaces. The deposits are attributed to rare, high-magnitude flood events that partially erode preexisting bar forms and channel margin sediments or to physical reworking of the bar surface during periods of normal flow.

Fine-Grained Sediment Lithofacies

The fine-grained lithofacies consists of deposits of coal and carbonaceous mudstone and siltstone with variable amounts of bioturbation and syngenetic sulfides. Deposits of fine-grained sediment may occur along the channel margins as overbank deposits or within the channel as mudstone plugs and thin mudstone drapes along channel-base bounding and accretion surfaces. Mudstone plugs, which may be more than 20 ft thick, are caused by distributary avulsion and channel abandonment. Clay drapes that form along basal channel-scour and bar-accretion surfaces suggest variable stream discharge with episodes of erosion and channel scouring, followed by periods of extremely low energy conditions and the deposition of fine-grained sediment from suspension over the top of the channel scour. The cohesive nature of the thin, fine-grained layer prevents erosion during subsequent periods of higher energy flow.

Distributary-Channel Complex Facies

Early-Stage Distributary-Channel Facies

These deposits are deeply incised into the delta front and are heterolithic (contain both mud and sand). Sandstone bodies (macroforms) are simple bar forms that have no internal large-scale-accretion surfaces and contain a low diversity of sedimentary structures. They are characterized by a 3- to 20-ft-thick, erosive-based, uniformly distributed medium- to coarse-grained sandstone sequence that consists of a thin, basal sand-rich lag and crossbedded sandstone couplet. The dominant stratification type is trough cross-stratification with large avalanche foresets locally present. However, bedding in sandstone units is typically faint to indistinct with evidence of dewatering and rapid sedimentation. A thin veneer of fine-grained, ripple-stratified sandstone may cap or flank the bar form. Closely associated deposits consist of thick, extensively deposited mudstone drapes that separate and compartmentalize individual sandstone macroforms. Bar forms and associated deposits may also display diagenetic sulfides, shark's tooth lags, and moderate bioturbation, including *Toledolites* bored logs.

Where the upper surface of the macroform coincides with the basal contact of an overlying macroform, it is highly irregular, and where the depositional topography of the macroform is preserved, it is convex upward. Channel incision, heterolithic composition, and uniform internal characteristics (grain size and low diversity of cross-strata types) reflect poor development of a waning-flow sequence during bar aggradation resulting from rapid aggradation and abandonment. This is a process that typically occurs under relatively uniform but episodic flow conditions caused by frequently recurring flood events within a mixed bedload, low-sinuosity distributary system (Allen, 1966).

Middle-Stage Distributary-Channel Facies

Laterally migrating channel deposits erosively overlie early-stage distributary-channel and delta-front deposits. These complexes are much more extensive than subjacent channel deposits and laterally shale out into overbank muds and silts, or are truncated by superjacent distributary-channel sandstones. The dominant characteristic of this channel type is the inclined erosive surfaces that dip gently toward the channel base and subdivide the channel belt into a series of multilateral sand bodies that are separated by thick, extensive mud-clast lag deposits. Strong vertical partitioning of stratal types produces a well-stratified system. Trough cross-stratified sandstones occupy the lower portion of the channel complex. Low-angle stratified sands abruptly overlie trough crossbeds, and the sequence is capped by moderately to highly contorted strata or, less commonly, ripple-laminated sandstones. Grain size in this interval decreases upward from poorly sorted, coarse sand at the base to moderately sorted, medium-fine sand at the top.

Late-Stage Distributary-Channel Facies

Late-stage distributary-channel deposits are considerably thicker and narrower than the underlying laterally expansive channel type. Typically, these deposits are perched above and erode deeply into subjacent sandstones. The basal contact is typically characterized by a deposit of mudstone/siltstone or a thick intraformational mud-clast lag. Internally, large inclined accretion surfaces divide the sand body into a series of subunits that are composed of a succession of stratal types. Each stratal type is characterized by a well-developed waning-flow sequence of small-scale sedimentary structures. In some cases, the upper surface is accentuated by a thin layer of fine-grained sediment that is 1 to 2 inches thick. Laterally, the channel type is closely associated with abandoned channel fill and crevasse splay deposits. These channel deposits are interpreted to reflect a mixed load, high-sinuosity channel within a highly aggradational setting.

Abandoned Channel Fill Facies

The abandoned channel fill facies is characterized by an erosive-based, 5- to 30-ft-thick mudstone plug, or alternatively, a mud-rich, upward-fining, interbedded sandstone and mudstone sequence that becomes increasingly mud-rich upward. Sandstone interbeds dip at a low angle and are concave upward from the bottom to the top. This facies is most often found in the upper portion of the system associated with the late-stage channel type. The abandoned channel fill facies is attributed to processes of distributary avulsion or channel cutoff and abandonment.

Crevasse Splay Facies

The crevasse splay facies is characterized by a 5- to 20-ft-thick, heterolithic, upward-coarsening sequence containing interbedded sandstone and laminated-to-bioturbated mudstone. The basal contact is sharp to erosional, whereas the upper contact is sharp and may be bioturbated. Sandstone beds are less than 1 inch to 3 ft thick and display trough cross-stratified sandstone that is interbedded with ripple cross-stratified and low-angle inclined sandstone. Sandstone beds in this sequence may contain a clay/coal clast lag at the base or along cross-strata foresets. Soft sediment deformation, indicated by deformed laminations up to 5 ft thick and load structures in underlying mudstones, is common in basal sandstone units. Crossbedding is dominantly unidirectional and normal to associated channel deposits. The deposits display a single story to multistory sheetlike geometry. Individual stories display low-angle, inclined surfaces that dip downcurrent. These deposits form in low-lying interdistributary bay and channel margin environments during flood stages in the distributary and typically are associated with sediments from the upper portion of the channel system. Temporal and spatial differences in magnitude and frequency of floods result in extreme variability.

Bounding Elements

Bounding elements are low-permeability, subhorizontal to inclined surfaces or strata that interrupt sandstone continuity and could act as baffles or barriers to flow in a reservoir. The most common bounding elements in Ferron GS 5 sandstones are contacts between different stratal types, channel scours, and lateral accretion surfaces. In the lower part of the distributary-channel complex, bounding elements separating individual sand bodies consist dominantly of a scoured surface overlain by poorly sorted, mud-clast-rich sandstone. In the middle to upper part of the complex, the bounding elements consist of scoured sand-on-sand contacts and lateral-accretion surfaces.

We find a four-order hierarchy of bounding elements and surfaces in the delta-front distributary-channel complex (table 2). First-order bounding elements relate to system changes such as the pinch-out of distributary sandstone into interdistributary bay mudstone. First-order bounding elements would behave as flow barriers in a reservoir because of the permeability contrast and lateral extent involved. Second-order bounding elements are defined largely by depositional or diagenetic facies changes. Typical examples are the interface between channel sandstones and floodplain muds or between relatively porous channel sandstones and tightly cemented transgressive sandstones. Third-order elements separate similar facies such as channel-on-channel contacts, which are commonly marked by mud-clast accumulations. Fourth-order elements define internal bounding surfaces within a facies. These elements probably constitute flow baffles that could reduce gas recovery efficiency.

PETROGRAPHY, DIAGENESIS, AND PERMEABILITY

Mineralogy of Ferron Sandstones

Transgressive, delta-front, and distributary-channel sandstones are volumetrically dominant in Ferron GS 5. Associated facies such as levee deposits, crevasse splays, and washover fans are volumetrically less important but were sampled because they may act as impediments to flow in a

Table 2. Hierarchy of bounding elements and surfaces in Ferron GS 5 fluvial-deltaic sandstones.

Order	Type	Examples
First	System change	Distributary-channel sandstone to interdistributary bay mudstone
Second	Facies change (depositional)	Abandoned channel fill Channel to levee Channel to floodplain Delta-front sandstones to mudstones
	(diagenetic)	Cementation change from delta front to distributary channel
Third	Interfaces	Channel-on-channel contact Channel base to channel margin
Fourth	Intrafacies	Lateral accretion surfaces Changes in stratal type Diagenetic front, paleosols

natural gas reservoir. We also collected and analyzed samples from the upper, fluvially influenced sandstones of Ferron GS 4.

Sandstone textures vary between the different facies. Transgressive and delta-front facies are uniformly either very fine or fine grained sandstones. Fluvial (GS 4) and distributary-channel (GS 5) facies range from very fine to coarse grained. Framework grains range from very poorly sorted to extremely well sorted; most are moderately well to well sorted.

Framework Grains

Quartz, feldspar, and rock fragments are the basic detrital component of Ferron sandstones. Common quartz with straight to slightly undulatory extinction is by far the most common quartz type present. Stretched metamorphic quartz (classification of Folk, 1974) is present in minor amounts in the coarser grained sandstones. Because the abundance of stretched metamorphic quartz is more closely related to grain size than to facies, its presence is not a good indicator of source rock type. Contacts between quartz are commonly concavo-convex to sutured, indicating that pressure solution has occurred.

Potassium feldspar is slightly more abundant than plagioclase, particularly in the coarser grained sandstones. Potassium feldspar is typically fresh, although minor amounts of partially leached potassium feldspar exist. Plagioclase grains may be fresh, highly sericitized or vacuolized, or partially to totally leached. Leached plagioclase and potassium feldspar provide microporosity that is recorded in the point-count data only if it amounts to more than 50 percent of the original grain volume.

The lithic component of Ferron sandstones is primarily chert and low- to medium-grade metamorphic rock fragments. Both chert and metamorphic rock fragments occur as fresh to highly leached grains. Significantly, the types of rock fragments present in the Ferron are relatively ductile grains that deform around more rigid quartz and feldspar during burial and compaction, thus reducing porosity and permeability.

Intergranular Material

Authigenic cements, porosity, and pseudomatrix fill the volume between detrital grains. Authigenic phases are either predominantly kaolinite, carbonate, or quartz. Kaolinite occurs mainly as pore-filling cement; less commonly it has a texture that reflects grain replacement. Carbonate is rarely a pore-filling cement; much more commonly it occurs as grain replacement. The size and shape of carbonate-replaced grains, as well as the rare observation of a feldspar grain partially replaced by carbonate, indicate that most carbonate-replaced grains were originally plagioclase feldspars. Electron microprobe analysis of carbonate cements shows that the chemical composition varies widely from pure calcite to Fe-calcite to dolomite. Stoichiometric ankerite is rare; most authigenic carbonate in Ferron sandstones is iron-rich dolomite.

Ferron sandstones contain both macroporosity and microporosity. Macroporosity is present as intergranular void space and as voids left by complete grain dissolution. Microporosity exists within partially leached grains (mostly plagioclase and chert fragments) and between crystallites in patches of authigenic kaolinite. Most macroporosity would be classified as secondary porosity according to the criteria of Schmidt and MacDonald (1979). Undoubtedly, some of the primary porosity that existed before the strata were uplifted during late Miocene to Holocene time (approximately 10 to 15 million years ago [m.y.a.]) has been enhanced by dissolution at the outcrop.

Pseudomatrix consists of locally derived clay rip-up clasts and mud chips introduced into the sands during bioturbation. After burial compaction, clay clasts are indistinguishable from clay laminae and clay introduced by bioturbation. Because clay clasts could not survive transport over any significant distance, and because they now so closely resemble bioturbated laminae, they are classified as intergranular material rather than detrital grains. Like rock fragments, pseudomatrix is easily deformed during burial compaction and severely reduces porosity and permeability by filling intergranular space. Pseudomatrix typically has weathered to a combination of Fe-Mn-oxide, Fe-Mn-hydroxide, and pyrite during exposure on the outcrop. Petrographic relations show that no appreciable volume change accompanied this conversion; thus, it did not affect rock texture.

Pseudomatrix commonly was the site for late carbonate nucleation; subsequent leaching of the carbonate creates isolated porosity within pseudomatrix.

Although all Ferron GS 5 sandstones contain the same types of grains, pseudomatrix, and cements, the relative proportions of each vary systematically with depositional environment and position in the facies tract.

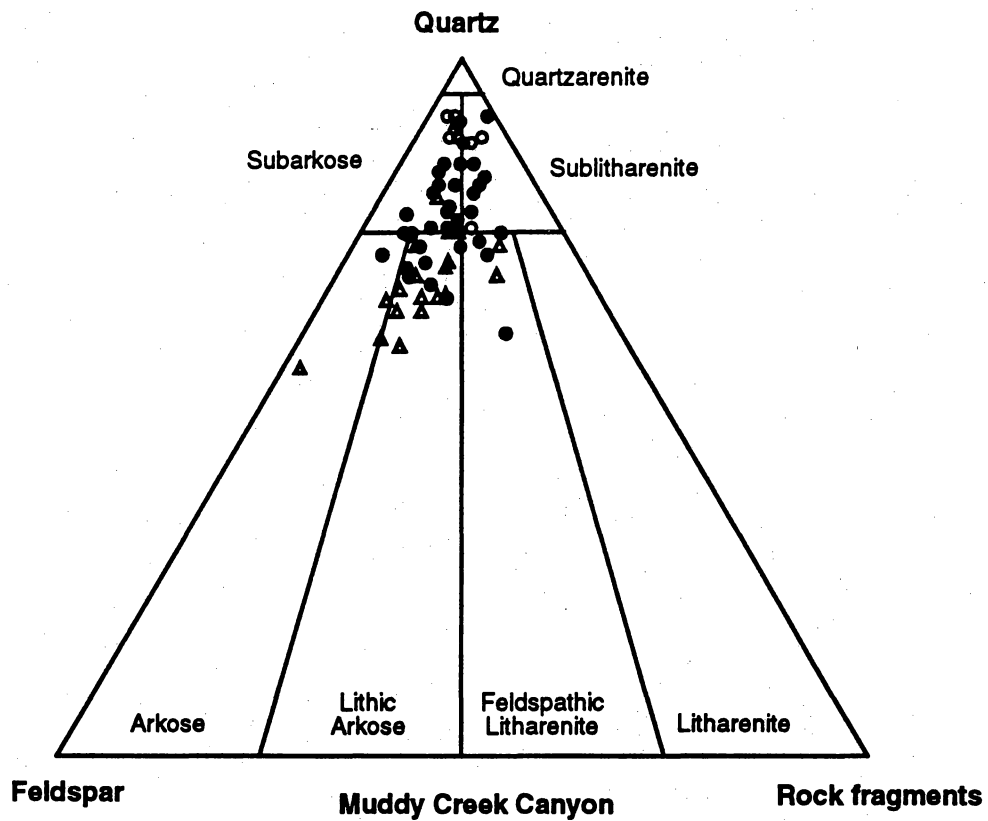
Ferron GS 5 Sandstones at Muddy Creek

Sandstone Types

Muddy Creek canyon exposes the Ferron GS 5 Sandstone at the most landward extent of the delta complex. At Muddy Creek we sampled distributary-channel, transgressive, delta-front, and associated facies of Ferron GS 5 and the upper sandstones of Ferron GS 4. Transgressive and delta-front sandstones are grouped together in the following discussion because there is no significant difference in composition between the two facies. Transgressive and delta-front sandstones are quartz-rich subarkoses and sublitharenites (fig. 6) with approximately equal amounts of feldspar and rock fragments. The mean Q:F:R composition of transgressive and delta-front sandstones is 88:7:5. Distributary-channel sandstones are subarkoses, sublitharenites, lithic arkoses, and feldspathic litharenites. Feldspars are slightly more abundant than rock fragments. Mean Q:F:R composition of distributary-channel sandstones is 77:13:10. In contrast, sandstones at the top of Ferron GS 4 contain relatively less quartz and are predominantly lithic arkoses. Mean Q:F:R composition of GS 4 sandstones is 68:20:12.

Intergranular Composition

Intergranular volume varies only slightly; distributary-channel, transgressive and delta-front, and GS 4 sandstones have mean values of 23.5 percent, 23.9 percent, and 22.9 percent, respectively (table 3). However, the composition of intergranular material does vary systematically. In GS 5



Explanation

- Distributary Channel
- Transgressive and Delta Front
- ▲ GS 4

QAa1963c

Figure 6. Framework grain composition of sandstones from Muddy Creek (classification of Folk, 1974).

Table 3. Summary of petrographic data for major constituents in Ferron GS 5 and GS 4 sandstones.

<u>Muddy Creek</u>			
	Distributary channel	Transgressive and delta front	GS 4
Quartz	77	88	68
Feldspar	13	7	20
Rock fragments	10	5	12
Intergrain volume	23.5	23.9	22.9
Matrix	3.9	1.5	4.7
Macroporosity	11.9	11.0	6.6
Microporosity	6.4	1.6	11.4
Total cement	7.1	10.5	11.1
Quartz cement	3.6	6.4	1.8
Carbonate cement	0.5	3.6	2.0
Kaolinite cement	3.0	0.5	7.3

<u>Picture Flats</u>		
	Distributary channel	Shoreface
Quartz	82	89
Feldspar	12	8
Rock fragments	6	3
Intergrain volume	21.0	24.1
Matrix	1.0	0.3
Macroporosity	13.0	9.9
Microporosity	3.1	0.9
Total cement	6.2	12.2
Quartz cement	4.2	5.2
Carbonate cement	0.8	6.9
Kaolinite cement	1.2	0.1

Table 3 (cont.)

<u>Cedar Ridge</u>		
	Distributary channel	Shoreface
Quartz	78	89
Feldspar	17	8
Rock fragments	5	3
Intergrain volume	18.9	21.7
Matrix	1.7	0.3
Macroporosity	11.9	7.9
Microporosity	2.8	0.6
Total cement	4.7	12.2
Quartz cement	2.3	3.3
Carbonate cement	1.0	8.7
Kaolinite cement	1.4	0.2

UURI cores

	Distributary channel
Quartz	78
Feldspar	16
Rock fragments	6
Intergrain volume	16.8
Matrix	1.8
Macroporosity	9.9
Microporosity	3.2
Total cement	4.9
Quartz cement	2.3
Carbonate cement	1.3
Kaolinite cement	1.3

Data for quartz, feldspar, and rock fragments are given as volume percent of framework grains; all other data are volume percent of the total rock. Intergrain volume is the volume not occupied by detrital quartz, feldspar, or rock fragments. Microporosity is the volume occupied by leached grains and kaolinite.

sandstones, pseudomatrix is more abundant in the distributary-channel facies than in transgressive and delta-front sandstones; GS 4 sandstones have the highest mean percent of pseudomatrix (table 3). Macroporosity is highest in distributary-channel and transgressive and delta-front sandstones (mean values of 11.9 percent and 11.0 percent, respectively), approximately twice the porosity of GS 4 sandstones (mean value of 6.6 percent; table 3). Cement volume varies from a low of 7.1 percent in distributary-channel sandstones to 11.1 percent in GS 4; transgressive and delta-front sandstones have a mean value of 10.5 percent cement. Quartz overgrowths, pore-filling and grain-replacing carbonate, and kaolinite are the predominant authigenic phases. Distributary-channel sandstones have approximately equal amounts of authigenic quartz and kaolinite. Transgressive and delta-front sandstones have mostly quartz and carbonate cement, whereas GS 4 sandstones contain abundant kaolinite. Among GS 5 sandstones, microporosity is greatest in distributary channels (mean 6.4 percent), reflecting both the amount of kaolinite cement and the volume of partially leached grains (table 3).

Ferron Sandstones from UURI Cores

Sandstone Types

The University of Utah Research Institute (UURI) cored two boreholes through the Ferron Sandstone approximately one-half mile east (landward) of Muddy Creek canyon. We sampled the distributary-channel facies of Ferron GS 5 in both cores to evaluate the effects of outcrop weathering on sandstone composition and petrophysical properties. Because of the proximity of core locations and Muddy Creek outcrop, substantial compositional differences between outcrop and core are unlikely. However, because the core samples are saturated with ground water and outcrop samples are exposed to weathering, compositional differences caused by surficial exposure are possible, even under the arid conditions of central Utah.

Distributary-channel sandstones from the UURI core are subarkoses with a minor amount of arkoses (fig. 7). The mean Q:F:R composition is 78:16:6 (table 3). The composition of distributary-

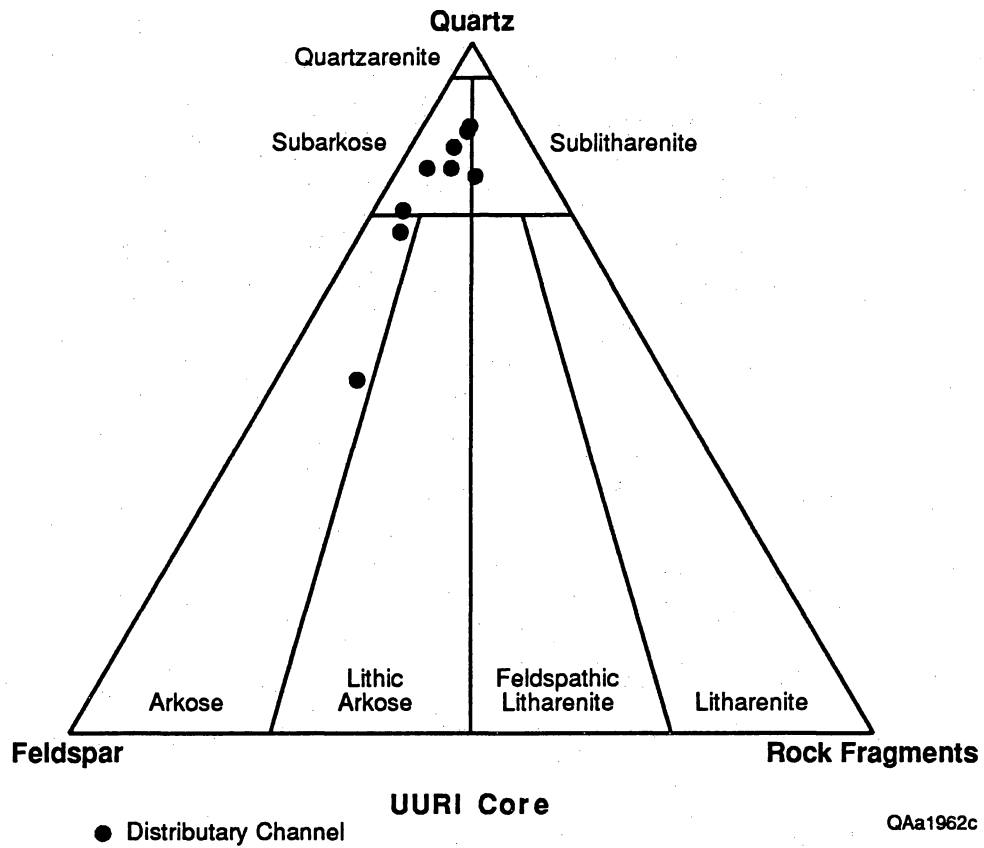


Figure 7. Framework grain composition of sandstones from UURI core (classification of Folk, 1974).

channel sandstones from the UURI cores falls within the range of compositions observed from distributary-channel sandstones at Muddy Creek. We did not find lithic arkose or sublitharenite sandstones in the UURI cores, but we did observe these rock-fragment-rich sandstones at Muddy Creek. We believe that the differences in sandstone composition between Muddy Creek outcrops and the UURI core samples simply reflect the fact that not all distributary-channel macroforms are represented in the core.

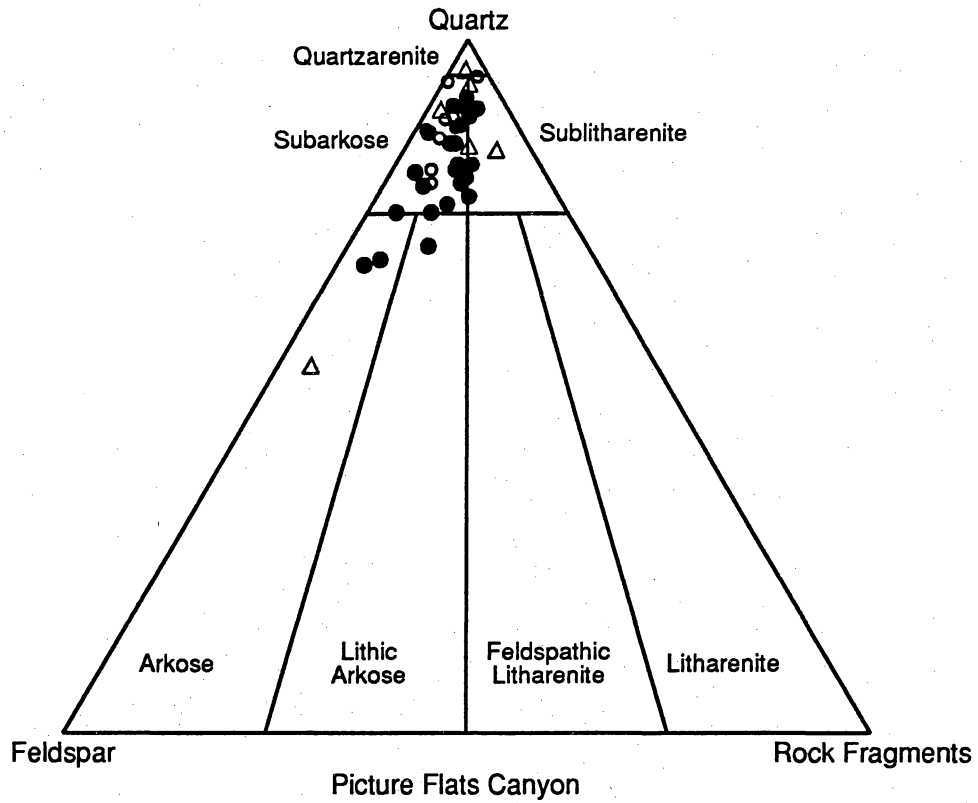
Intergranular Composition

The intergranular volume of distributary-channel sandstones from the UURI cores averages 16.8 percent, significantly lower than that of Muddy Creek distributary-channel samples (23.5 percent; table 3). Pseudomatrix content is also lower in the UURI cores, as are macroporosity and microporosity (table 3). Total cement volume is 4.9 percent of the whole rock, with quartz cement slightly more abundant than carbonate or kaolinite.

Ferron Sandstones at Picture Flats

Sandstone Types

Picture Flats canyon exposes the delta complex sandstones near the center of the facies tract. Both distributary-channel and shoreface (transgressive and delta-front) sandstones exposed at Picture Flats are predominantly subarkoses (fig. 8). However, as at Muddy Creek (table 3), shoreface sandstones contain more quartz (mean Q:F:R of 89:8:3) than the distributary-channel sandstones (mean Q:F:R of 82:12:6). In both distributary-channel and shoreface sandstones, feldspars are approximately twice as abundant as rock fragments.



- Distributary Channel
- Transgressive and Delta Front
- △ GS 4

QAa1961c

Figure 8. Framework grain composition of sandstones from Picture Flats (classification of Folk, 1974).

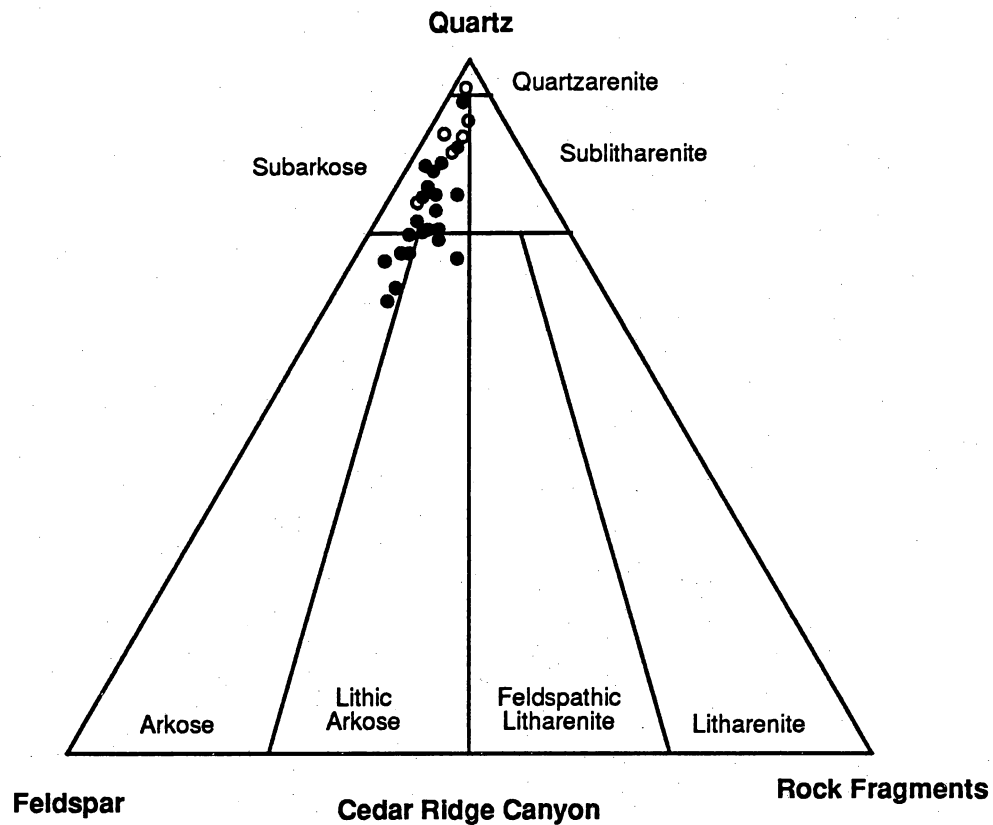
Intergranular Composition

Intergranular volume averages 21.0 percent in distributary-channel sandstones and 24.1 percent in shoreface sandstones. Pseudomatrix is only a minor component of the rocks, averaging 1.0 percent in distributary-channel sandstones and 0.3 percent in shoreface sandstones. Macroporosity is slightly higher in distributary-channel sandstones than in shoreface sandstones (13.0 percent versus 9.9 percent); microporosity is substantially higher in distributary-channel sandstones (3.1 percent versus 0.9 percent), reflecting the greater abundance of both kaolinite cement and leached grains in distributary-channel sandstones. Total cement volume in shoreface sandstones is approximately twice that of distributary-channel sandstones (12.2 percent and 6.2 percent, respectively [table 3]). Authigenic quartz and carbonate are present in subequal amounts in shoreface sandstones, whereas quartz cement is the most abundant authigenic material in distributary-channel sandstones. Kaolinite cement occurs only in trace amounts regardless of sandstone facies.

Ferron Sandstones at Cedar Ridge

Sandstone Types

Cedar Ridge canyon provides exposures of the most seaward extent of the Ferron GS 5 delta complex. Distributary-channel sandstones here are predominantly subarkoses with minor amounts of arkoses and lithic arkoses (fig. 9). Feldspars are approximately three times as abundant as rock fragments. The mean Q:F:R composition of Cedar Ridge distributary-channel sandstones is 78:17:5 (table 3). Shoreface sandstones are mostly quartz-rich subarkoses with a minor amount of quartzarenites. The mean Q:F:R composition of Cedar Ridge shoreface sandstones is 89:8:3.



Explanation

- Distributary Channel
- Shoreface

QAa1960c

Figure 9. Framework grain composition of sandstones from Cedar Ridge (classification of Folk, 1974).

Intergranular Composition

Intergranular volume averages 18.9 percent and 21.7 percent for distributary-channel and shoreface sandstones, respectively. Pseudomatrix content is low (1.7 percent and 0.3 percent for distributary-channel and shoreface sandstones, respectively). Macroporosity is higher in distributary-channel sandstones than in shoreface sandstones (11.9 percent versus 7.9 percent, respectively), whereas microporosity is generally low (2.8 percent in distributary-channel sandstones versus 0.6 percent in shoreface sandstones). Total cement content is significantly higher in shoreface sandstones (12.2 percent versus 4.7 percent in distributary-channel sandstones). Authigenic quartz, carbonate, and kaolinite are present in approximately equal, low amounts in distributary-channel sandstones. In shoreface sandstones, carbonate dominates the volume of authigenic material (table 3).

Sandstone Texture and Petrophysical Properties

Tables 4, 5, and 6 present sample descriptions, results of grain-size analyses, and petrophysical data, respectively. Relations between petrophysical parameters and textural and petrographic data and the implications for translating outcrop properties to reservoir conditions are reported separately (Miller and others, in preparation).

PERMEABILITY CHARACTERISTICS OF LITHOFACIES AND FACIES

We measured permeability directly on the outcrop and collected data for statistical analysis and for determining permeability population and spatial characteristics of lithofacies (stratal types) and facies. More than 10,000 outcrop permeability values have been obtained from GS 5; these include measurements on more than 75 vertical and horizontal transects and several sample grids. By comparing stratal architecture with permeability values, we evaluated the influence of depositional processes on sandstone heterogeneity and the factors that control permeability

Table 4. Descriptions of samples collected for petrophysical property measurements.

ESEL#	GS	Location	Facies	Characteristics	
1	6	5	Muddy Creek	Transgressive	Highly bioturbated
2	1	5	Muddy Creek	Distributary channel	Top of contorted zone
2	2	5	Muddy Creek	Distributary channel	Horizontally laminated
2	3	5	Muddy Creek	Distributary channel	Base of channel, trough crossbedded
2	4	5	Muddy Creek	Delta front	Top of delta front
2	5	5	Muddy Creek	Distributary channel	Planar crossbedded
2	6	4	Muddy Creek	Channel	Top of channel
2	7	4	Muddy Creek	Channel	Base of channel
2	8	4	Muddy Creek	Channel	Indistinct bedding
2	9	5	Muddy Creek	Distributary channel	Base of channel
2	10	4	Muddy Creek	Channel	Top of channel
2	11	5	Muddy Creek	Distributary channel	Upper channel, planar crossbedded
2	12	5	Muddy Creek	Distributary channel	Small-scale trough crossbedded, lateral accretion point-bar deposit
2	13	5	Muddy Creek	Distributary channel	Lower channel, lateral accretion deposit
3	1	5	Picture Flats	Levee deposit	Horizontally laminated
3	2	5	Picture Flats	Delta front	Base of deposit
3	3	5	Picture Flats	Delta front	Top of delta front
3	4	5	Picture Flats	Distributary channel	Massive bedding
3	5	5	Picture Flats	Distributary channel	Top of channel, horizontally bedded
3	6	5	Picture Flats	Distributary channel	Base of channel, mud-clast-rich
3	7	5	Picture Flats	Distributary channel	Small-scale trough crossbedded, lateral accretion deposit
3	8	5	Picture Flats	Distributary channel	Levee/crevasse splay deposit
3	9	5	Picture Flats	Distributary channel	Mouth-bar deposit
4	2	5	Muddy Creek	Distributary channel	Base of channel, ripple-laminated
5	1	5	Picture Flats	Distributary channel	Fine-grained, abundant mud chips
5	2	5	Cedar Ridge	Delta front	Fine-grained, well-sorted, swaley/hummocky bedding
5	3	5	Picture Flats	Washover	Fine-grained, trough crossbedded, bioturbated
5	4	5	Picture Flats	Washover	Medium- to coarse-grained, trough crossbedded, bioturbated
5	5	5	Picture Flats	Delta front	Very fine to fine-grained, highly bioturbated, near landward pinch-out
5	6	5	Picture Flats	Washover	Fine-grained, bioturbated, horizontal bedding
5	7	5	Picture Flats	Delta front	Fine-grained, swaley/hummocky bedding
5	8	5	Picture Flats	Washover	Fine-grained, horizontal bedding
5	9	5	Picture Flats	Distributary channel	Fine- to medium-grained, trough crossbedded

Table 4 (cont.)

ESEL#	GS	Location	Facies	Characteristics
5 10	5	Picture Flats	Distributary channel	Very coarse grained, trough crossbedded
5 11	5	Picture Flats	Distributary channel	Contact between distributary channel and delta front
5 12	5	Picture Flats	Distributary channel	Very fine grained, ripple-laminated levee deposit
5 13	5	Picture Flats	Distributary channel	Fine- to medium-grained, trough crossbedded
5 14	5	Picture Flats	Distributary channel	Fine- to medium-grained, trough crossbedded
5 15	5	Picture Flats	Distributary channel	Fine- to medium-grained, trough crossbedded
5 16	2	I-70	Mouth bar	Fine- to medium-grained, well-sorted, trough crossbedded
5 17	2	I-70	Distal mouth bar	Fine-grained, bioturbated
5 18	2	I-70	Delta front	Very fine to fine-grained, bioturbated
5 19	2	I-70	Distal mouth bar	Fine-grained, stacked ripples
5 20	2	I-70	Delta front	Very fine grained, bioturbated
5 21	2	I-70	Lower delta front	Very fine grained, hummocky bedding, interbedded sandstone and shale
6 1	5	UURI-1	Distributary channel	Fine- to medium-grained, trough crossbedded
6 2	5	UURI-2	Distributary channel	Medium-grained, trough crossbedded, horizontal specimen
6 3	5	UURI-2	Distributary channel	Fine-grained, ripple crossbedded
6 4	5	UURI-1	Distributary channel	Trough crossbedded, organic laminae, horizontal specimen
6 5	2	UURI-1	Mouth bar	Very fine grained, parallel bedding, shale laminae
6 6	2	UURI-2	Distal mouth bar	Mud clasts
6 7	5	UURI-2	Distributary channel	Medium-grained, trough crossbedded, vertical specimen
6 8	5	UURI-1	Distributary channel	Trough crossbedded, organic laminae, vertical specimen
6 9	5	UURI-1	Distributary channel	Fine-grained, trough/horizontal bedded, organic laminae
6 10	5	UURI-1	Distributary channel	Mud- and coal-clast lag deposit
6 11	5	UURI-2	Distributary channel	Mud- and coal-clast lag deposit
6 12	2	UURI-2	Mouth bar	Fine-grained, massive, rooted
6 13	2	UURI-1	Mouth bar	Fine-grained, shale laminae
6 15	5	UURI-2	Distributary channel	Medium- to coarse-grained, massive
6 16	2	UURI-1	Mouth bar	Medium-grained, planar/trough crossbedded, well sorted
6-17	2	UURI-1	Mouth bar	Medium-grained, trough crossbedded, well sorted
6-18	5	UURI-1	Distributary channel	Medium-coarse grained, massive
6-19	5	UURI-1	Distributary channel	Trough crossbedded, organic laminae, horizontal bedded
6-20	2	UURI-2	Mouth bar	Medium-grained, trough crossbedded
6-21	2	UURI-1	Mouth bar	Massive sandstone with rooted
6-22	2	UURI-2	Mouth bar	Medium-grained, trough crossbedded, rooted

ESEL#: Earth Science and Engineering Laboratory Identification, consisting of set and block number.

GS: Genetic sequence number.

Table 5. Results of grain-size distribution analysis of sandstone blocks collected for petrophysical measurements.

Sample	% Sand	% Silt	% Clay	Mean	Sorting	Skewness	Kurtosis
2-1	85	11	4	2.68	0.47	0.03	0.83
2-2	82	16	2	2.78	0.44	-0.24	0.92
2-3	86	10	4	2.27	0.38	0.46	1.07
2-4	90	8	2	2.96	0.30	0.03	1.23
2-5	81	14	5	2.49	0.26	0.09	1.16
2-6	84	14	2	2.19	0.36	0.22	1.16
2-7	90	7	3	-0.29	0.53	0.03	1.09
2-8	78	15	7	2.03	0.42	0.04	1.38
2-9	85	13	2	1.18	0.47	-0.01	0.97
2-10	75	21	4	2.51	0.36	0.00	0.91
2-11	84	13	3	1.52	0.47	0.01	1.02
2-12	84	11	5	2.40	0.33	0.10	1.00
2-13	90	8	2	1.64	0.42	0.00	0.94
3-1	77	16	7	2.65	0.34	0.00	1.18
3-2	95	4	1	1.76	0.34	-0.08	1.32
3-3	84	14	2	3.28	0.19	0.13	0.95
3-4	87	7	6	1.20	0.46	-0.07	0.98
3-5	87	8	5	2.99	0.21	-0.04	1.33
3-6	90	8	2	2.56	0.39	-0.10	1.07
3-7	90	7	3	2.82	0.23	-0.13	1.32
3-8	84	14	2	3.01	0.26	0.13	1.22
3-9	92	6	2	1.61	0.47	-0.09	0.98
5-2	88	7	5	2.96	0.23	-0.08	1.24
5-5	88	9	3	2.57	0.42	-0.05	0.95
5-6	90	7	3	2.95	0.38	-0.09	1.23
5-7	90	6	4	2.28	0.44	0.09	0.98
5-8	90	5	5	2.62	0.39	-0.14	1.22
5-9	90	9	1	1.90	0.48	0.05	1.26
5-12	89	9	2	2.89	0.28	-0.15	1.21
5-13	90	4	6	2.10	0.61	0.43	0.66
5-14	90	6	4	0.77	1.16	-0.52	1.21
5-15	86	8	6	1.74	0.62	-0.40	1.47
5-16	90	6	4	2.05	0.58	0.38	1.20
5-18	90	6	4	3.05	0.42	-0.20	1.50
5-19	82	10	8	2.56	0.39	0.06	1.23
5-21	67	25	8	3.91	0.34	0.15	1.09
6-1	78	16	7	2.56	0.63	-0.24	0.97
6-2	91	7	3	1.71	0.44	0.05	1.43
6-3	90	6	4	2.56	0.56	-0.14	0.88
6-4	77	18	5	2.69	0.61	-0.02	0.99
6-7	86	11	3	2.83	0.53	-0.40	1.54
6-8	71	20	9	2.35	0.75	-0.08	0.94
6-9	79	13	8	2.56	0.69	-0.21	0.91
6-10	82	11	7	1.78	0.61	-0.04	1.32
6-11	83	10	7	2.41	0.39	-0.44	1.32
6-12	78	16	6	3.89	0.58	-0.01	1.08
6-15a	87	7	6	1.68	0.45	-0.10	0.50
6-15b	86	10	4	1.38	0.60	-0.12	1.07
6-16a	78	13	9	1.97	0.63	-0.15	1.05
6-16b	82	13	5	2.12	0.49	-0.10	0.96
6-17	82	11	7	1.74	0.48	0.12	1.06
6-18	84	12	4	2.29	0.62	0.04	0.95
6-20a	88	9	3	2.13	0.38	0.26	1.35
6-20b	85	14	1	1.77	0.50	0.13	1.24
6-21a	75	14	11	1.99	0.41	0.04	1.08
6-21b	79	15	6	2.30	0.66	0.05	1.02
6-22a	81	15	4	2.23	0.42	0.03	1.16
6-22b	81	17	2	1.70	-0.53	1.08	-0.17

Percent sand, silt, and clay were determined from sieve and pipette analyses. Mean, standard deviation, skewness, and kurtosis values are graphic moments (Folk, 1974). Sets of samples labeled a and b are repeat sand-size distribution analyses using different subsamples of the disaggregated sandstone. Comparisons show that moments are generally reproducible to within 0.1 phi unit.

Table 6. Results of ESEL petrophysical analyses.

ESEL no.	Porosity %	Kg (lab) md	Kg (mp) md	Kw md	Form. fac.	Sat. exp.	Swi %	Sgr %	Kgr @ Swi	Kwr @ Sgr
1-06	12.5	20.4	155.4	4.5	29.3	1.3	44	14	0.54	0.20
2-01	17.3	0.8		0.5	13.5	2.3	46	40	0.33	0.07
2-02	13.0	1.9	5.6	0.8	19.5	1.5	39	22	0.49	0.05
2-03	16.0	11.2		3.8	20.9	1.5	56	30	0.32	0.10
2-04 ^a	17 ^d	43.7								
2-05	21.0	115.0		43.0	11.1	2.0	55	5	0.45	0.45
2-06	15.1	1.5	11.5	0.9	15.8	1.5	39	26	0.38	0.05
2-07 ^b										
2-08	15.0	2.3	11.3	1.1	18.8	1.7	45	15	0.52	0.06
2-09	18.1	79.0		47.0	16.3	1.5	47	30	0.19	0.12
2-10 ^c	9 ^d	720 ^e								
2-11	17.7	16.0		8.0	15.1	2.0	50	20	0.70	0.13
2-12	16.0	12.8	53.2	5.3	14.1	1.5	60	10	0.99	0.03
2-13	18.0	68.0		31.1	16.2	1.5	54	23	0.17	0.15
3-1A	12.7	7.3	26	3.5	25.6	1.8	45	18	0.69	0.11
3-1B	14.0	0.1	18	0.0	35.5	1.2	31	25	0.23	0.14
3-02	12.5	0.1	0.2	0.1	20.7	2.0	35	11	0.49	0.10
3-03	17.6	35.8	92.1	31.4	15.6	1.6	36	29	0.30	0.02
3-04	15.4	16.0		10.2	11.6	3.0	58	20	0.28	0.05
3-05	16.3	69.3	121	33.9	15.8	1.6	44	30	0.47	0.05
3-06	18.0	85.0	261.2	22.0	19.9	2.8	55	11	0.76	0.54
3-07	18.0	217.0	275	54.0	13.4	1.8	45	21	0.40	0.10
3-08	14.3	42.4		34.1	18.4	1.5	41	13	0.38	0.08
3-09	16.8	153.0	474.1	87.9	13.0	2.5	52	26	0.73	0.15
4-01 ^a	17 ^d									
4-2A	16.0	12.3		3.5	14.2	1.7	49	10	0.90	0.07
4-2B	16.0	0.4		0.1	19.4	1.1	24	29	0.55	0.16

Note: a = failed test; b = core loss, no test; c = test terminated, low permeability; d = estimated from bulk specimen weight; e = value in nanodarcys

Table 6 (cont.)

ESEL no.	Porosity %	Kg (lab) md	Kg (mp) md	Kw md	Form. fac.	Sat. exp.	Swi %	Sgr %	Kgr @ Swi	Kwr @ Sgr
5-01	17.8	18.1	36.2	8.9	19.7	2.8	65	8	0.43	0.17
5-02	19.8	49.4	203.8	30.3	11.2	1.6	49	23	0.38	0.06
5-03 ^a	24 ^d		404.9							
5-04	12.9	16.8	416.3	5.1	47.3	1.5	57	8	0.41	0.06
5-05	15.8	49.1	103.6	30.6	15.0	2.0	45	18	0.44	0.09
5-06	16.2	58.2	229.0	33.8	16.6	1.9	49	13	0.65	0.27
5-07	16.1	76.4	239.7	32.0	13.5	1.8	47	6	0.63	0.12
5-08	18.3	105.0	178.6	43.8	11.9	1.3	40	31	0.59	0.05
5-09	19.2	259.6	439.5	176.6	13.0	2.0	57	8	0.65	0.25
5-10 ^a	17 ^d		152.2							
5-11 ^c	14 ^d	2.1 ^e	184.4							
5-12	14.9	20.7	47.3	13.5	18.0	1.6	54	15	0.33	0.09
5-13	16.6	56.2	91.5	33.8	15.2	2.1	63		0.43	
5-14	18.0	286.6	477.3	116.8	14.3	2.3	60	8	0.45	0.14
5-15	21.0	181.8	344.5	36.0	13.0	1.4	45	7	0.33	0.09
6-01	17.1	6.2	7.1	3.2	16.1	1.6	51.5	10	0.42	0.21
6-02	17.9	198.3	331.6	113.0	12.3	1.8	48	17	0.62	0.18
6-03	16.3	125.4		55.7	11.2	2.8	57	12	0.51	0.35
6-04	15.0	5.8		2.0	18.6	1.6	54	12	0.7	0.2
6-07	16.1	24.6	140.7	12.9	18.9	1.6	35	8	0.44	0.51
6-08	14.6	0.2	13.7	0.1	29.0	1.0	29	22	0.2	0.1
6-09	13.9	0.06	30.7	0.01	25.2	1	27	11	0.3	0.12
6-10	14.9	2.4	36.3	0.7	21.6	1.8	55	18	0.86	0.23
6-11	15.8	0.8	87.5	0.3	36.1	1.1	24.5	27	0.35	0.09
6-14 ^c	15 ^d	550 ^e	12.4							
6-15	16.8	58.5	474.3	17.1	14.4	1.5	52	20	0.23	0.16
6-18	13.3	36.5	63.0	17.3	21.1	1.7	36	27	0.58	0.1
6-19 ^a	18 ^d		21.7							
6-23 ^b	15 ^d		115.7							

Note: a = failed test; b = core loss, no test; c = test terminated, low permeability; d = estimated from bulk specimen weight; e = value in nanodarcys

variation. In the following discussions, we use the central tendency, variance, and distribution type to characterize the relationship of permeability to facies and lithofacies, and to describe scale dependence. The spatial correlation of permeability within lithofacies was estimated by semivariogram analysis.

Factors Controlling Mean Permeability

Because different sedimentary processes operate in different depositional environments, we first examined permeability variation at the facies scale. Comparing log permeability with cumulative percent for distributary-channel and delta-front sandstones shows mean permeability of the distributary-channel sandstones to be nearly an order of magnitude higher than that of delta-front sandstones (fig. 10). Variation is nearly four orders of magnitude in both facies. However, the range of permeability in the distributary-channel sandstones is slightly greater than in delta-front sandstones. The lower limit of permeability in both facies is less than the detection limit of our field minipermeameter (~ 0.1 md); the upper limit of permeability is much higher in distributary-channel sandstones (fig. 10).

To examine the relationship of permeability to lithofacies, permeability measurements for the distributary-channel and delta-front sandstones were subdivided according to lithofacies. Within the distributary channel, four lithofacies-related permeability groups exist (fig. 11). Trough cross-stratified sandstones have an average permeability of 500 md. Sandstones having low-angle stratification have intermediate permeabilities, averaging 100 md. Ripple-stratified sandstones and lag deposits average 55 and 44 md, respectively. Contorted sandstones have intermediate but variable permeability. Permeability variation in the contorted strata is closely related to the original bedding of the sediment: higher when the original sand deposits were trough cross-stratified and lower when the original deposits were ripple stratified. Permeability in mudstones and siltstones is very low, averaging less than 0.1 md.

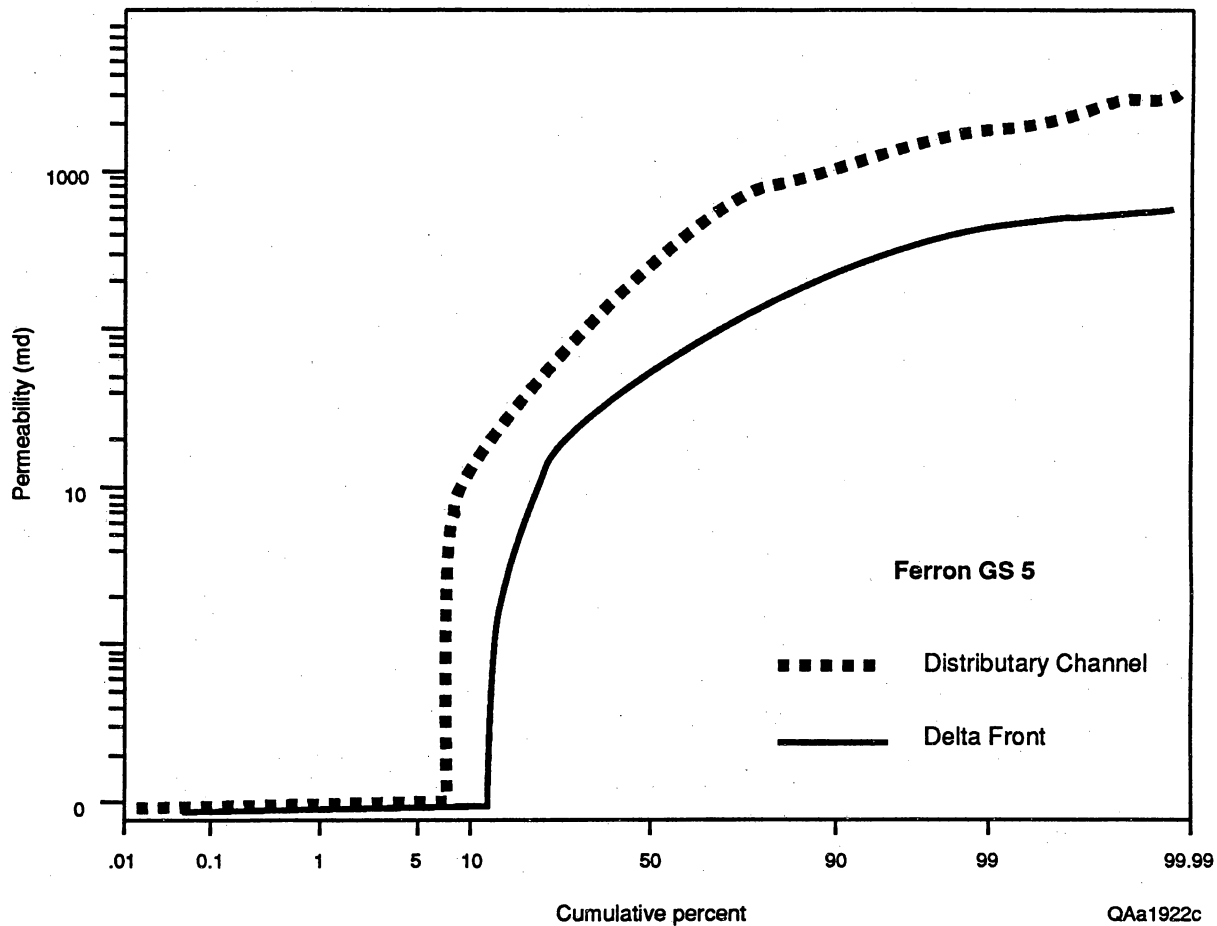
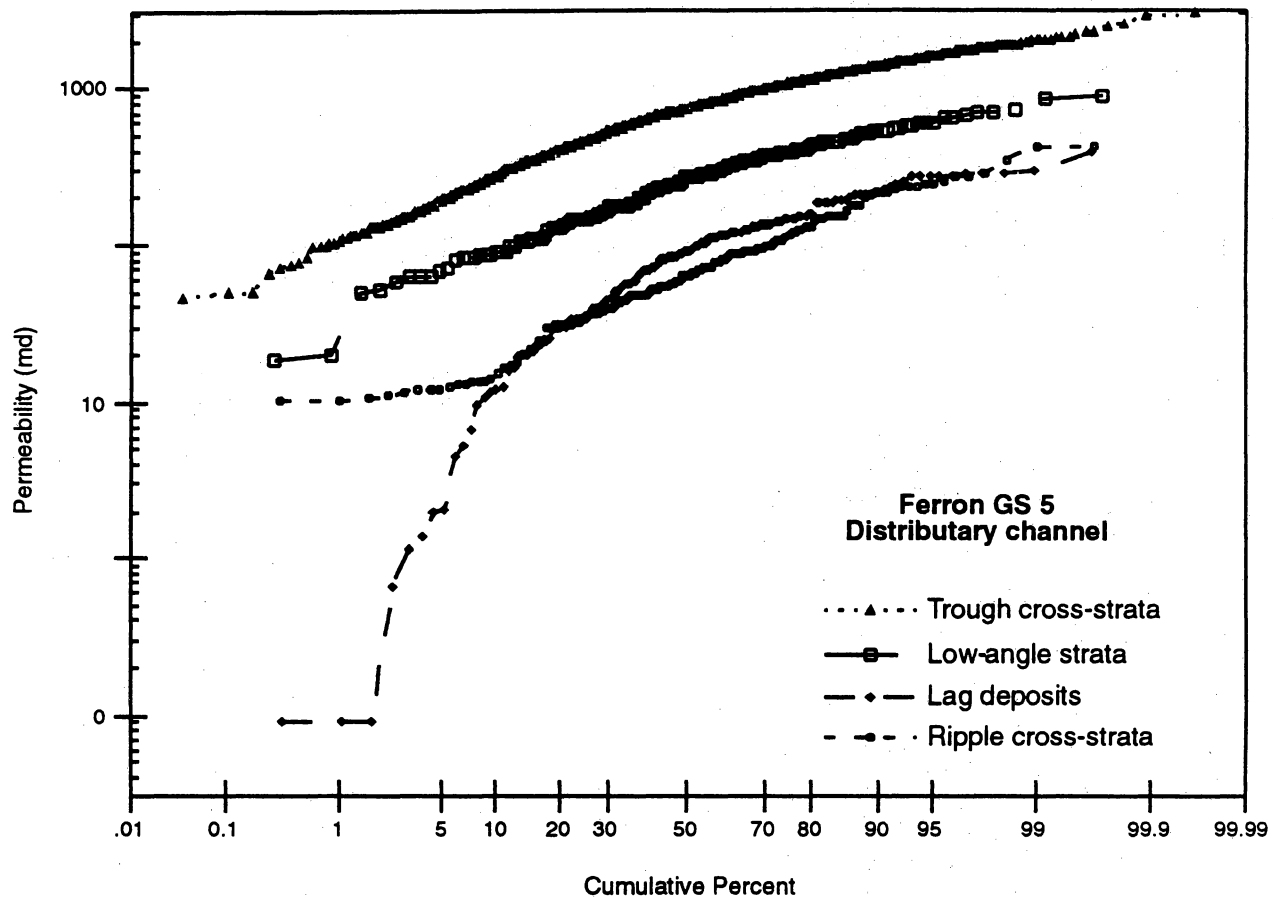


Figure 10. Cumulative percent plot of permeability comparing distributary-channel and delta-front deposits. Data from a log normally distributed population would plot as a straight line in these coordinates.



QAa1923c

Figure 11. Cumulative percent plot of permeability comparing lithofacies types from distributary-channel facies.

We attribute the observed relation between permeability and lithofacies to both textural and compositional factors. For example, comparing stratal types shows a predictable increase in permeability with increasing grain size. Very fine to fine-grained ripple-stratified sandstones have the lowest permeabilities, fine- to medium-grained low-angle stratification sandstones have intermediate permeabilities, and medium-fine to coarse-grained trough cross-stratified sandstones have the highest permeabilities. However, comparing stratal types of equivalent grain size (that is, fine-grained ripple-stratified sandstones with fine-grained trough cross-stratified sandstones) indicates differences in permeability between the two sets are not significant; fine-grained ripple deposits and fine-grained trough cross-strata have similar permeabilities. Likewise, comparing permeability with grain size for a single facies shows permeability increases through medium-grained sandstone (fig. 12). However, as grain size increases beyond coarse sand size (0 phi), average permeability decreases slightly. Comparing samples of similar grain size indicates that this trend is partly attributable to the effects of decreasing sorting with increasing grain size beyond medium-coarse sand. Additionally, lag deposits have an average permeability that is much lower than would be predicted from grain size alone. SEM examination indicates that decreased permeability is related to the presence of clay clasts that have been distorted into pseudomatrix during burial and compaction, a process that drastically reduces porosity and permeability in these sediments.

Permeability characteristics closely reflect grain size and sorting trends within delta-front deposits as well (fig. 13). Swaley-stratified sandstones comprise the coarsest and best sorted sediments and have the highest permeabilities, averaging 260 md. Finer grained hummocky and ripple cross-stratified sandstones have intermediate permeabilities, averaging 110 md and 30 md, respectively. Poorly sorted, intensely bioturbated sandstones have the lowest permeabilities, averaging 14 md.

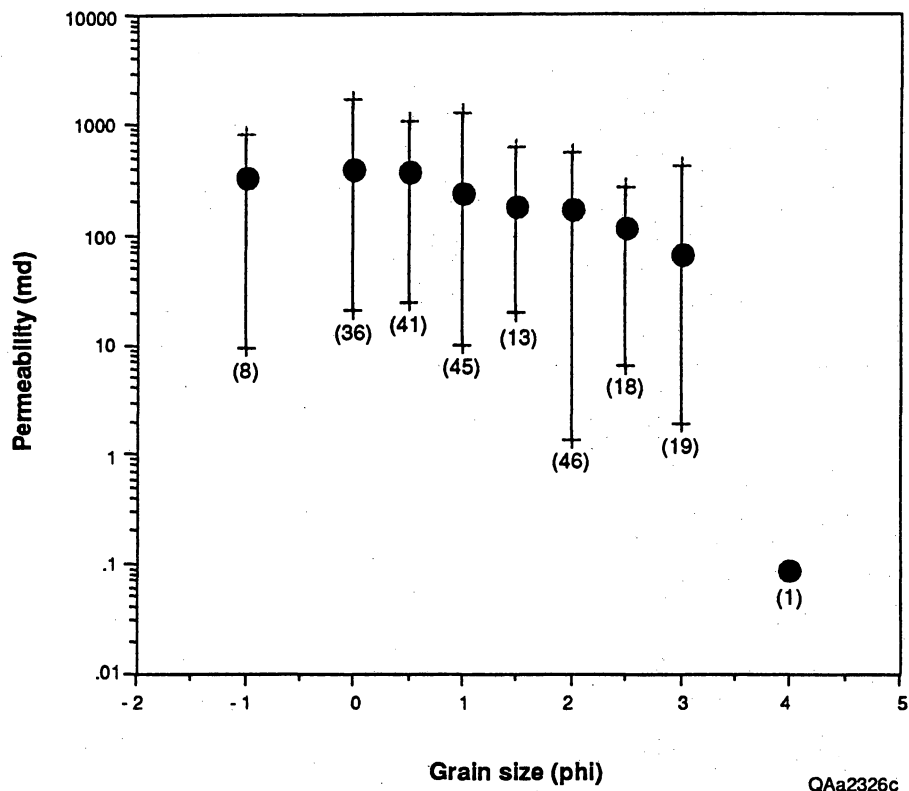
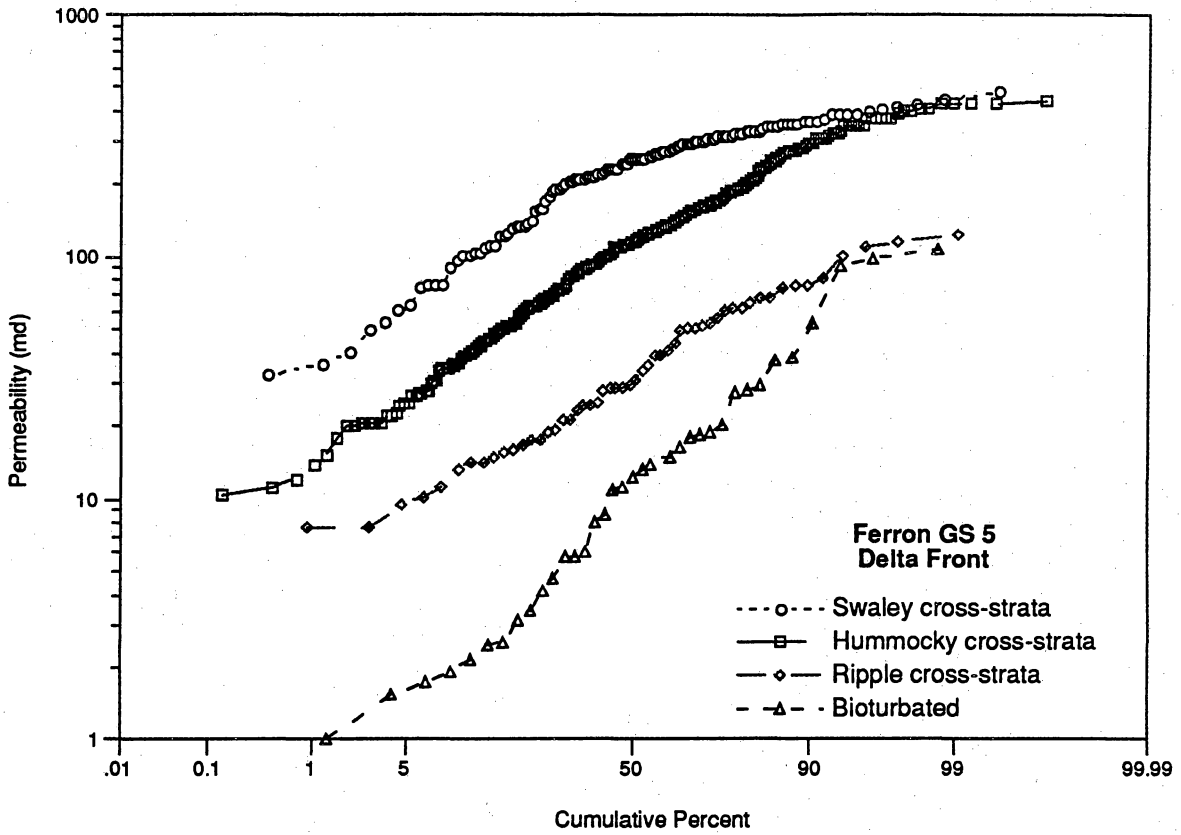


Figure 12. Plot of permeability versus grain size for the distributary-channel facies showing mean permeability, range, and number of analyses for each grain size.



QAa1924c

Figure 13. Cumulative percent plot of permeability comparing stratal types from delta-front deposits.

Geologic Controls on Permeability Variation

We next examined geologic controls on permeability by separating permeability values according to facies, lithofacies, and bedsets. At the facies scale, permeability within the distributary-channel sandstones displays a high degree of variation, spanning more than four orders of magnitude. Variation within individual lithofacies is much less, however, spanning one to three orders of magnitude. Permeability within individual stratal types is highly dependent on grain size variation. For example, ripple-stratified and trough cross-stratified sandstones show a higher degree of grain size variation than low-angle stratified sandstones. Predictably, ripple and trough cross-stratified sandstones, which span two orders of magnitude, also display a higher degree of permeability variation than low-angle stratified sandstones, which have a variation of one order of magnitude. Additional factors such as mineralogical composition also influence permeability variability. For example, permeability within bounding lithologies ranges over three orders of magnitude, from less than 0.1 md to greater than 200 md. This is an exceptionally high degree of variation, particularly because there is no significant difference in grain size between bounding lithologies and other lithofacies. The greater permeability variation in bounding elements is attributed to variation in both grain size and amount of ductile grains, as opposed to only grain size in other strata; bounding strata contain more ductile clay clasts that occlude porosity and reduce permeability.

At the smallest scale, variation within and between individual bedding sets that compose different stratal types was investigated. Within the trough cross-strata, variation in average permeability among bedding sets is approximately one order of magnitude (less than 100 md to 1,000 md). Likewise, permeability variation within a single bed set is also approximately one order of magnitude. These two components combine to explain the total variation observed within the trough cross-stratified lithofacies.

These results show that permeability variation is scale dependent and hierarchical. Permeability variation decreases as we subdivide sample sets into fundamental geologic and

depositional units. At the smallest scale examined, permeability variation is related to variation within and between single bedding sets of strata. These components combine to explain the degree of variation observed at the lithofacies scale. Likewise, permeability at the facies level is related to variation among lithofacies and the proportion of each lithofacies within the distributary-channel facies.

Delta-front lithofacies have a more homogeneous permeability distribution than distributary-channel lithofacies, a characteristic consistent with their uniform grain size and high degree of sorting. The range of permeability values within delta-front lithofacies is slightly greater than an order of magnitude, compared to approximately two orders of magnitude for distributary-channel lithofacies. As would be expected, uniformly fine-grained, well-sorted swaley-stratified sandstones have the least amount of variance, having permeability values ranging from a high of 457 md to a low of 33 md. Conversely, very fine to fine-grained hummocky cross-stratified sandstones show the greatest amount of variation (less than 10 md to greater than 400 md).

Permeability Distribution

Permeability is typically considered to be log normally distributed. However, a plot of log permeability versus cumulative percent for the distributary-channel and delta-front sandstones (fig. 10) shows that the data are neither normally or log normally distributed. Instead, the data fit a multimodal distribution type, as indicated by protuberances in the probability plot, and are intermediate between normal and log-normal distributions. These features indicate that permeability at the facies scale is not represented by a single population but by a mixture of several distinct permeability populations.

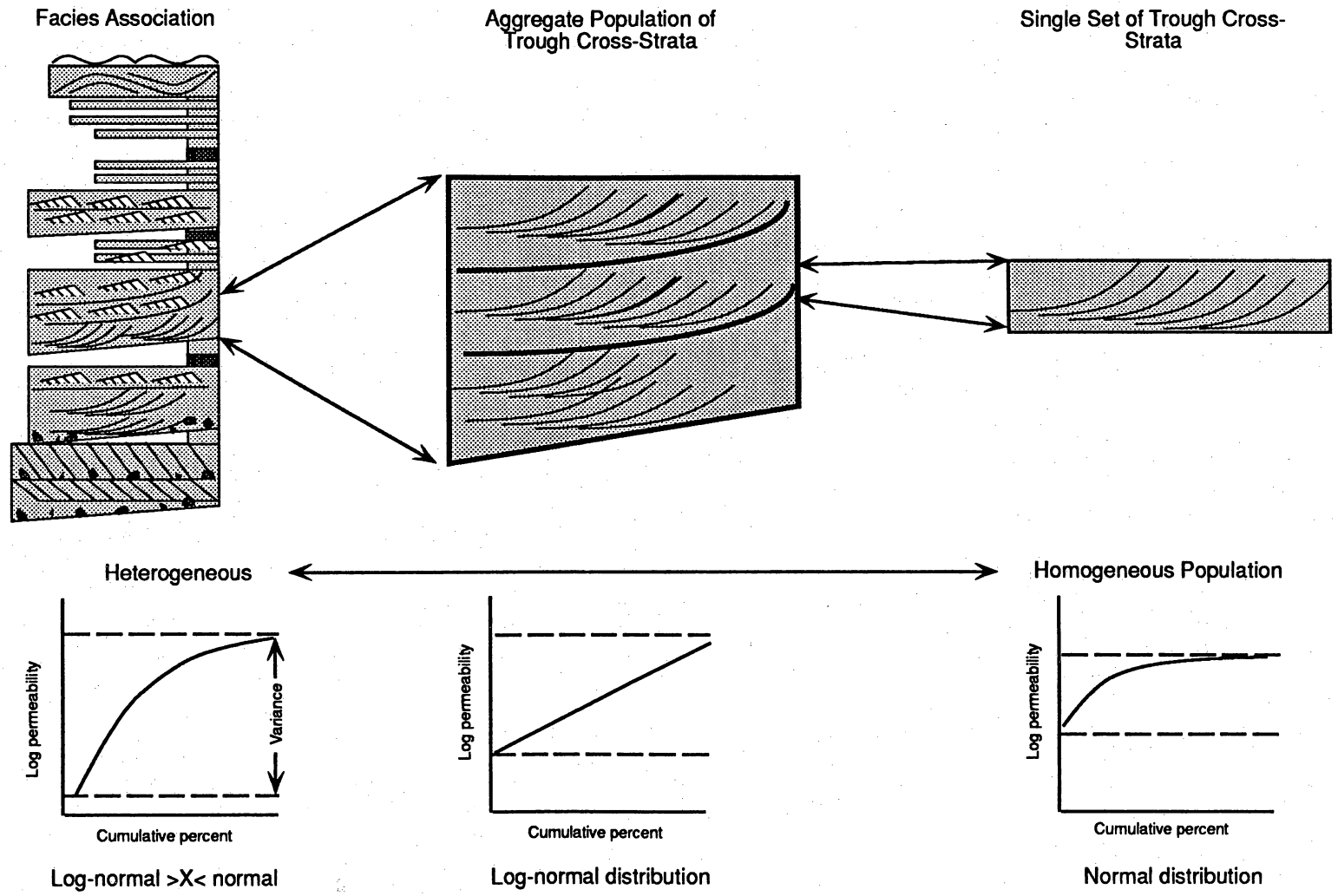
At the lithofacies scale, plots of log permeability versus cumulative percent are approximately symmetrical (figs. 11 and 13), indicating that populations consisting of individual lithofacies approach a log-normal distribution. Exceptions to this trend occur with the contorted and bounding lithologies. Contorted strata are composed of several different stratification types that

have undergone postdepositional modification. Thus, contorted strata are not a primary depositional lithofacies but are a syndepositional modification of original bedding types. Nonspatial permeability characteristics of the contorted strata closely reflect those of the original bedding type, and therefore the contorted strata reflect several different permeability groups. The permeability distribution of bounding lithologies also indicates the presence of multiple populations that reflect variations in grain size, composition, or cementation. At the smallest scale examined, permeability within single bedsets of trough cross-strata approximate a normal distribution.

Permeability distribution type is a function of scale and is arranged in a hierarchical fashion that is related to geologic scale-dependent factors. Figure 14 illustrates the scale-dependent permeability structure displayed by the different stratal elements. To understand why permeability distributions change with scale, we must examine how permeability variation is partitioned between and within lithofacies. At the facies scale, distributions are unique and not characterized by a normal or log normal distribution, but rather by an intermediate distribution type. The actual distribution varies and depends on the proportion of preserved lithofacies, the permeability contrast between lithofacies, and the variance and distribution of permeability of each lithofacies.

At the lithofacies scale permeability approximates a log-normal distribution (fig. 14). Factors that define the collective distribution are the permeability variation within bedsets and the variance and distribution of permeability between bedsets. The variance within and between bedsets is approximately one order of magnitude and is normally distributed within single sets. Given that the collection of sets is normally distributed, a combination of these attributes produces a population that is distinctly skewed to the left, approximating a log-normal distribution. These results are similar to those noted by Jensen and others (1986), who attributed the log-normal distribution of undifferentiated permeability statistics to a mixture of more than one distribution type. Aggregate populations at the scale of the distributary-channel facies tended to fit a Poisson distribution.

Delta-front lithofacies tend to have permeability distributions that approximate a log-normal distribution. Similar to distributary-channel lithofacies, this trend is scale dependent, with individual beds displaying highly uniform, normal distributions, and bedsets displaying more



QAa1925c

Figure 14. Scale-dependent permeability characteristics of stratal elements.

variable log-normal distributions. An exception to this trend is the highly uniform swaley-stratified sandstones. In this lithofacies, the distribution type more closely approximates a normal distribution.

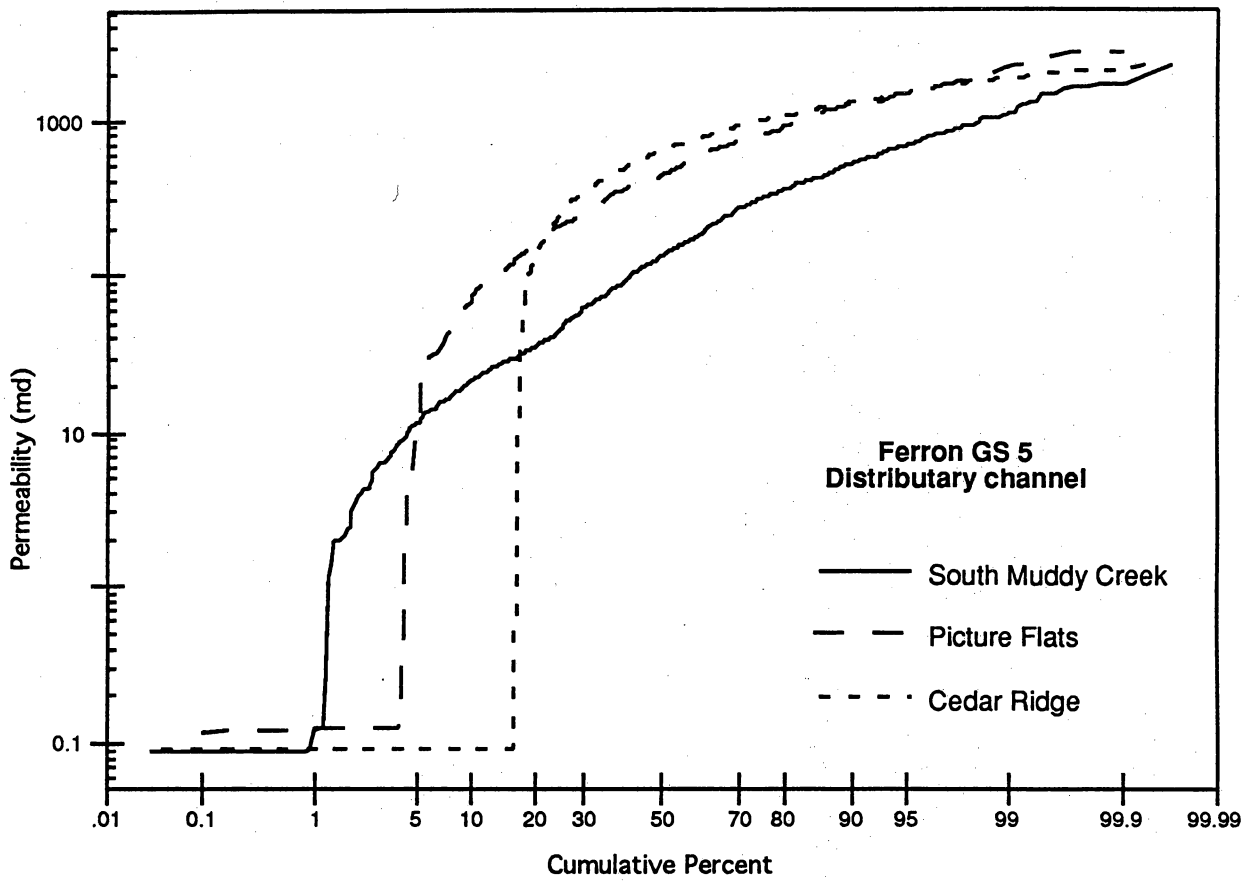
Stationarity of Permeability Measures

Having established the fundamental geologic controls on permeability mean, range, and distribution type, we now assess permeability heterogeneity at the gas-field scale. To provide outcrop-based information for constructing realistic reservoir models, we evaluated permeability characteristics from proximal to distal positions in the facies tract. We examined the stationarity (constancy of values) of permeability mean, variance, and distribution type by comparing data from South Muddy Creek (near the proximal limit of deltaic influence), Picture Flats (near the middle of the facies tract), and Cedar Ridge (at the distal limit of deltaic sandstone deposition). The degree of stationarity was assessed by t- and f-tests. These tests are statistical measures that compare the equivalency of two populations in terms of their mean and variance, respectively. The two populations are assumed to be equivalent if test results comparing their characteristics are within an accepted significance level, in this case 0.05; if test results are outside this range we reject the assumption that the two populations are equivalent. Permeability characteristics were examined at the facies and lithofacies scale, and results are summarized in table 7.

At the level of the distributary-channel facies, the mean and variance were found not to be stationary between South Muddy Creek, Picture Flats, and Cedar Ridge. Mean permeability progressively increases seaward from an average of 300 md in South Muddy Creek to 550 md in Picture Flats and to 700 md at Cedar Ridge (fig. 15). Variance progressively decreases seaward. At the lithofacies scale (figs. 16 through 18), seaward trends are similar, although less dramatic than those observed at the distributary-channel scale. Statistical comparison among equivalent lithofacies indicates permeability characteristics are significantly different at each locality (table 7). Comparing equivalent lithofacies and channel types verifies stationarity permeability characteristics between

Table 7. Permeability characteristics of stratal types.

Ferron outcrop samples				
Sample	Mean (md)	Standard deviation (md)	Distribution type	Number
Early-stage distributary channel				
Trough cross-strata	710	295	log normal	1054
Low-angle strata	263	105	log normal	49
Ripple cross-strata	32	24	log normal	36
Lag deposits	49	40	multi-normal	51
Shale/siltstone	<0.08	—	—	195
Contorted strata	502	287	log normal	20
Middle-stage distributary channel				
Trough cross-strata	430	204	log normal	384
Low-angle strata	150	78	log normal	72
Ripple cross-strata	38	27	log normal	65
Lag deposits	45	31	multi-normal	80
Shale/siltstone	<0.08	—	—	12
Contorted strata	170	87	multi-normal	55
Late-stage distributary channel				
Trough cross-strata	287	123	log normal	309
Low-angle strata	87	50	log normal	160
Ripple cross-strata	24	15	log normal	39
Lag deposits	35	21	multi-normal	25
Shale/siltstone	<0.08	—	—	3
Contorted strata	54	39	multi-normal	9
Ferron UURI core samples				
Distributary channel				
Trough cross-strata	246	98	log normal	69
Horizontal	106	65	log normal	81
Ripple cross-strata	26	31	log normal to multi-normal	18



QAa1926c

Figure 15. Cumulative percent plot of permeability for distributary-channel deposits from South Muddy Creek, Picture Flats, and Cedar Ridge.

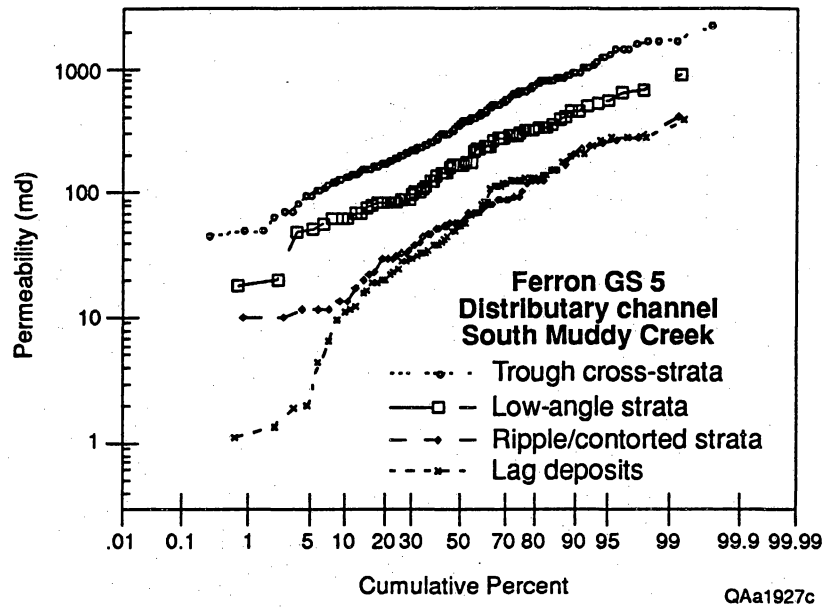


Figure 16. Cumulative probability plot of permeability for stratal types from distributary-channel facies at South Muddy Creek.

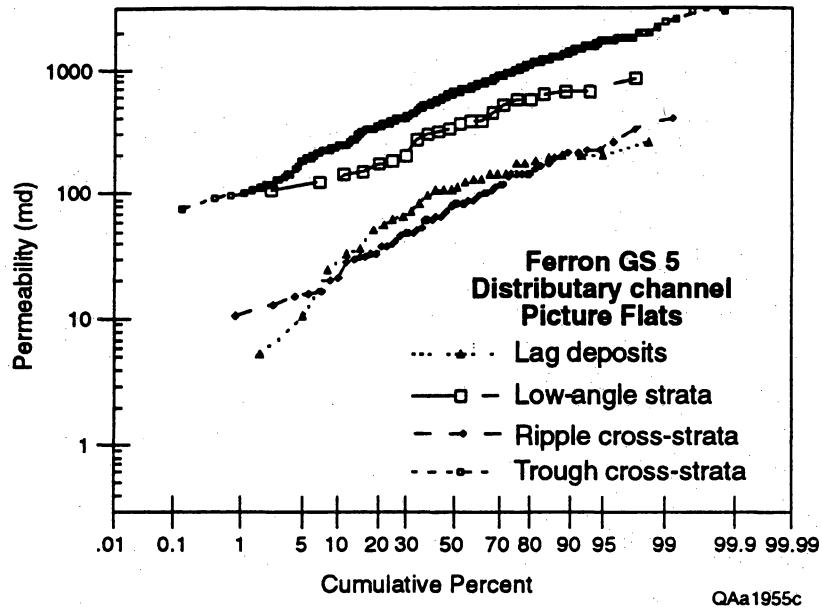
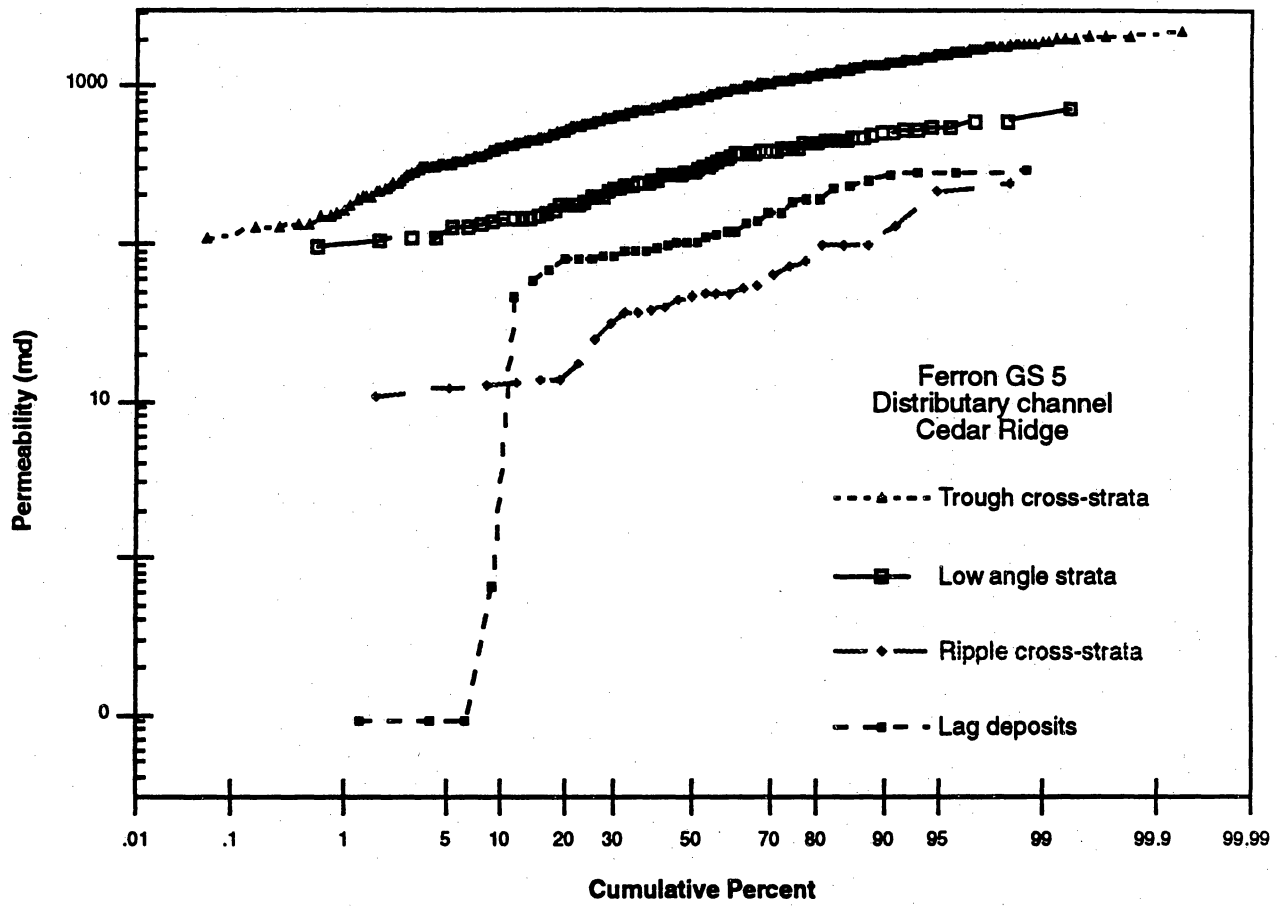


Figure 17. Cumulative probability plot of permeability comparing stratal types from distributary-channel facies at Picture Flats.



QAa1956c

Figure 18. Cumulative probability plot of permeability comparing stratal types from distributary-channel facies at Cedar Ridge Canyon.

each locality. These results demonstrate that shifts in permeability characteristics are related to shifts in the proportion of stratal types. Seaward increases in permeability are attributed to increases in the proportion of high permeability lithofacies, whereas decreases in variance are attributed to an increase in the proportion of the more homogeneous early-stage distributary-channel facies.

Stationarity of the distribution type is qualitatively assessed by examining cumulative percent plots for various permeability groups. Results are similar to trends observed for the mean and variance of permeability, with distribution type displaying much greater constancy at the lithofacies scale than at the facies scale. At the facies scale, permeability of distributary-channel deposits lies between a normal and log-normal distribution and becomes progressively less skewed seaward (fig. 15). The change in distribution type reflects a change in the proportion of lithofacies, with the trough cross-stratified and fine-grained lithofacies comprising a greater proportion of the channel fill downstream. However, the distribution type displayed by each lithofacies group approaches a log-normal distribution and remains relatively unchanged from each locality (figs. 16 through 18).

Similar analysis of delta-front sandstones indicates that constancy of permeability characteristics is greater at the lithofacies than at the facies scale. Significant changes in mean, variance, and distribution type are observed between South Muddy Creek, Picture Flats, and Cedar Ridge, with changes in permeability characteristics at the facies scale reflecting changes in the proportion of lithofacies. Delta-front deposits progressively thin and contain an increasing proportion of low-permeability lithofacies seaward. In addition, near the landward pinch-out of the delta-front facies, distributary channels selectively eroded and removed high-permeability upper delta-front sands.

In contrast to the lithofacies scale, at the facies scale, variations in permeability characteristics reflect differences in the diversity of preserved strata. At the lithofacies scale, variations in permeability characteristics are related to differences in mineralogic characteristics. The fact that permeability characteristics are more constant within lithofacies than within facies suggests that the petrographic features that determine the permeability characteristics at the lithofacies scale are relatively uniform throughout the facies tract for each stratal type. Stratal diversity, which

determines permeability characteristics of the preserved facies, varies with position in the facies tract and reflects the amount of sediment that is ultimately preserved. At the facies scale, aggregate permeability characteristics are not stationary over a distance of more than a few thousand feet, whereas at the lithofacies scale, permeability characteristics appear to be constant over tens of thousands of feet.

Petrology-Permeability Relations

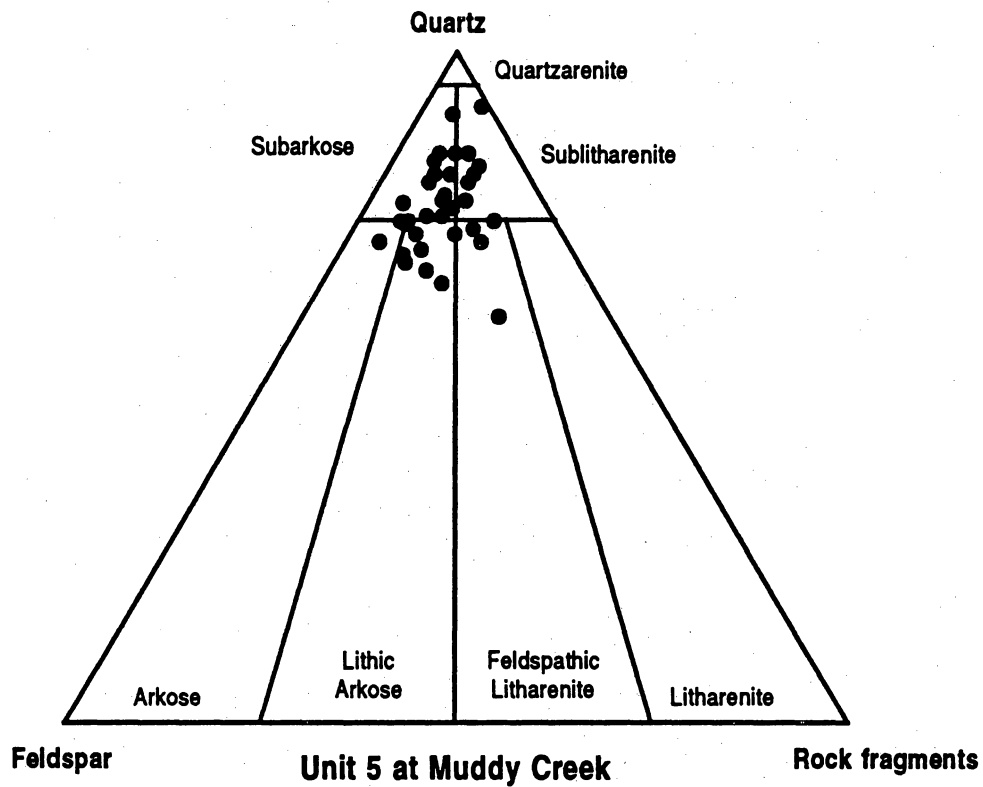
Systematic mineralogical differences accompany the observed permeability differences between sandstone facies and at the three outcrop locations. As previously discussed, delta-front, shoreface, and transgressive sandstones have lower mean permeability and lower permeability variation than distributary-channel sandstones. Regional variation in mean and maximum permeability values in delta-front sandstones is not statistically significant. Delta-front, shoreface, and transgressive sandstones are also relatively homogeneous mineralogically (table 3); there are no significant mineralogical variations between landward and seaward positions in the facies tract.

There are, however, marked regional variations in both mineralogy and permeability of distributary-channel sandstones. The compositional trends exhibited by sandstones in Muddy Creek correspond to systematic differences in permeability between facies. Distributary-channel sandstones have the highest mean permeability and, except where occluded by pseudomatrix, relatively high porosity (compared with that of matrix and cement), and have subequal amounts of kaolinite and quartz cement. GS 4 sandstones have the lowest mean permeability (29 md), subequal amounts of cement, matrix, and porosity, and relatively large amounts of kaolinite cement, which fills intergranular voids and retards fluid flow. Delta-front and transgressive sandstones have intermediate values of mean permeability (54 and 129 md, respectively), small amounts of pseudomatrix, and predominantly quartz cement, which results in smooth grain surfaces and little resistance to fluid flow.

Relations between permeability, channel type, and position in the facies tract have been previously documented. Figures 19, 20, and 21 show the changes in Q:F:R grain composition for distributary-channel sandstones at Muddy Creek, Picture Flats, and Cedar Ridge canyons, respectively, along with the mean permeability values for all samples measured at each outcrop. Trends in sand grain composition from South Muddy Creek to Cedar Ridge indicate that permeability is unaffected by the percent of feldspar and quartz but decreases with an increase in the percent of rock fragments. Because rock fragments in the Ferron are dominantly ductile grains that have been pressed into primary intergranular pore space during burial compaction, at least part of the seaward increase in permeability can be attributed to the increased removal of rock fragments as a result of increased physical reworking of sediments in the more seaward parts of the facies tract. The down-facies tract decrease in ductile rock fragments and the corresponding increase in permeability suggest that increased mechanical reworking with downstream transport produces a more mineralogically mature, permeable sandstone.

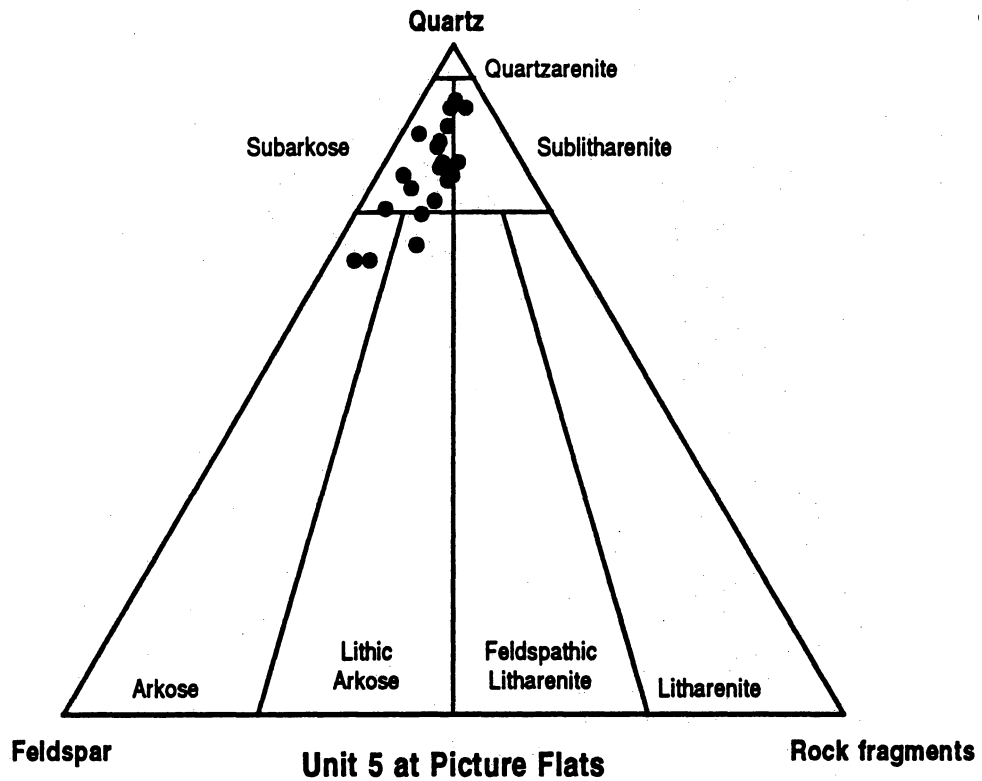
To more quantitatively explore relations between petrology and permeability, we used simple correlation coefficient analysis between sandstone point-count data and the logarithm of permeability measured on the plugs from which thin sections were cut. For the set of all distributary-channel sandstones (77 cases), the most significant correlations are between log permeability and percent pseudomatrix, grain size, percent rock fragments, percent connected porosity, and percent feldspar, in descending order. Multiple regression of these variables against log permeability results in a correlation coefficient (r^2) of 0.42. Deletion of outliers from the data set improves the correlations only slightly to 0.46.

Because the analysis of factors controlling permeability values and distribution types indicated that lithofacies are the essential building blocks of sandstone, we performed a similar investigation on the subset of all trough crossbedded distributary-channel sandstones (34 cases). In descending order, log permeability best correlates with percent rock fragments, percent feldspar, percent connected porosity, grain size, and percent pseudomatrix. Multiple regression against log



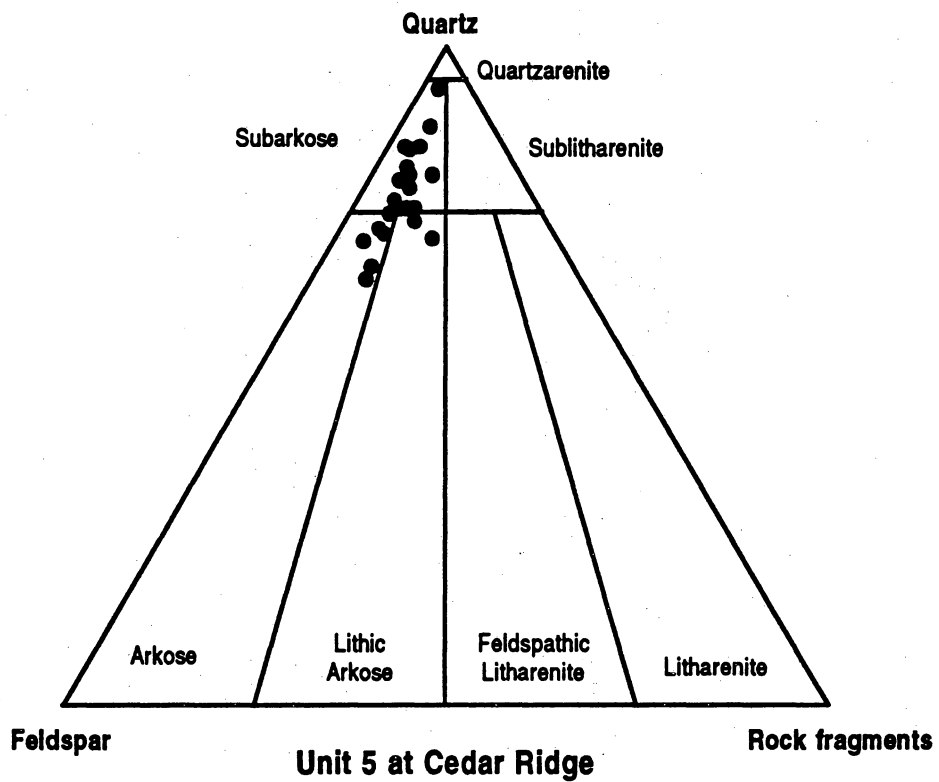
QAa601c

Figure 19. Framework grain composition of distributary-channel sandstones from Muddy Creek (classification of Folk, 1974).



QAa602c

Figure 20. Framework grain composition of distributary-channel sandstones from Picture Flats (classification of Folk, 1974).



QAa604c

Figure 21. Framework grain composition of distributary-channel sandstones from Cedar Ridge (classification of Folk, 1974).

permeability produces a correlation coefficient of 0.55. Deletion of outliers improves the correlation coefficient to 0.69.

This statistical analysis is not intended to precisely predict permeability from petrographic information. It does, however, identify those petrologic factors that strongly influence permeability. Most previous studies have found that permeability typically correlates with grain size and porosity. In a landward-stepping depositional setting with relatively short transport distance from sediment source to basin, we would expect physical processes in the depositional environment to strongly influence sandstone fabric and therefore petrophysical properties as well. The diagenetic overprint is mild because Ferron sandstones experienced only low to moderate burial temperatures. Chert and low-grade metamorphic rock fragments are ductile and relatively easily removed by sediment reworking. Where these grains are present they will partly occlude pore space during burial compaction; where they have been removed by sediment reworking more primary porosity will be preserved. Feldspar grains are also subject to removal by abrasion and commonly reduce porosity by fracturing during compaction. Pseudomatrix in the Ferron GS 5 is locally derived, ductile, and completely fills primary intergranular porosity during burial compaction. In landward-stepping sandstones, one could predict that pseudomatrix would be more abundant in the proximal channels (where mud is distributed throughout the sandstones as mud clasts and clay chips) and would be less abundant in distal channels (where mud is segregated into shale and mudstone strata).

Comparison of Outcrop and Subsurface Permeability

Our purpose in conducting outcrop geologic characterizations and permeability measurements is to obtain data that will increase our understanding of sandstone reservoirs. Other studies discussed previously showed that useful permeability information can be carried from outcrop to reservoir. We have an opportunity to directly test the similarity of permeability measures in the Ferron by comparing results obtained from outcrop with those measured in nearby cores.

In 1991 the University of Utah Research Institute (UURI), under contract to the Gas Research Institute, drilled and cored two boreholes through the entire Ferron Sandstone. In UURI well No. 2, a complete sequence through a Ferron GS 5 distributary channel was obtained. The sequence, approximately 25 ft thick, is composed of several distinct intervals. The basal portion of the channel erosionally overlies organic rich mudstones in GS 4 and consists of about 8 ft of medium-grained trough cross-stratified to indistinctly bedded sandstone that contains thin zones of mud rip-up clasts. Abruptly overlying this interval is approximately 10 ft of fine-grained sandstone in which laminae dip at very low angles ($\leq 10^\circ$). The uppermost interval consists of about 5 ft of ripple cross-stratified and contorted sandstone that records the final phase of channel fill. Capping the sequence is a series of thinly bedded, moderately bioturbated mudstones and siltstones.

The UURI well No. 2 is located about 0.5 mi from Muddy Creek canyon. Comparison of core and equivalent outcrop intervals in Muddy Creek shows a close match of lithologies and their distribution. In South Muddy Creek distributary channels have a well-developed succession of stratal types that include a basal interval composed of medium to coarse trough cross-stratified sandstone and mud-clast-bearing lag deposits, an intermediate interval of low-angle stratification, and an upper interval of ripple cross-stratified and contorted bedded sandstone. These features suggest that the channel is a late-stage distributary channel.

Permeability in the core was measured at 0.1-ft spacing and along an equivalent vertical outcrop transect at 0.5-ft spacing. Figure 22 shows the relationship of permeability to stratification type for the interval tested in the UURI core. Core permeabilities have the same relation with stratification type as at the outcrop. Trough cross-stratified sandstones have the highest permeabilities, ripple cross-stratified sandstones are lowest, and low-angle inclined strata have intermediate permeability. Statistical comparison also shows a close correlation in permeability mean, coefficient of variation, and distribution type in core and at outcrop (table 7). Additionally, comparison of the cored interval with a nearby transect (fig. 23) shows a strong similarity in permeability patterns between the two settings. Each interval displays a well-developed upward-decreasing permeability trend that reflects the strong vertical partitioning of stratal types. A

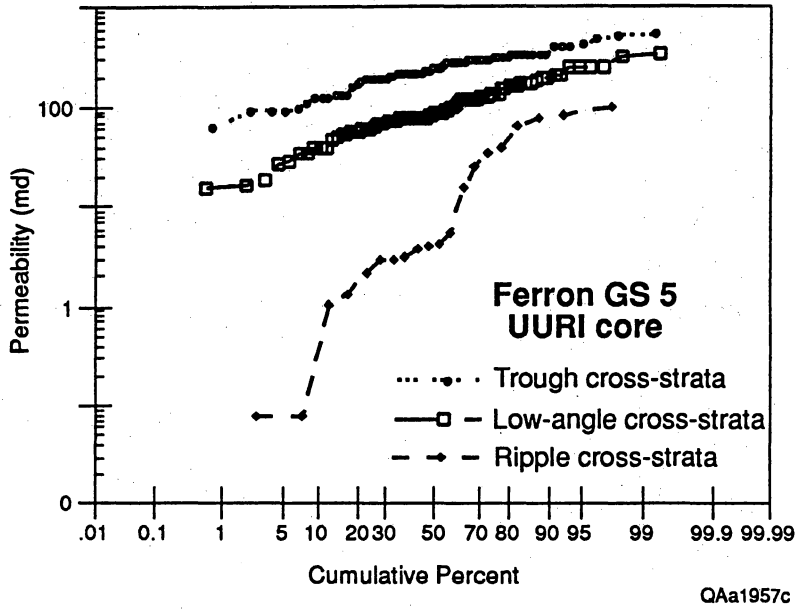
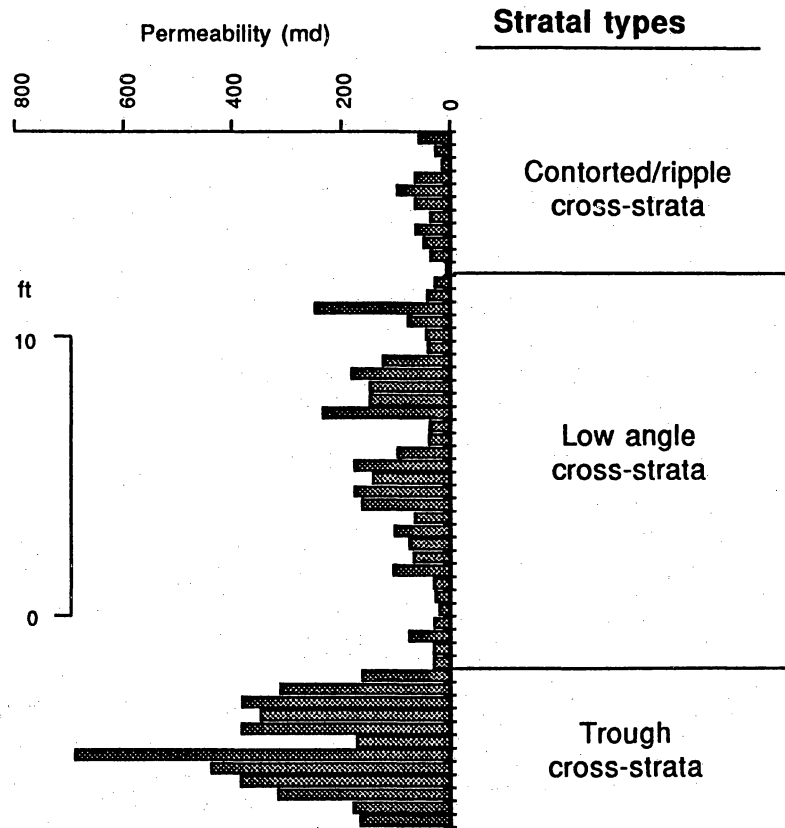
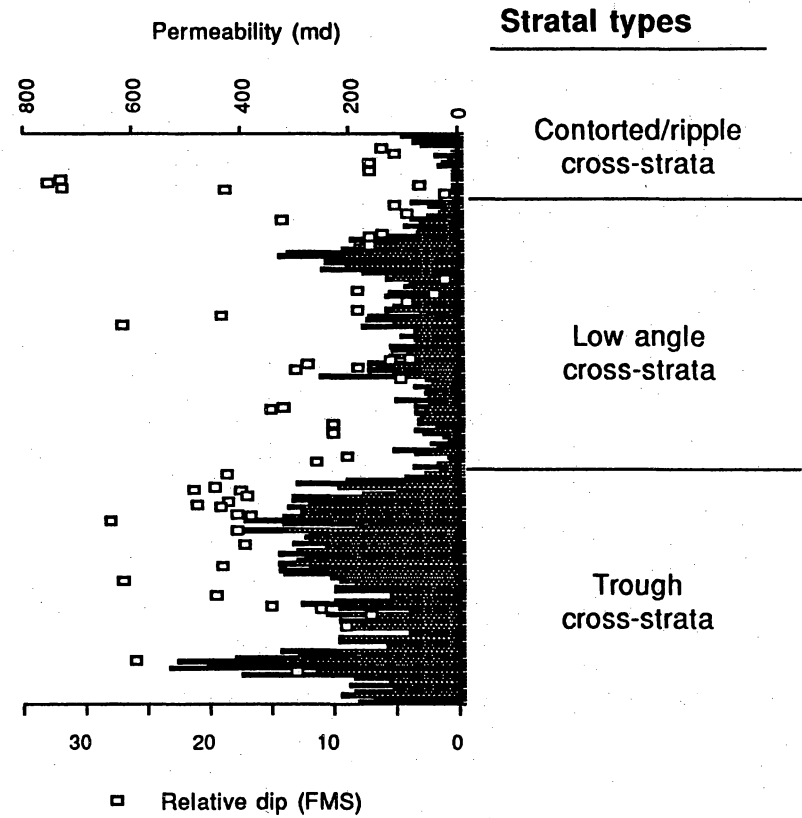


Figure 22. Cumulative probability plot of permeability for stratal types within distributary-channel facies from UURI Well No. 2.

**Outcrop South Muddy Creek
permeability profile**



**UURI Core No. 2
permeability profile**



08

QAa1200c

Figure 23. Comparison of permeability profiles between outcrop and UURI Well No. 2.

correlation also exists between relative dips and permeability for the UURI cored interval; permeability generally increases with increasing dip angle. This relation is attributed to permeability differences between the high-angle trough cross-strata and the low-angle and ripple stratification types. These results confirm that permeability structure determined on outcrop can be extrapolated to nearby subsurface equivalent sandstones.

Spatial Permeability Variation

The scale, magnitude, and distribution of heterogeneities reflect the processes that formed them. Furthermore, in many depositional systems the distribution of such heterogeneities is often a function of orientation. Therefore, we expect that sandstones deposited under different conditions will show different degrees of anisotropy. Detailed transects and sample grids were constructed within specific lithofacies to examine permeability patterns within lithofacies and across bounding surfaces. Characterizing permeability patterns at this scale is necessary to evaluate permeability anisotropy in the scale-up of petrophysical properties.

We used the semivariogram to examine spatial permeability variation. The variogram is a statistical tool that estimates the variability of a property such as permeability as a function of distance. The variogram is calculated by summing the squares of the differences of all data pairs separated by a given lag distance (h) and dividing this sum by the number of pairs. This value is then plotted on the ordinate of a graph, and the distance between pairs is plotted on the abscissa. A property that is correlated over the scale examined will show increasing semivariance (γ) with increasing lag distance. A property that is not correlated will not display an increasing variogram function.

The variogram is characterized by several parameters. The range is the distance over which a property is correlated. The sill is the semivariance value (γ) at which the variogram function no longer increases with distance and correlation ceases. Theoretically, if measurement error is nonexistent the semivariance should approach zero as the lag distance becomes infinitesimally

small. However, most experimental variograms do not pass through the origin. This unexplained variance is referred to as the nugget effect and may be attributable either to measurement error or to correlation on a scale that is less than sample spacing. In addition, a change in slope of the variogram function indicates a change in the style of correlation.

Figures 24, 25, and 26 show the vertical and horizontal variograms for the contorted, low-angle, and trough crossbedded stratal types, respectively, from the distributary-channel facies in South Muddy Creek. Data were collected within each lithofacies at 0.5-ft intervals along an 80-ft transect that paralleled lithofacies boundaries in the direction of sediment transport. The trough crossbedded lithofacies is composed of downcurrent-descending crossbed sets that range from about 0.33 to 1.0 ft in thickness. Internally this facies can be subdivided into cosets of trough cross-strata, each displaying an upward-fining grain-size trend. The low-angle stratification is composed of a series of thin beds that vary from several inches to several feet in thickness. Discontinuities separating beds are characterized by thin mudstone and siltstone layers that extend laterally for several hundred feet. Internally, beds consist of fine-grained low-angle strata. The contorted interval is composed of fine-grained, low-angle to ripple cross-stratified sandstones that have been syndepositionally deformed and display chaotic, vertical, and overturned bedding or laminae.

Estimated correlation ranges show a close relation to stratification type. In the vertical direction, deposits displayed similar correlation lengths, 2.5 ft within the contorted interval, 3.5 ft within the trough cross-stratified sandstones, and 5 ft within the low-angle lithofacies. Differences in estimated correlation lengths in the horizontal direction are more pronounced, with trough cross-stratified sandstones displaying a range of approximately 24 ft, low-angle strata 10 ft, and contorted strata 2.5 ft. Comparison of permeability patterns with geologic characteristics shows that estimated correlation lengths reflect small-scale bedding features within the deposits. For example, bedding features within the contorted interval were destroyed or highly disrupted shortly after deposition. As a result, these deposits display a poorly defined correlation range that lacks a preferred orientation, that is, horizontal and vertical correlation ranges are equal. However, within the low-angle and trough cross-stratified intervals, primary bedding features are preserved.

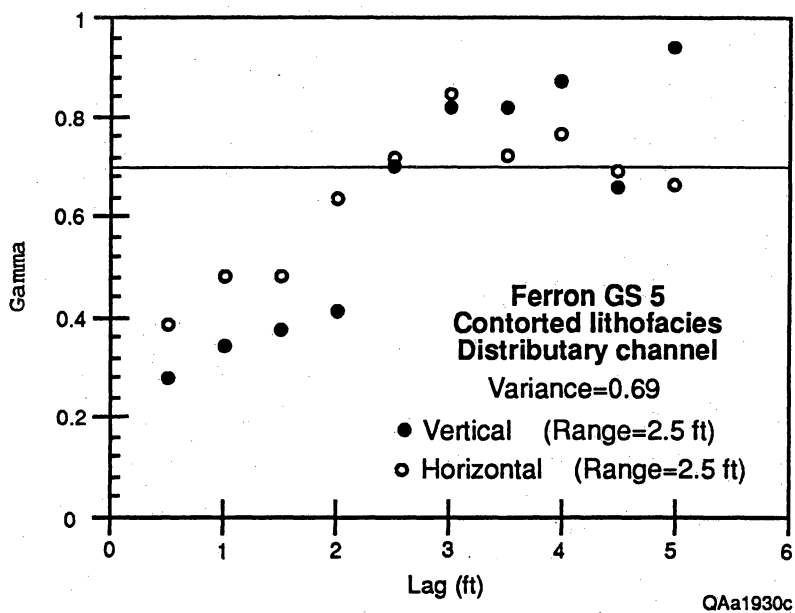


Figure 24. Horizontal and vertical variograms for contorted lithofacies, distributory-channel facies.

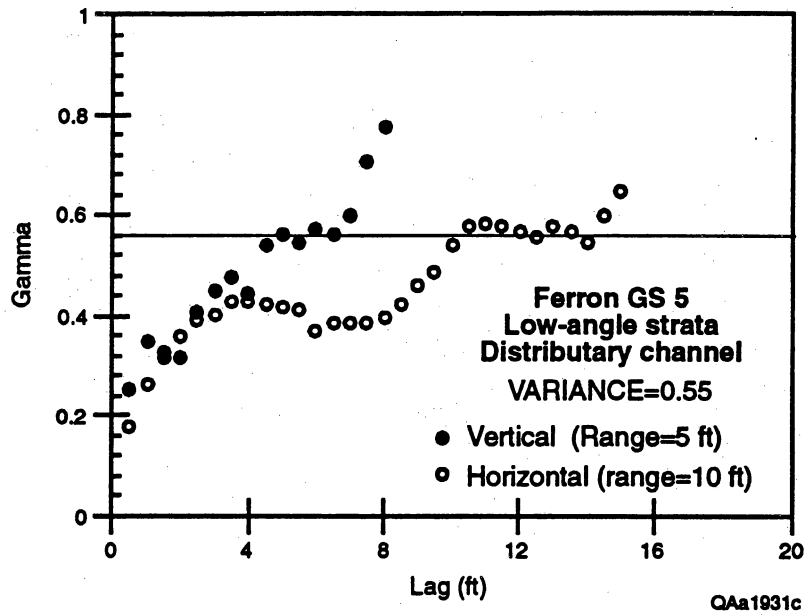


Figure 25. Horizontal and vertical variograms for low-angle strata, distributary-channel facies.

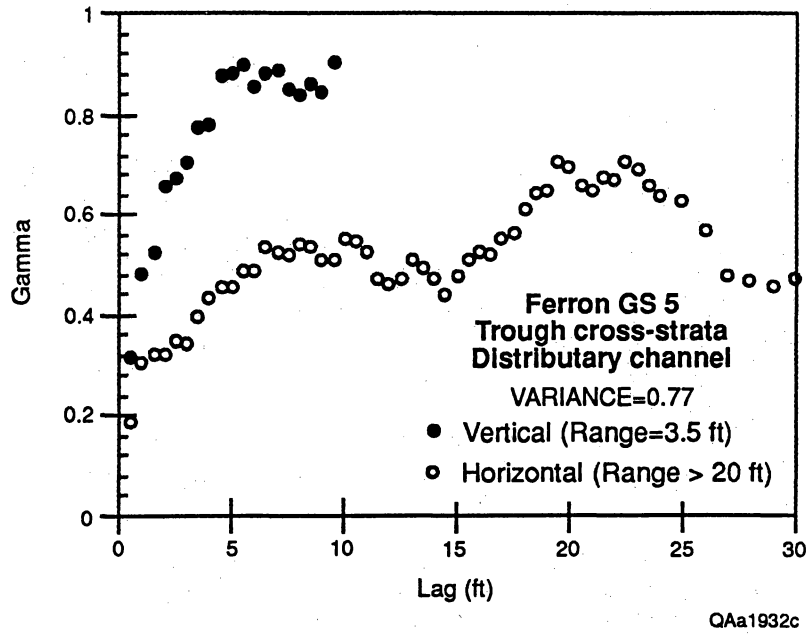


Figure 26. Horizontal and vertical variograms for trough cross-strata, distributary-channel facies.

Correlation ranges within these deposits are well defined and display a preferred orientation; horizontal correlation ranges significantly exceed vertical ranges. Results similar to these were also obtained from a 40- by 40-ft sample grid constructed within the distributary-channel facies in Muddy Creek.

Within the trough cross-stratified lithofacies, the horizontal correlation ranges should be regarded as a minimum because straight line measurements along an inclined sand body likely underestimate the lateral extent of these zones. However, this correlation distance is probably most appropriate to use in reservoir studies because flow to a gas well will also have to cross internal bedding set boundaries. In addition, correlation ranges derived from permeability profiles and semivariogram analysis indicate that stratification types show the same repetitive patterns horizontally as they do vertically, but the horizontal scale is larger.

Permeability patterns within highly bioturbated and swaley-stratified sandstones of the delta front were also investigated (figs. 27 and 28). Results are similar to those of the distributary-channel lithofacies, with stratified sandstones displaying greater horizontal correlation lengths than disrupted sandstones. Within the delta front, swaley-stratified sandstones have a correlation length of several hundred feet, compared with that of several feet in highly bioturbated sandstones.

Permeability Anisotropy

We can use the magnitude and distribution of heterogeneities to infer directional permeability trends within and between stratification types. The effect of permeability variations caused by small-scale heterogeneities between bedsets and cosets on anisotropy will depend on several factors. These include cross-set orientation, dimension, arrangement, and degree of permeability variation. Weber (1972) derived an expression for horizontal permeability anisotropy caused by the effects of crossbed foresets and bottomsets. However, the algorithm assumed all cross sets were similarly oriented. The importance of small-scale anisotropy may be reduced if considerable variation in orientation of individual sets exists at a scale smaller than the well spacing.

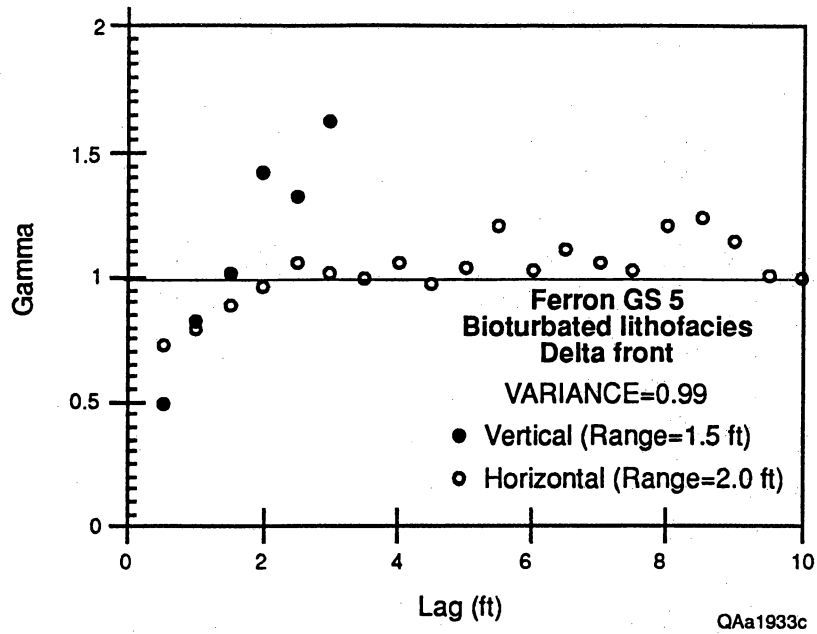


Figure 27. Horizontal and vertical variograms for bioturbated lithofacies, delta-front facies.

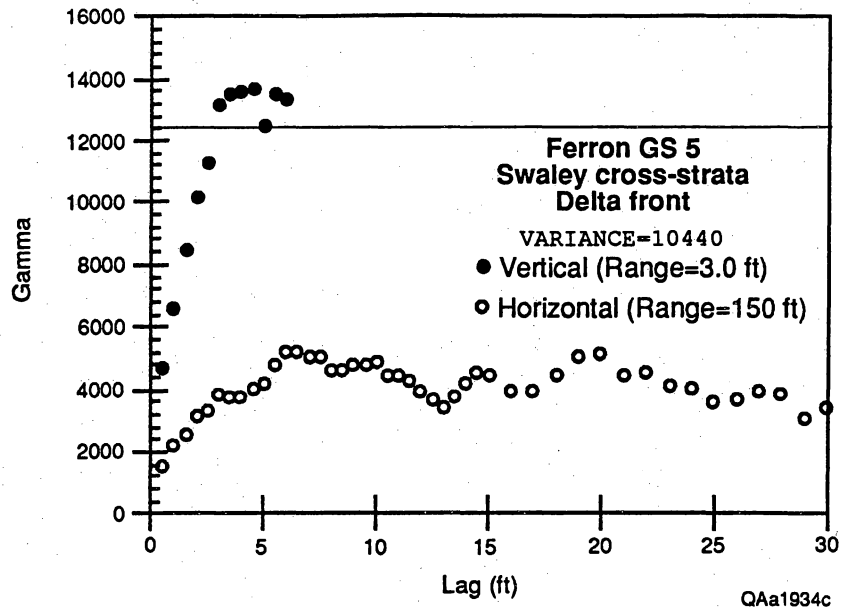


Figure 28. Horizontal and vertical variograms for swaley cross-strata, delta-front facies.

A comparison of horizontal to vertical correlation ranges is used to infer the directional dependence of permeability. The ratio of estimated horizontal to vertical correlation ranges are high (2 to 50) within lithofacies that display well-defined stratification (trough, low-angle, and swaley) and low (1 to 2) within lithofacies that lack well-defined stratification (bioturbated or convolute). For example, the ratio of horizontal to vertical correlation ranges is greater than 10 for trough crossbedded, low-angle, and swaley stratified sandstones, and approximately equal to 1 for the contorted and extremely bioturbated sandstones. However, the magnitude of permeability variation is not the same in all cases. In the trough and swaley cross-stratified sandstones, vertical permeability is disrupted by set boundaries that have low permeability. In trough cross-strata, the permeability contrast across boundaries is approximately an order of magnitude and may not be sufficient to produce significant horizontal to vertical anisotropy. However, in ripple and low-angle stratification types, permeability continuity is severely disrupted by clay drapes that separate strata sets and cosets. Bioturbation and syndepositional deformation disrupt primary bedding features that impart permeability patterns. Bioturbation increases vertical connectivity by disrupting bedding and bounding surfaces but also decreases mean permeability by introducing clay and matrix into the sandstones. Syndepositional deformation reduces lateral continuity by disrupting the original fabric of the sandstones.

In trough crossbedded sandstones, horizontal permeability is greatest in the direction of sediment transport. Sets of cross-strata are aligned approximately parallel to the depositional axis and are approximately 5 to 10 times longer than they are wide, ranging from 5 to 20 ft wide and 20 to several hundred feet long. However, the orientation of individual sets varies considerably and reduces horizontal anisotropy.

PERMEABILITY RELATIONS AND SANDSTONE ARCHITECTURE

Having established the permeability characteristics of facies and their component lithofacies, we can now evaluate probable patterns of fluid flow in an analogous sandstone reservoir. To do this,

we determine the vertical and lateral variation of facies and how well they are connected by comparing the permeability variations with the lithofacies arrangements at (1) Muddy Creek canyon, the most landward exposure of deltaic sedimentation, (2) Picture Flats canyon, approximately 1.5 mi from Muddy Creek and near the center of the facies tract, and (3) Cedar Ridge canyon, approximately 1.5 mi seaward of Picture Flats canyon and at the most seaward exposure of GS 5 sandstones.

Muddy Creek Canyon

Sandstone Architecture

Delta-Front Sandstones

The transgressive facies that marks the base of deltaic GS 5 in Muddy Creek is thin (less than 3 ft), laterally extensive, but locally discontinuous where eroded during deposition of overlying sandstones.

Directly above the transgressive facies are upper delta-front sandstones that have been extensively eroded by overlying distributary channels. Thicknesses vary from 0 to 25 ft over short lateral distances. Internally, the upper delta front is composed of a series of subintervals. Bedding in the subintervals consists of hummocky to swaley stratification, whereas grain size ranges from very fine to fine and is relatively uniform throughout. Lateral facies variation is subtle; no well-defined facies boundaries are apparent. However, vertical variation is pronounced. The lower bounding surface of each delta-front subinterval is erosional; upper bounding surfaces are composed of laterally continuous interbedded siltstone and mudstone layers. The uppermost layer of each subinterval is the thickest.

Internally, individual sandstone subunits are sigmoidal; each sigmoidal subinterval extends downdip for several kilometers. Thus, the dominant style of heterogeneity in the delta-front sandstones is vertical stratification, with subintervals ranging from 3 to 15 ft in thickness. Lateral

heterogeneity resulting from depositional processes in the subintervals is minimal. Lateral variability of the delta-front sandstones is caused primarily by erosion associated with deposition of the superposed distributary sandstones.

Distributary-Channel and Associated Deposits

Four spatially dependent permeability structures occur within the distributary-channel system at Muddy Creek. Three styles are related to within-channel variation: (1) variation within lithofacies, (2) variation between lithofacies, and (3) variation between the distributary-channel center and margin. The fourth reflects variations between channel types, that is, early- versus middle- versus late-stage channel. Each channel type has a characteristic geometry, arrangement of lithofacies, and stratigraphic position.

Preserved distributary channels and associated sediments vary considerably from landward to seaward extent of the facies tract and from early to late deposits. We recognize three stages of distributary-channel sedimentation. Early-stage channels are exposed along the entire system from landward to seaward extent; middle-stage and late-stage channels are present only in the more proximal settings. Significant landward to seaward variations also occur in the relations between channels deposits, abandoned channel fills, and crevasse splay deposits.

Early-Stage Distributary Channels.—At the base of the distributary channel complex and deeply incised into the underlying delta front are a series of narrow, laterally isolated early-stage distributary channels. Geometry varies considerably, reflecting the amount of erosion as overlying distributary channels were deposited. These channels typically are very heterolithic; individual channels are isolated from one another by extensive mudstone drapes. Bedding within the macroforms is dominantly trough cross-strata with large avalanche foresets locally present. Small-scale bounding surfaces are indistinct and lack well-defined lithologies.

Middle-Stage Distributary Channels.—Laterally migrating channel deposits erosively overlie early-stage distributary-channel and delta-front deposits. These deposits are much more extensive than

subjacent early-stage channel deposits. Two laterally migrating distributary-channel complexes exposed in Muddy Creek are 1,200 and 1,320 ft wide. Laterally, these channel complexes shale out into overbank muds and silts or are truncated by superjacent distributary-channel sandstones. A typical vertical sequence begins with a basal zone of clay-clast-bearing trough crossbeds that overlie a sharp erosional base. These mud clasts typically deform into pseudomatrix during compaction. As previously discussed, these mud-clast-rich zones have substantially lower permeabilities than do adjacent stratal types and probably would interfere with fluid flow in a reservoir. Trough cross-stratified sandstones occupy the lower portion of the channel complex. Grain size in this interval decreases upward from coarse, poorly sorted at the base to medium-fine, moderately sorted at the top. Low-angle cross-stratified sandstones abruptly overlie trough crossbeds and also display an upward-decreasing trend from medium to fine moderately sorted sand. The sequence is capped by fine to very fine grained, moderately to highly contorted strata or, less commonly, ripple-laminated sandstones.

Inclined erosive surfaces that dip gently toward the channel base at angles of 5° to 15° characterize this channel type. The dimensions of the sandstone packages bounded by the accretion surfaces vary considerably. Widths of the sigmoidal sand bodies average 360 ft but range from 75 to 700 ft. Individual lenses are 3 to 20 ft thick and erosionally overlap to form multilateral sand bodies with a cumulative thickness of 15 to 40 ft and belt widths of 1,200 to 1,500 ft.

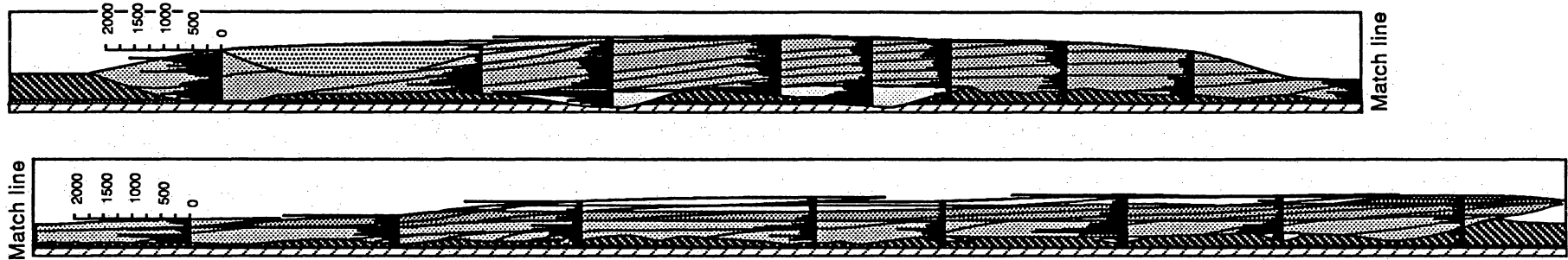
Laterally across the complex in the direction of migration, the three main stratal types are not continuous but pinch out over the underlying strata. The lower trough crossbedded facies is as much as 20 ft thick and has the greatest lateral dimensions, extending 1,200 ft across the channel belt. The low-angle stratified facies is as much as 15 ft thick and extends approximately 800 ft. The upper contorted facies is as much as 10 ft thick and 500 ft wide. Small-scale bounding surfaces or discontinuities that divide channel forms and stratal types into subsets are not extensive or well defined by a distinct lithology, nor are clay drapes common in the middle-stage distributary channel type.

Late-Stage Distributary Channels.—Late-stage distributary-channel deposits are considerably thicker and narrower than the underlying channel types. Typically, late stage channels are perched above and deeply eroded into middle-stage channel sandstones. The basal contact is generally marked by a mudstone or siltstone layer or by a thick intraformational mud-clast lag. Internally, large inclined accretion surfaces divide the sand body into a series of subunits, each composed of a succession of stratal types. These stratal types are characterized by a well-developed waning-flow sequence of small-scale sedimentary structures. Occasionally, the upper surface is accentuated by a thin layer of fine-grained sediment as much as 2 inches thick. Laterally, these channels are encased by abandoned channel fill and crevasse splay deposits.

Permeability Characteristics

Permeability patterns reflect the vertical and horizontal distribution of lithofacies (fig. 29). Within distributary-channel deposits, channel bases have generally low permeabilities and the highest permeabilities occur in the lower channel fill. Overall, permeability displays a well-developed upward-decreasing trend that extends laterally across the entire channel fill. Laterally, slightly higher permeabilities exist in the central portion of the channel than on its margins. Because average permeability decreases from 308 md in the trough cross-strata to 145 md in the low-angle strata and to 88 md in the contorted strata, we conclude that the upward-decreasing permeability trend is caused by the vertical arrangement of stratal types and grain size change. Laterally and vertically, this trend is disrupted by the lower permeability bounding lithologies that occur along the channel base, accretion, and reactivation surfaces. Erosional discontinuities and bounding lithologies have the lowest permeabilities in the distributary-channel facies (average of 44 md).

Within the distributary-channel facies, estimated permeability correlation lengths reflect the arrangement of lithofacies groups. Comparison of vertical transects within the laterally migrating (middle stage) distributary-channel complex shows permeability to be correlated laterally over a



94

100 ft/30 m
 No vertical exaggeration

Permeability profile



- Delta front
- Transgressive
- Delta plain
- Abandoned channel fill

- Distributary channel
- Trough cross-strata
- Low-angle stratification
- Ripple/contorted strata

QAa1198c

Figure 29. Permeability profiles and distributary-channel architecture from South Muddy Creek.

distance of 600 ft (fig. 30). The large-scale correlation range is interpreted to reflect the lateral distribution of stratal types and the gradual decrease in permeability along the channel margins. A significant scale of heterogeneity not revealed at this scale of analysis but observable by inspection of the cross section is the variation related to low-permeability lag deposits that define the laterally migrating inclined channel forms. A correlation range and semivariance can be predicted for such a feature on the basis of the relationship of permeability to depositional architecture depicted in the cross section. The correlation range is a rough estimate of one half the thickness of the fundamental element causing the permeability variation; in this case, variation between channel forms. Channel forms display an average lateral dimension of approximately 400 ft, suggesting a lateral correlation length of approximately 200 ft.

In the vertical direction permeability is correlated over several scales, one at 6 ft and another at 20 ft (fig. 31). The 6-ft correlation range reflects the vertical distribution of low-permeability lag deposits along channel-base-bounding surfaces and reactivation surfaces. The larger correlation range of about 20 ft reflects the vertical partitioning of high-permeability trough cross-stratified sandstones along the lower portion of the channel and overlying lower permeability low-angle and contorted strata.

Picture Flats Canyon

Sandstone Architecture

As at Muddy Creek canyon, distributary-channel and associated deposits erosionally overly delta-front sediments at Picture Flats (fig. 32). However, at Muddy Creek thickly bedded hummocky to swaley cross-stratified sandstones directly overlie the basal bioturbated transgressive sandstone. At Picture Flats a thick interval of thinly interbedded hummocky cross-stratified sandstone and siltstone, which coarsens and thickens upward, separates the bioturbated basal interval from the thickly bedded hummocky to swaley cross-stratified sandstones. Hummocky cross-stratified sandstones in this interval vary from several inches thick near the base to a few feet thick near the

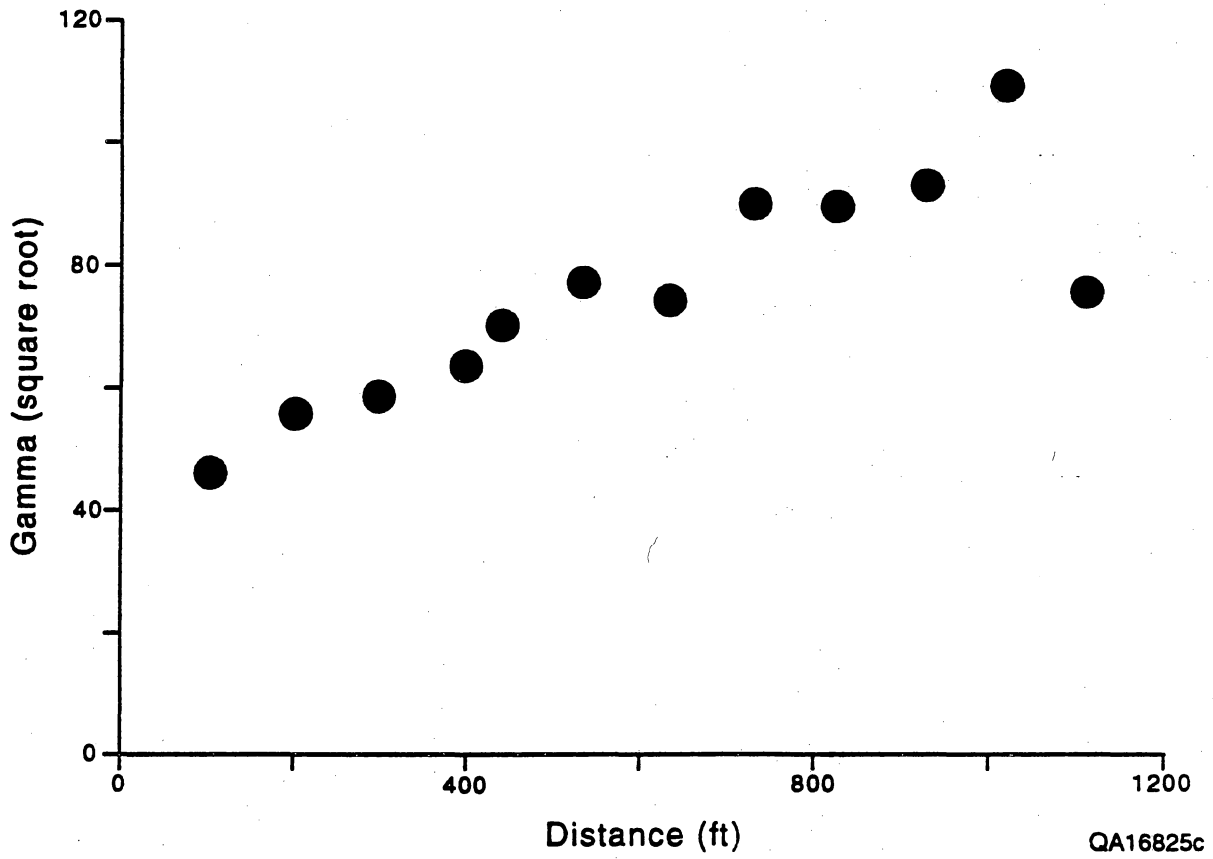


Figure 30. Horizontal variogram from distributary-channel facies from South Muddy Creek.

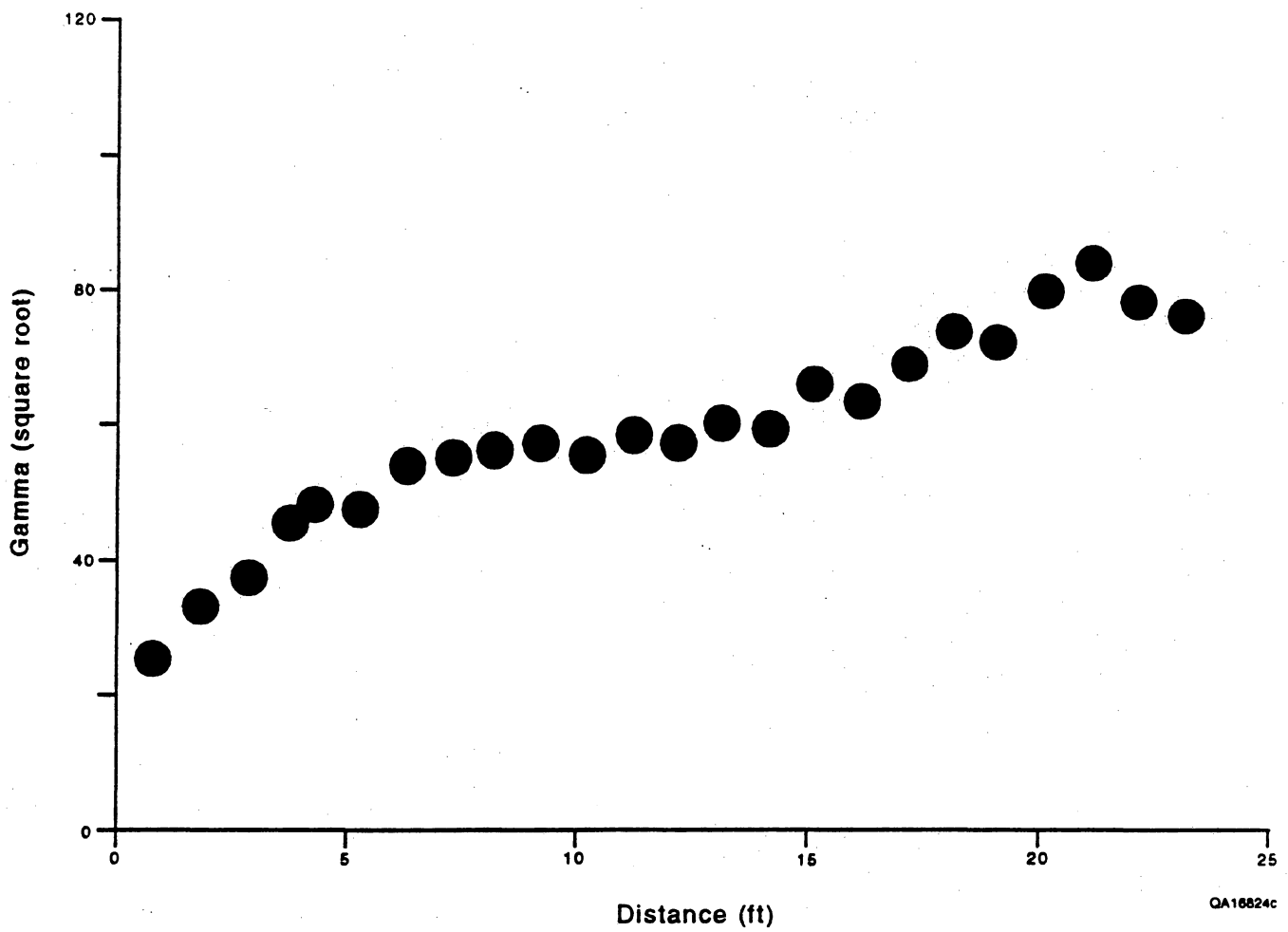


Figure 31. Vertical variogram within distributary-channel facies from South Muddy Creek.

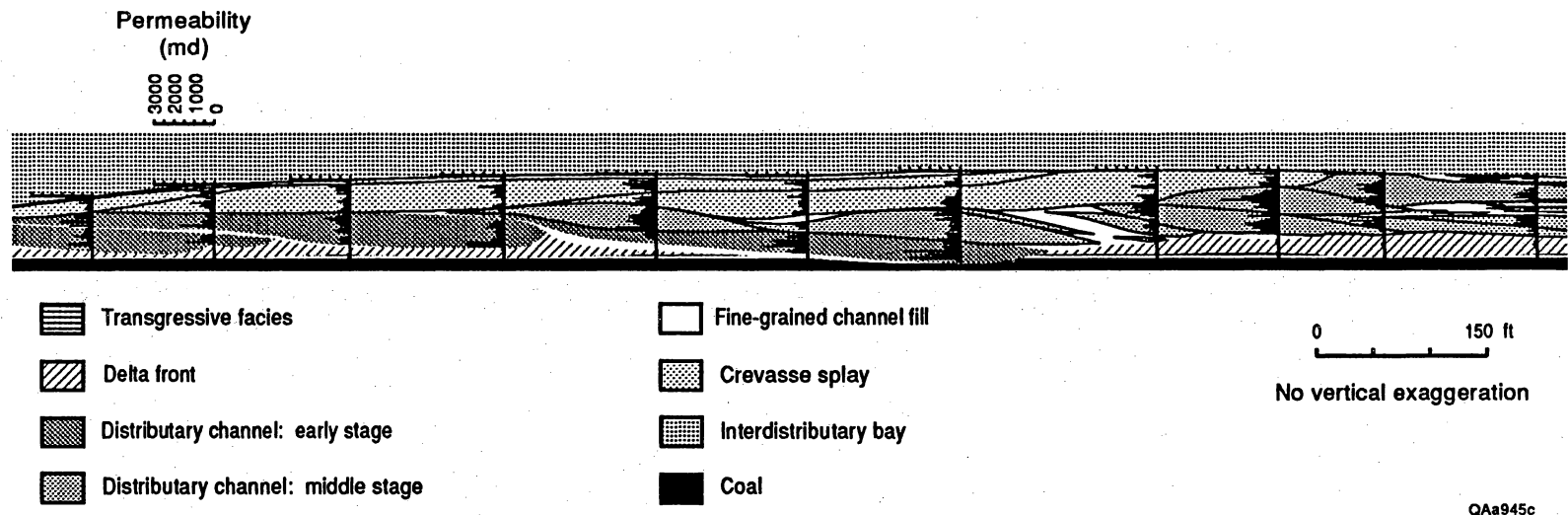


Figure 32. Permeability profiles and distributary-channel architecture from Picture Flats.

top. Thick hummocky to swaley cross-stratified sandstone units are poorly preserved because of extensive erosion by overlying distributary channels; they occur only as thin, discontinuous lenses separated laterally from one another by adjacent distributary-channel sand bodies. Overall, the thickness of the delta-front facies ranges from 0 (where completely eroded by overlying distributary channels) to approximately 15 ft. Lateral extent of individual hummocky cross-stratified beds is several hundred to several thousand feet.

The distributary-channel belt at Picture Flats consists of several stories of multilateral channel forms. In the lower channel story, sand bodies 10 to 20 ft thick and 100 to 300 ft long erosionally overlie delta-front deposits. Internally, these sand bodies consist of a poorly developed lag deposit overlain by relatively uniform trough cross-strata or indistinctly bedded sandstones. Grain size typically ranges from medium coarse to medium fine and displays a weakly developed upward-fining trend. Closely associated with these deposits are thick mudstone drapes that isolate these sand bodies from the underlying delta front and laterally adjacent sand bodies. These facies associations are interpreted as the early-stage, incised-channel type.

Erosionally overlying the early-formed channel deposits and the delta front is a series of laterally migrating sand bodies. These sand bodies have thick, well-developed lag deposits at their base and distinct bedforms such as trough and low-angle stratification above the base. Locally preserved within this facies are large avalanche foresets. The facies association is interpreted as the middle-stage, laterally migrating channel type. Capping the succession are crevasse splay and abandoned channel fill deposits that represent the final phase of channel aggradation and abandonment. The thick, narrow, late-stage distributary-channel sandstones that are present at Muddy Creek canyon are represented in Picture Flats only by these overbank deposits.

Unlike Muddy Creek, where variation in the distributary-channel and associated deposits reflects the dominance of middle- to late-stage distributary-channel types, at Picture Flats lateral and vertical variation reflects the distribution of early- to middle-stage distributary channels. In comparison to Muddy Creek, sand bodies at Picture Flats are thicker, less laterally extensive, and more separated by continuous shale layers. In addition, the lateral and down-channel migration

that results in a predictable arrangement of stratal types or upward-fining grain-size trend at Muddy Creek is not well developed at Picture Flats.

Permeability Character

The relationship of permeability to depositional architecture at Picture Flats is shown in figure 32. Trends in permeability mean, variation, and distribution type between the distributary-channel facies and the delta front are similar to those observed in Muddy Creek; distributary-channel facies display about an order of magnitude higher permeability than does the delta front. In addition, within the distributary-channel facies, permeability relates to grain size and stratification type, as it does in Muddy Creek. Although absolute permeability between similar lithofacies is somewhat higher at Picture Flats than at Muddy Creek, the relationships of permeability between lithofacies is the same: trough cross-strata have the highest permeabilities and bounding lithologies have the lowest.

Differences in permeability structure between Muddy Creek and Picture Flats result from changes in the channel architecture, which in turn reflect the proportions of the different distributary-channel types. Zones of highest permeability are more evenly distributed throughout the channel fill and are not concentrated in the lower part as in Muddy Creek. At the largest scale, the permeability pattern reflects the vertical and lateral stacking of individual macroforms. Permeability continuity corresponds to channel geometries and is disrupted laterally and vertically by low-permeability lithofacies, such as mudstone drapes, ripple-laminated sandstones, and mud-clast-rich lag deposits. Within the channel deposits, permeability is higher in the central and downstream portions than along the flanks or upstream portions; permeability does not display a well-developed vertical trend. In contrast, crevasse splay deposits generally show an erratic upward-increasing permeability trend and no well-developed lateral trend.

Cedar Ridge Canyon

Cedar Ridge canyon exposes the most seaward delta-front and distributary-channel sandstones of the landward-stepping Ferron GS 5. We studied these outcrops at two locations. Cedar Ridge I exposes the distributary-channel complex at the most seaward extent of deposition, whereas Cedar Ridge II exposes the laterally associated distal delta-front deposits.

Cedar Ridge Distributary-Channel Architecture

The Cedar Ridge I locality represents the seawardmost extent of distributary-channel influence within deltaic GS 5. A deeply incised distributary-channel complex provides contrast to the laterally continuous but vertically stratified delta-front sandstone. The channel belt is approximately 700 ft wide and 60 ft thick; it is incised through the entire thickness of GS 5 and into underlying GS 4. Channel forms within the channel belt are inclined and arranged in a multistory to multilateral fashion. The channel fill is extremely heterolithic, with large homogeneous sand bodies separated by thick, extensive mudstone and siltstone layers. Bedding within sand bodies is predominately trough cross-stratified or indistinct. Channel architecture is characteristic of the early-stage distributary-channel type.

Adjacent to the channel, delta-front deposits extend from the top of the G coal overlying GS 4 to the base of GS 6, a distance of approximately 40 ft. Within this sequence, grain size increases and beds thicken dramatically from the base upward. Lower delta-front deposits range from 20 to 25 ft in thickness and overlying upper delta-front deposits range from 12 to 17 ft in thickness. Delta-front deposits display a high degree of vertical heterogeneity with individual sandstone beds separated from each other by thin, extensively deposited bioturbated mudstones. Laterally, however, individual sandstone beds extend from about 1,000 to 10,000 ft. Bedding within the delta front is dominantly hummocky cross-stratified in the lower two-thirds and swaley stratified in the upper one-third.

Cedar Ridge Distributary-Channel Permeability Characteristics

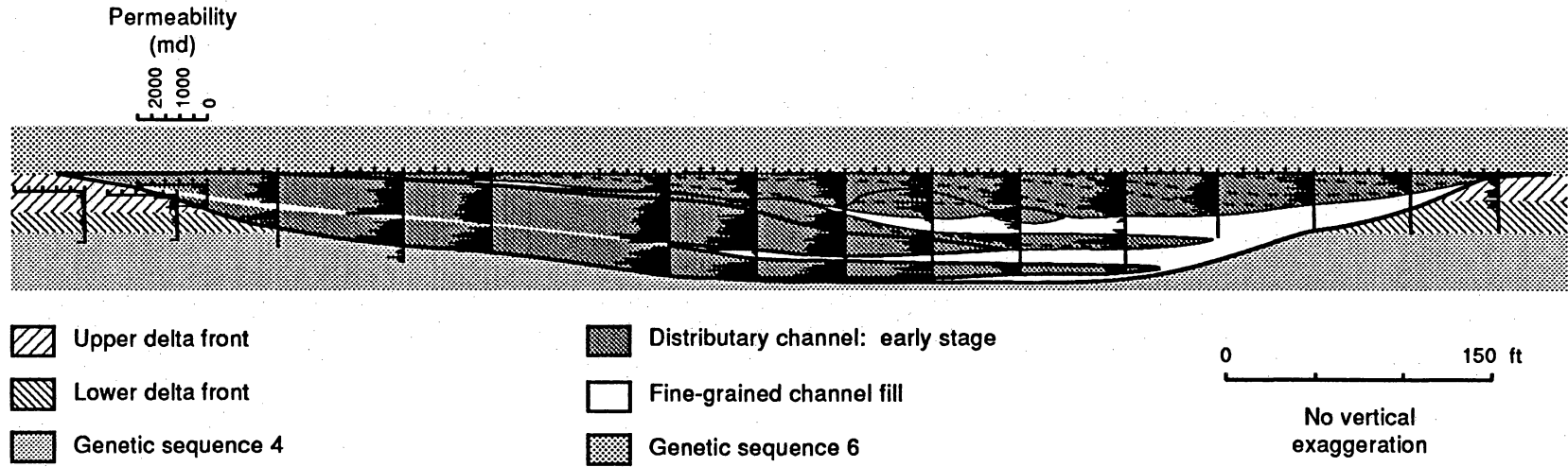
The relationship of permeability to channel architecture in Cedar Ridge canyon is shown in figure 33. Permeability varies greatly within the distributary-channel facies, from less than 0.1 md to greater than 2,500 md. The primary source of this variation is the contrast between channel forms that are composed of high-permeability trough cross-stratified sandstones and low-permeability mudstone and siltstone layers that vertically and laterally separate channel forms. As a result of this stacking arrangement, zones of very high permeability are isolated both laterally and vertically from one another by zones of low permeability. Despite the very heterolithic character, average permeability of the channel fill exceeds 700 md.

Zones of high permeability are uniformly distributed throughout the channel fill. Laterally, the highest permeabilities are in the center of the channel fill. Within individual channel forms, permeability is uniformly high and lacks a well-developed upward trend. In addition, permeability is relatively homogeneous.

Permeability within the adjacent delta-front sandstone displays a very consistent upward-increasing trend. Permeability ranges from several millidarcys in the hummocky cross-stratified sandstones of the lower delta front to several hundred millidarcys in the swaley-stratified sandstones of the upper delta front.

Cedar Ridge Distal Delta-Front Architecture

Cedar Ridge II exposes a strike-oriented cross section of deltaic GS 5 approximately 2.5 mi seaward of South Muddy Creek. Distributary-channel deposits are absent here; the section is composed entirely of delta-front sediments. Strata consist of lower to upper shoreface facies associations that form a 40-ft upward-coarsening, bed-thickening sequence of interbedded sandstone and laminated to bioturbated mudstone. Lithofacies are strongly partitioned vertically into discrete intervals. A highly bioturbated interval lies at the base of the sequence and marks the maximum flooding surfaces across the preexisting deltaic unit. Gradationally overlying this interval



QAa941c

Figure 33. Permeability profiles and distributary-channel architecture from Cedar Ridge.

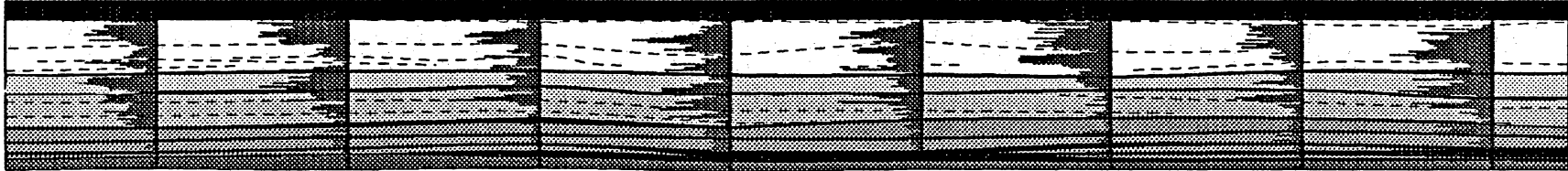
are lower delta-front deposits that consist of thinly interbedded very fine to fine-grained sandstones and laminated to bioturbated mudstones. Sandstone interbeds have a sharp erosive base overlain by cosets of hummocky cross-strata and are capped by a thin veneer of ripple stratification. The sequence is capped by a thick interval of extremely homogeneous fine-grained, well-sorted sandstone composed of amalgamated sets of hummocky to swaley cross-stratification. Lateral variation is minimal. Lithofacies thickness and distribution remain extremely constant across the section. The upward-coarsening grain size and regular vertical distribution of stratal types is attributed to a general shallowing of the water depth during deposition.

Cedar Ridge Distal Delta-Front Permeability Characteristics

Permeability variation in delta-front sandstones was examined in detail at Cedar Ridge canyon. Measurements were taken at 0.5-ft intervals along a series of vertical transects spaced every 50 ft. The relationship of permeability to architecture is shown in figure 34.

At the largest scale permeability displays a well-developed upward-increasing trend that reflects the vertical arrangement of lithofacies. Low-permeability bioturbated sandstones are overlain by wave-ripple and hummocky cross-stratified sandstones of intermediate permeability, which in turn are overlain by high-permeability swaley cross-stratified sandstones. Laterally, the upward-increasing permeability trend is extremely consistent across the section. Maximum permeabilities, located in the upper portion of the interval, consistently range between 400 and 450 md. Vertically, permeability variation decreases upward through the section. Lower delta-front deposits have the greatest lithofacies diversity and the greatest permeability variation. Conversely, upper delta-front deposits have low lithofacies diversity and a low degree of permeability variation.

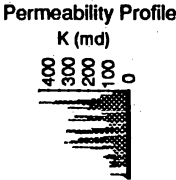
Ferron GS 5
Cedar Ridge Canyon
Delta front



EXPLANATION

- Upper shore face (dominantly swaley cross-strata)
- ▨ Middle shore face (dominantly hummocky cross-strata)
- ▩ Lower shore face (hummocky and ripple cross-strata)
- ▧ Intensely bioturbated sandstone
- Laminated siltstone/mudstone

Scale: 50 ft
No Vertical Exaggeration



QAa2408c

105

Figure 34. Permeability profiles and delta-front architecture from Cedar Ridge.

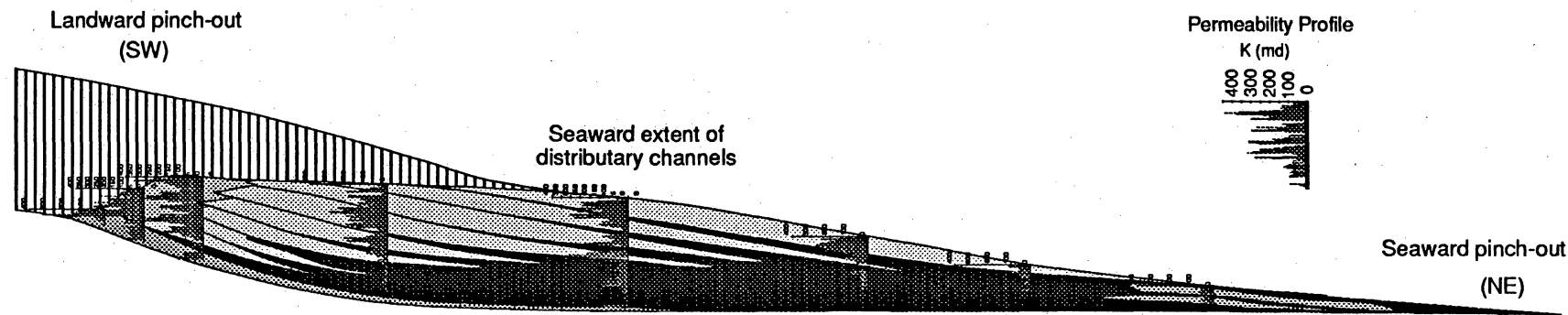
Regional Architecture and Permeability Relations

Delta-Front Sandstones

To investigate regional variation in sandstone geometry and permeability structure we collected data along a depositional profile from the landward pinch-out of shallow marine strata in Muddy Creek to the seaward extent of lower delta-front sandstones near Dry Wash, a distance of approximately 4 mi (fig. 35). Shallow marine strata consist of lower to upper shoreface associations. These are characterized by a 15- to 40-ft-thick upward-coarsening, bed-thickening sequence consisting of interbedded sandstone and laminated to bioturbated mudstone. Areally, the delta-front facies form a strike-aligned deposit elongated northwest to southeast. Along depositional strike, where the delta-front facies has not been removed by erosion, lateral variation in depositional characteristics is minimal. Lithofacies arrangements and thicknesses remain extremely constant and continuity of individual sand bodies is very high. Along depositional dip the cross-sectional geometry is characterized by a broadly lenticular sand body that gradually thins to a feather edge at the seaward extent and abruptly thickens at the landward pinch-out. Laterally extensive, thin mudstones divide the delta front into a series of offlapping seaward-dipping subunits. Individual subunits consist of amalgamated hummocky to swaley cross-strata overlain by a thin veneer of wave-ripple-stratified sandstone that displays a sharp to erosional basal contact and sharp to bioturbated upper contact. Subunits range from several feet to tens of feet thick. Lithofacies associations progressively change along depositional dip. Proceeding seaward from the landward pinch-out, swash and multidirectional trough cross-strata are replaced by upper shoreface swaley and hummocky cross-strata, which in turn are gradually replaced by the lower shoreface succession of interbedded hummocky and laminated to bioturbated mudstones.

Delta-front deposits are highly stratified vertically but extremely continuous laterally. The deposits display a well-developed upward-increasing grain-size distribution and bed-thickening trend. In a seaward direction the lower delta front thickens from a few feet near the landward pinch-out in Muddy Creek to more than 20 ft at Cedar Ridge. Upper delta-front deposits abruptly

Ferron GS 5 Delta front facies



107

EXPLANATION

- | | |
|---|--|
| <ul style="list-style-type: none"> Delta Plain Upper Shore face (Hummocky/Swaley) Foreshore (Swash laminations) | <ul style="list-style-type: none"> Slump Interval Lower Shoreface (Interbedded Sand/Silt) Transgressive (biotubated) |
|---|--|

SCALE:

 Hor. 1000 ft
 Ver. 20 ft

QAa2411c

Figure 35. Regional cross section along depositional dip displaying permeability profiles and delta-front architecture.

thicken (approximately 25 ft) near the landward pinch-out and gradually thin to the seaward pinch-out at Dry Wash. The preserved thickness of the delta front, however, is highly variable because overlying distributary channels eroded into the underlying deposits.

Permeability trends progressively change along depositional dip (fig. 35). Vertical permeability profiles display an upward-increasing trend that becomes more pronounced seaward. Near the landward pinch-out in Muddy Creek, zones of high permeability are present throughout the interval. However, seaward from this location high-permeability zones become increasingly restricted to the upper portion of the profile. Maximum permeabilities change along depositional dip. Between the landward pinch-out of the delta front in Muddy Creek and the seaward extent of distributary-channel influence near Cedar Ridge canyon, maximum permeabilities in the delta front remain near 400 to 450 md, whereas seaward of this position maximum permeabilities gradually decrease. Lateral permeability trends reflect the distribution of lithofacies caused by a gradual deepening of water depth during deposition. Within the delta front, permeability variation reflects the stacking of subintervals, each of which displays a general upward-increasing permeability trend except at the upper part of unit, where permeability slightly decreases.

This analysis of permeability variation in preserved sandstones is complicated by the fact that the overlying distributary channels erosively remove much of the delta front shortly after it is deposited. A comparison of the delta-front facies from Muddy Creek and Picture Flats, where much of the upper delta-front facies has been removed, with the delta-front facies at Cedar Ridge canyon, where the delta-front facies is intact, shows an increase in average permeability from about 50 md at Muddy Creek and Picture Flats to 130 md at Cedar Ridge. The comparison demonstrates that distributary channels selectively remove the upper, most permeable, part of the delta-front facies.

Distributary-Channel Sandstones

Detailed architectural and permeability analysis of distributary-channel facies along the depositional profile of a retrogradational delta cycle in the Ferron GS 5 reveals systematic changes in

channel morphology and permeability structure. The dynamic evolution of channel-belt architecture records a complete cycle of base-level fall and rise that corresponds to channel incision, expansion, and aggradation. In landward reaches, near the landward pinch-out of coeval delta-front facies, middle- and late-stage, expansive to aggradational macroforms are volumetrically dominant; in seaward channel reaches, early-stage, incised macroforms are volumetrically dominant. This overall landward onlap pattern displayed by early- to late-stage macroforms corresponds to changes in channel geometry, connectivity, and permeability structure.

A comparison of all measured distributary-channel sandstone dimensions (fig. 36) shows that late-stage channels are nearly twice as thick as early- or middle-stage channels and wider than most early- or middle-stage channels. However, late-stage channels are relatively rare in Ferron GS 5. Early- and middle-stage channels have the same range of lateral dimensions, but early-stage channels are generally thicker than middle-stage distributary channels (fig. 36). These geometric differences between channel types reflect differences in depositional and preservation processes as well as differences in the facies tract. Comparing channel dimensions of early-stage channels at the three locations (fig. 37) shows that the preserved channel deposits are widest and thickest at the seaward extent of the depositional system; they become progressively thinner and narrower landward. Middle-stage channel sandstones occur only at the Muddy Creek and Picture Flats locations. Middle-stage channel dimensions do not differ significantly between the middle (Picture Flats) and the landward limit (Muddy Creek) of channel deposition in the facies tract (fig. 38). Late-stage channels occur only at the Muddy Creek outcrop. We cannot document regional changes in late-stage channel geometry.

Variations in distributary-channel dimensions at a fixed point in the facies tract can be examined at Muddy Creek and Picture Flats; only early-stage channels were deposited at Cedar Ridge. In Muddy Creek canyon, preserved early-stage channel deposits are generally not as laterally extensive as those in middle-stage channels; however, the two channel types are approximately equally thick (fig. 39). Near the center of the facies tract at Picture Flats, early-stage channels are wider and thicker than middle-stage channels (fig. 40).

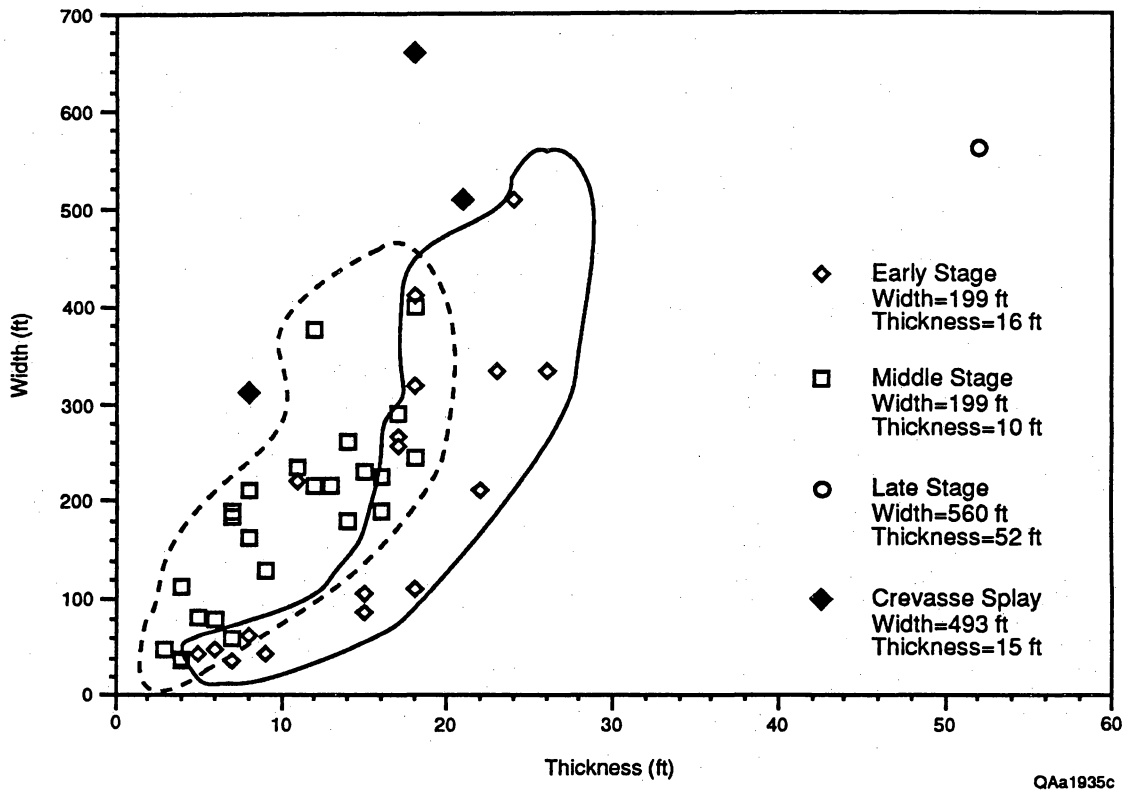


Figure 36. Comparison of channel dimensions for early-, middle-, and late-stage distributary channels.

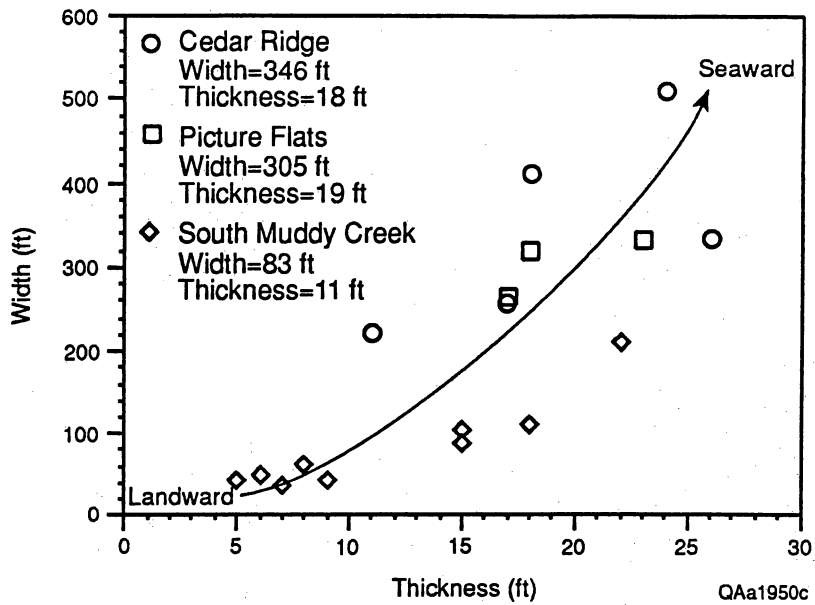


Figure 37. Comparison of early-stage distributary-channel dimensions at Muddy Creek, Picture Flats, and Cedar Ridge. Dimensions of early-stage distributary channels increase systematically from landward to seaward.

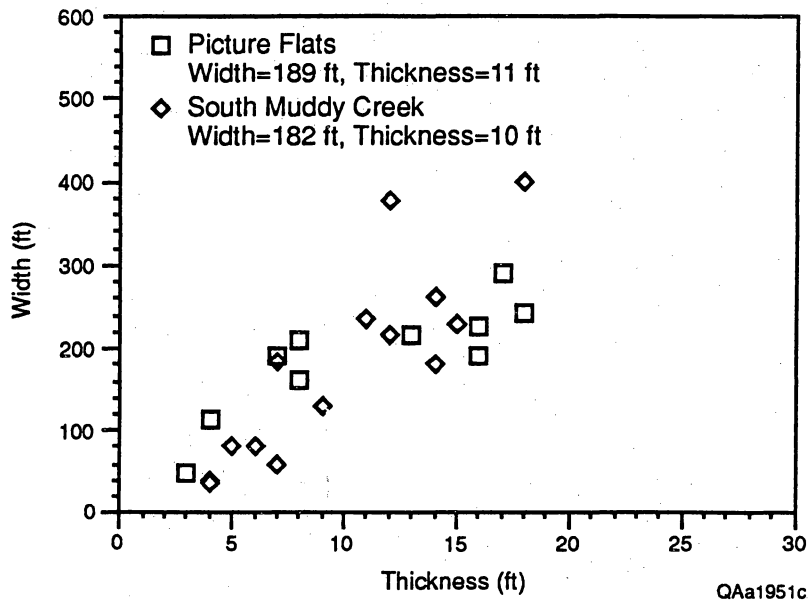
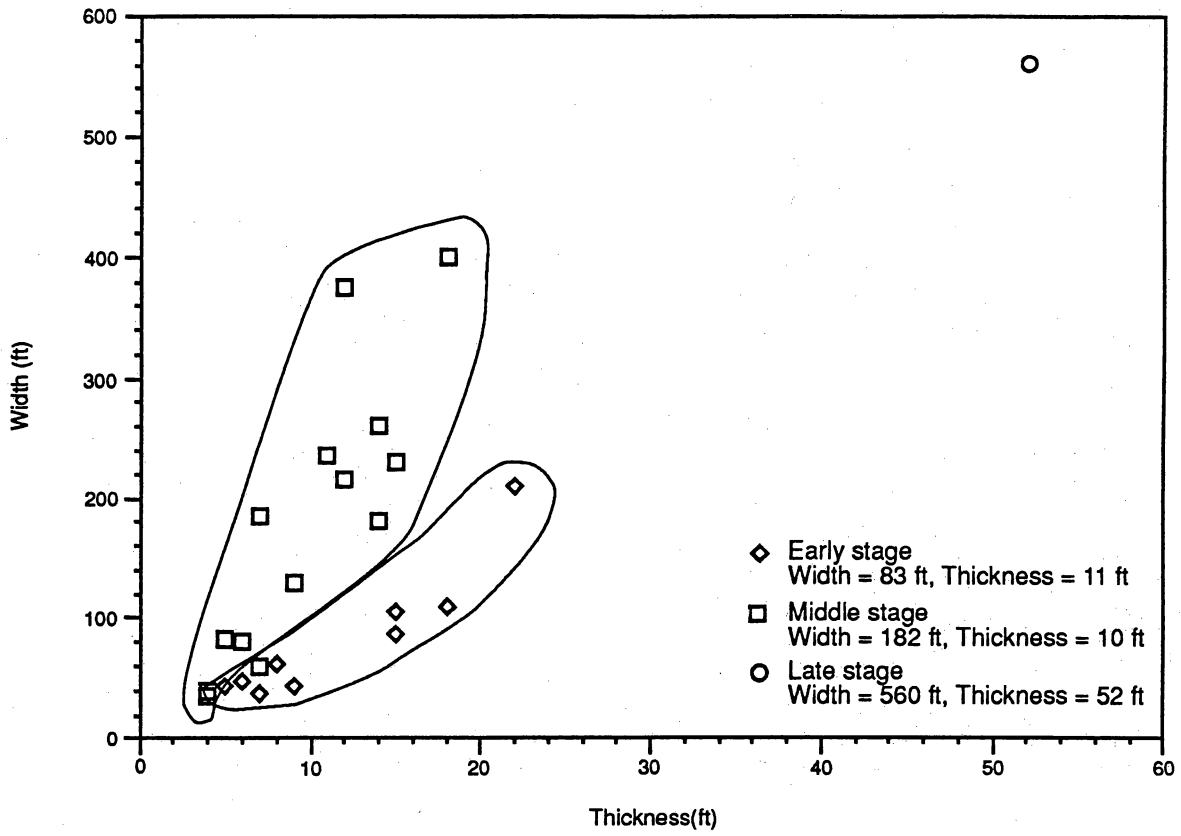
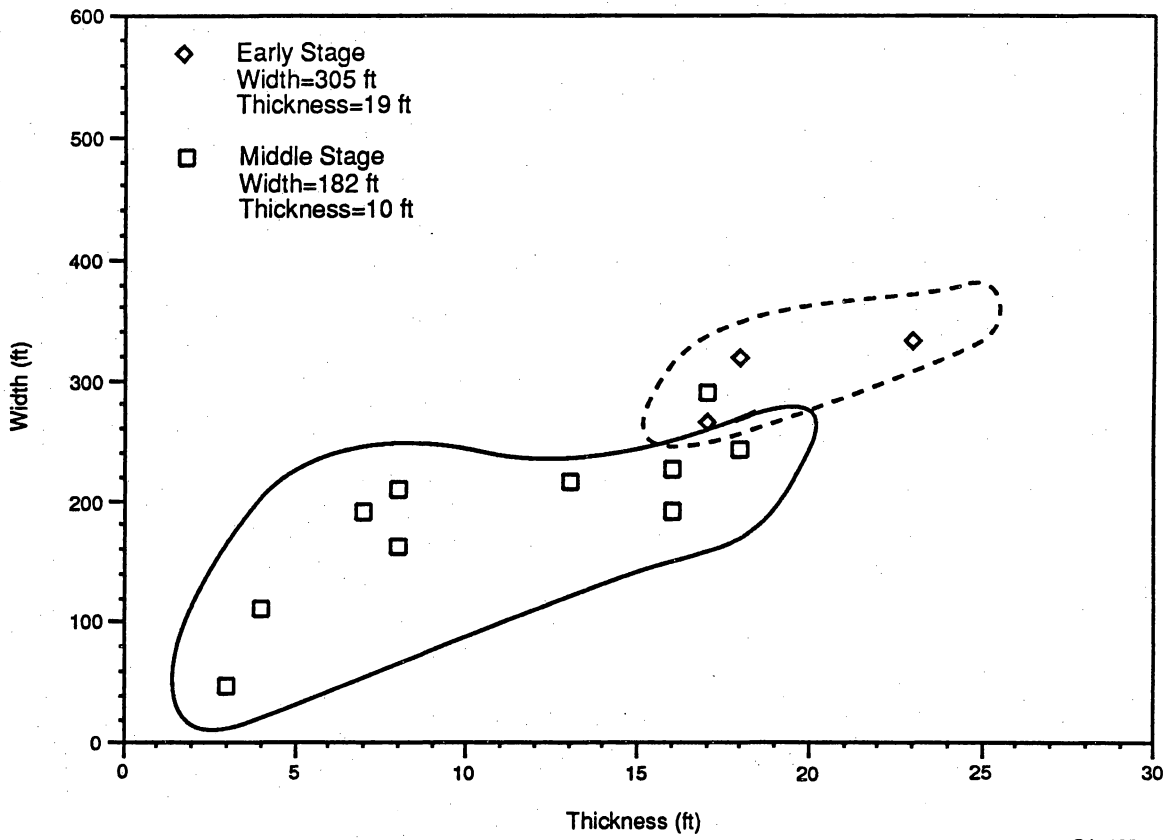


Figure 38. Comparison of middle-stage distributary-channel dimensions at Muddy Creek and Picture Flats. Dimensions of middle-stage distributary channels do not significantly change from landward limit to center of the facies tract.



QAa1952c

Figure 39. Comparison of early-, middle-, and late-stage distributary-channel dimensions at Muddy Creek. Middle-stage distributary channels are generally wider and thinner than early-stage channels.



QAa1953c

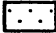




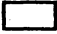





Figure 40. Comparison of distributary-channel dimensions at Picture Flats. Early-stage distributary channels are thicker and wider than middle-stage channels.

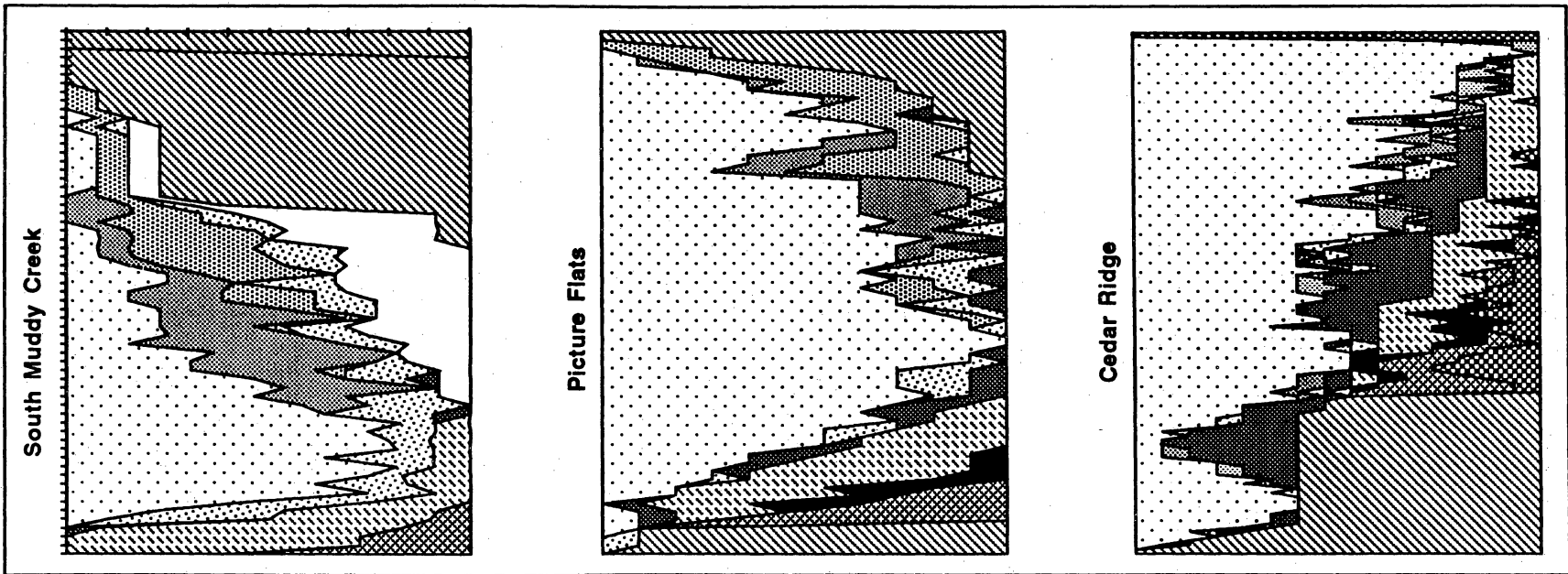
Variations in the geometry of distributary-channel sandstones that reflect both channel type and position along the facies tract affect permeability structure. At Cedar Ridge where early-stage distributary channels deeply erode into delta-front deposits, channel complexes are composed of laterally restricted multilateral channel forms that are separated from each other by thick, laterally extensive mudstones. Channel forms contain a high proportion of trough cross-strata, and permeability is uniformly high throughout the channel fill (fig. 33). Upstream from this locality, early-stage channels are overlain by middle-stage, laterally expansive channel forms. At Picture Flats, channels are composed of subequal amounts of early-, middle-, and late-stage channel forms arranged in a multilateral to multistoried fashion. Zones of high permeability are erratically distributed throughout the channel fill (fig. 32). At Muddy Creek, near the landward pinch-out of coeval delta-front deposits, middle- to late-stage distributary-channels dominate. Channel complexes are composed of multilateral channel forms that vary laterally from thick, aggrading channels to thin, laterally expansive channels. Strong vertical partitioning of lithofacies results in a well-developed upward-decreasing permeability trend that is disrupted by inclined, low-permeability mud-clast lag deposits (fig. 29).

Regional Variations in Distributary-Channel Lithofacies Proportions, Macroform Types, and Sandstone Architecture

Lithofacies proportion curves of distributary-channel deposits at each locality characterize seaward changes in the vertical arrangement lithofacies associations (figs. 41 and 42). The proportion of both high (trough crossbedded) and low (bounding elements) permeability lithofacies progressively increases in a seaward direction.

Along with these systematic changes in sandstone architecture, average permeability increases but the degree of interconnectedness between channel forms decreases. In addition, the degree of vertical lithofacies partitioning decreases seaward. Overall vertical permeability trends shift from upward-decreasing in landward portions to uniform or erratic in seaward portions (figs. 29, 32, and 33). In a seaward direction, mean permeability and lateral continuity increase as the volume of

-  Trough cross-strata
-  Low-angle strata
-  Ripple cross-strata
-  Lag deposits
-  Mud/silt
-  Abandoned channel fill
-  Delta plain
-  Hummocky cross-strata
-  Ripple stratification (delta front)
-  Bioturbated sediments
-  Mud/silt (delta front)



QAa1203c

Figure 41. Comparison of vertical lithofacies proportion curves within GS 5 from South Muddy Creek, Picture Flats, and Cedar Ridge.

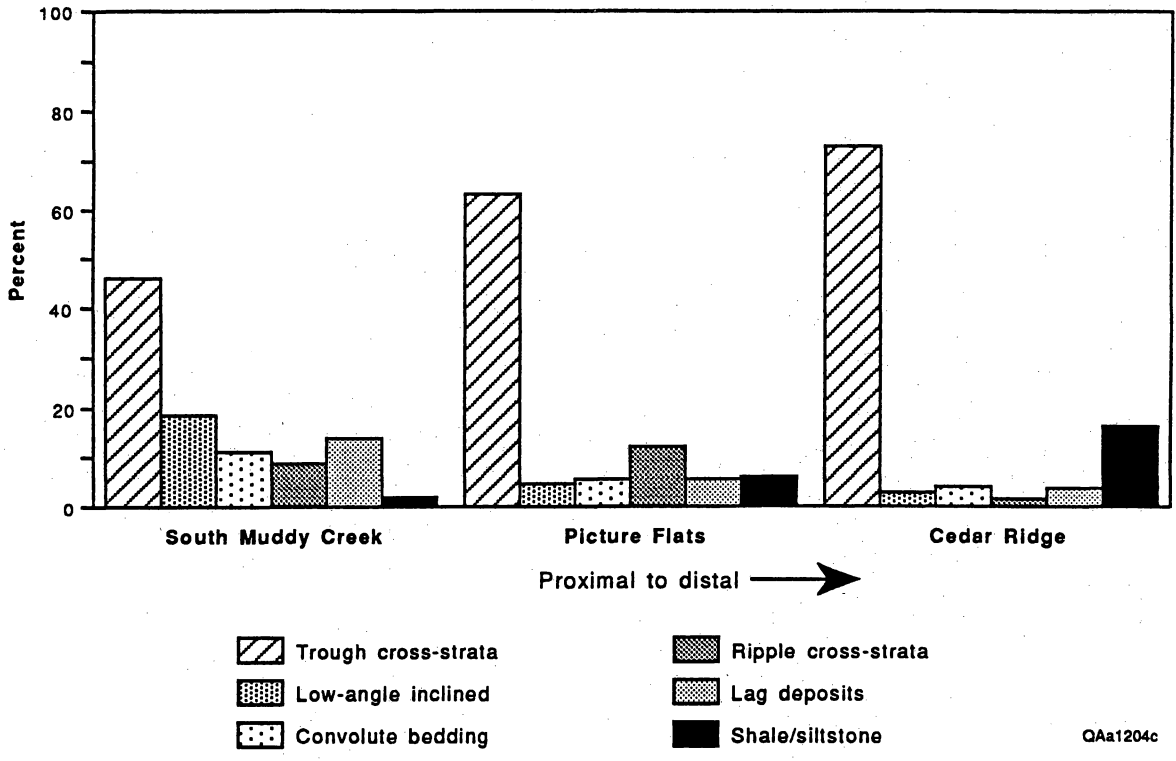


Figure 42. Comparison of stratal diversity within distributary-channel facies between South Muddy Creek, Picture Flats, and Cedar Ridge.

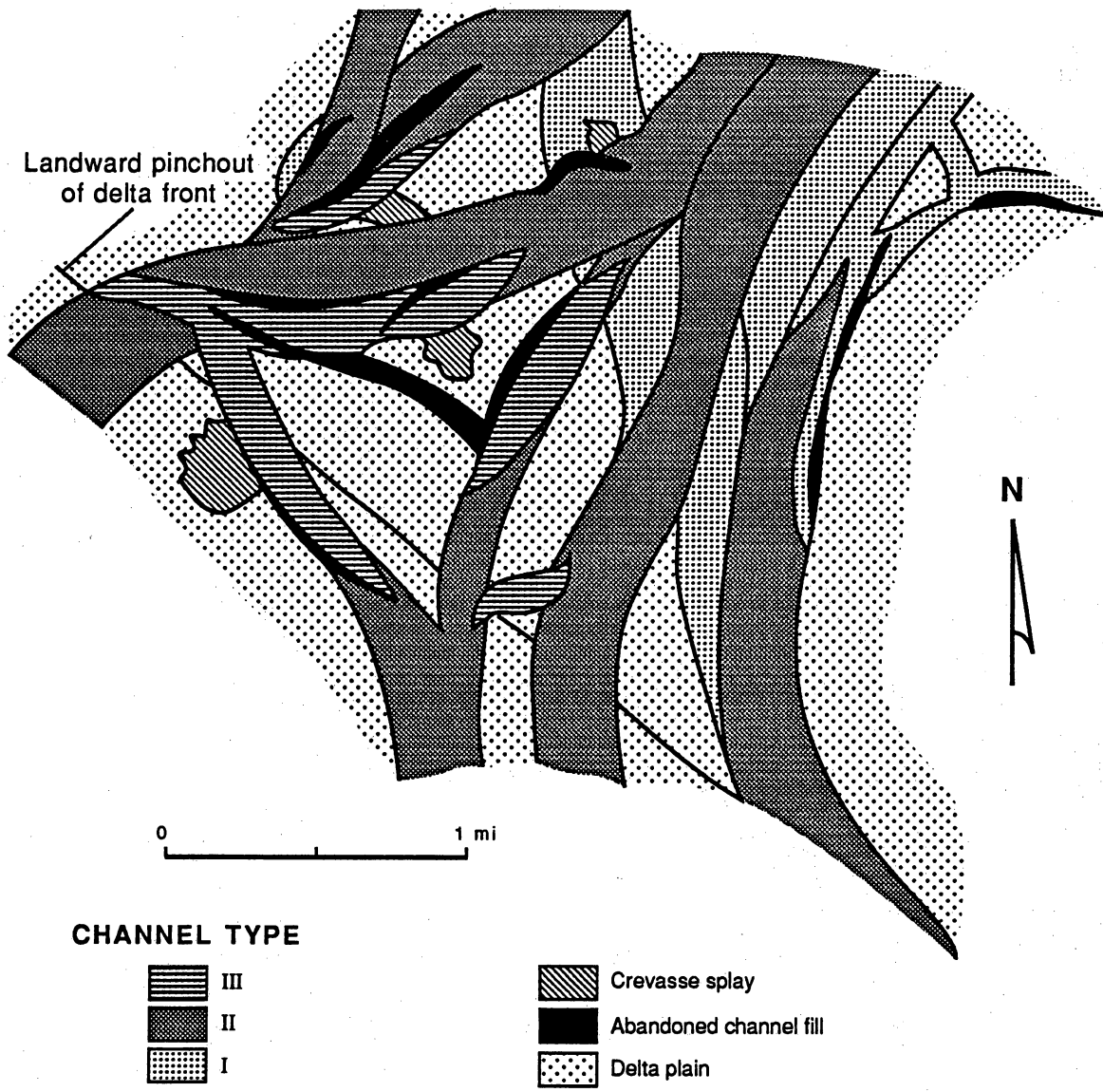
early-stage distributary-channel facies increases. Early-stage distributary channels average 700 md, compared with 300 md in late-stage distributary channels. Internally, early-stage macroforms are relatively homogeneous, displaying uniformly high permeabilities. In the landward section of the facies tract, dominant middle- and late-stage macroforms have higher stratal diversity and greater overall permeability variation. However, the thickness and lateral extent of low-permeability strata separating individual channels increases seaward. Early-stage macroforms are poorly interconnected vertically and are segmented by laterally continuous mudstones. Landward, middle- and late-stage macroforms are separated by extensive, discontinuous, and low-permeability mud-clast lag deposits.

Therefore, the regional trend in distributary-channel sandstones is from relatively low-permeability late- and middle-stage channel complexes with good vertical connection near the landward limit to high-permeability early-stage channel complexes with poor vertical connection between individual channel sandstones near the seaward limit of deposition. Thick, late-stage channels are found only near the landward limit of distributary-channel deposition, whereas the widest and most permeable channel sandstones are well-preserved, early-stage channels deposited near the seaward limit of the facies tract.

IMPLICATIONS FOR INFILL DRILLING

Selective or targeted infill drilling within known natural gas fields and plays can be an effective and cost-efficient way to increase recovery of an important energy resource. Outcrop characterization studies of the Ferron Sandstone provide guidelines to maximize the yield of additional wells in areas of known gas production.

Outcrop characterization of Muddy Creek, Picture Flats, and Cedar Ridge canyons, combined with intercanyon tracing of channel and interchannel sandstones, provides a field-scale map of architectural sandstone relations in the landward-stepping Ferron GS 5 (fig. 43). Permeability measurements show that the best reservoir analog sandstones reside in the distributary-channel deposits; delta-front, shoreface, and transgressive sandstones have a mean permeability that is an



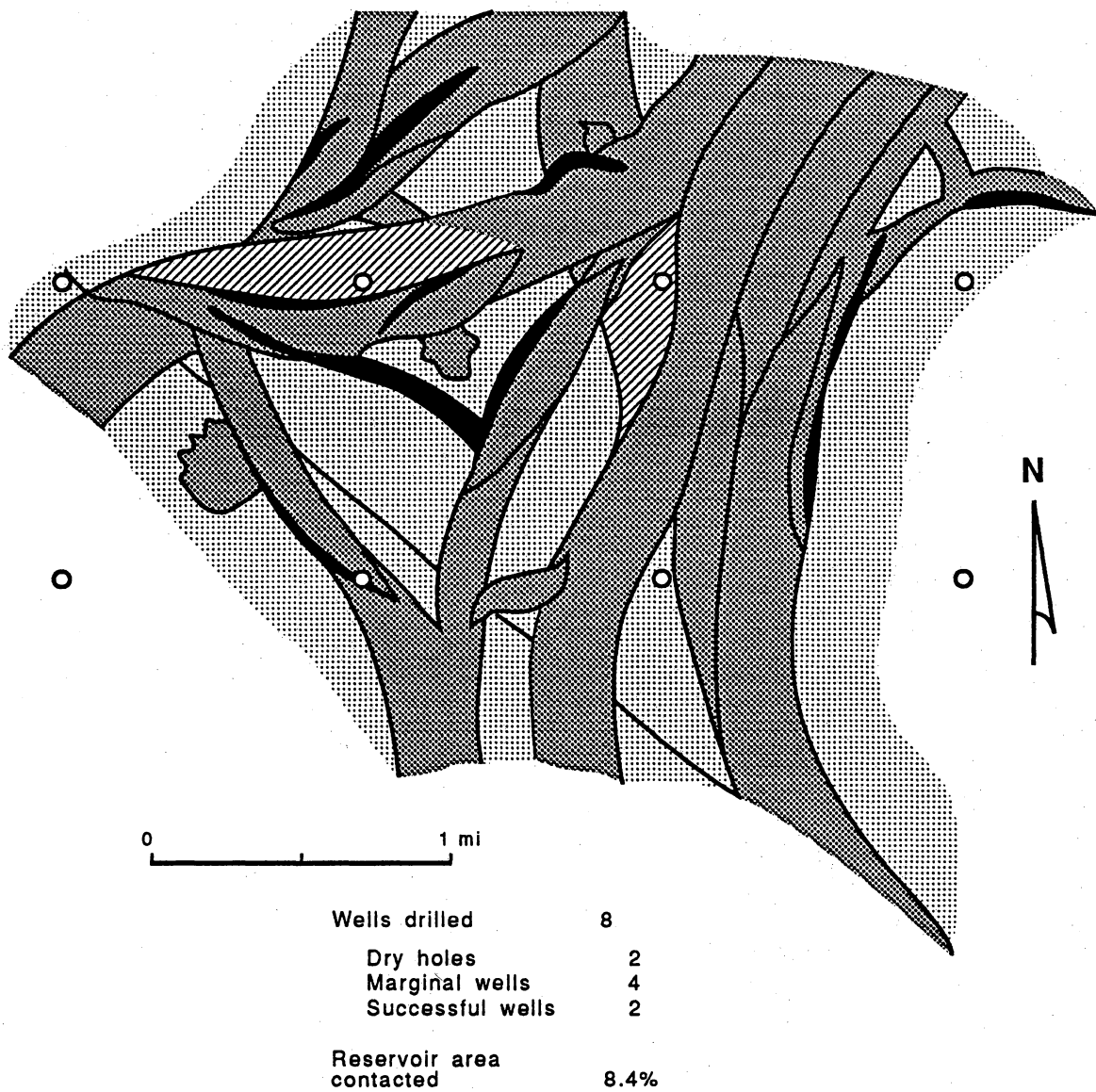
QAa949c

Figure 43. Map of distributary-channel and interdistributary strata in Ferron GS 5 from the landward extent near Muddy Creek to the seaward limit near Cedar Ridge.

order of magnitude lower. Because GS 5 is a landward-stepping sequence, it is laterally compressed and extends only about 4 mi from landward to seaward pinch-out. Distributary-channel sandstones, the drilling targets, have complex geometries and are poorly interconnected at the between-well scale.

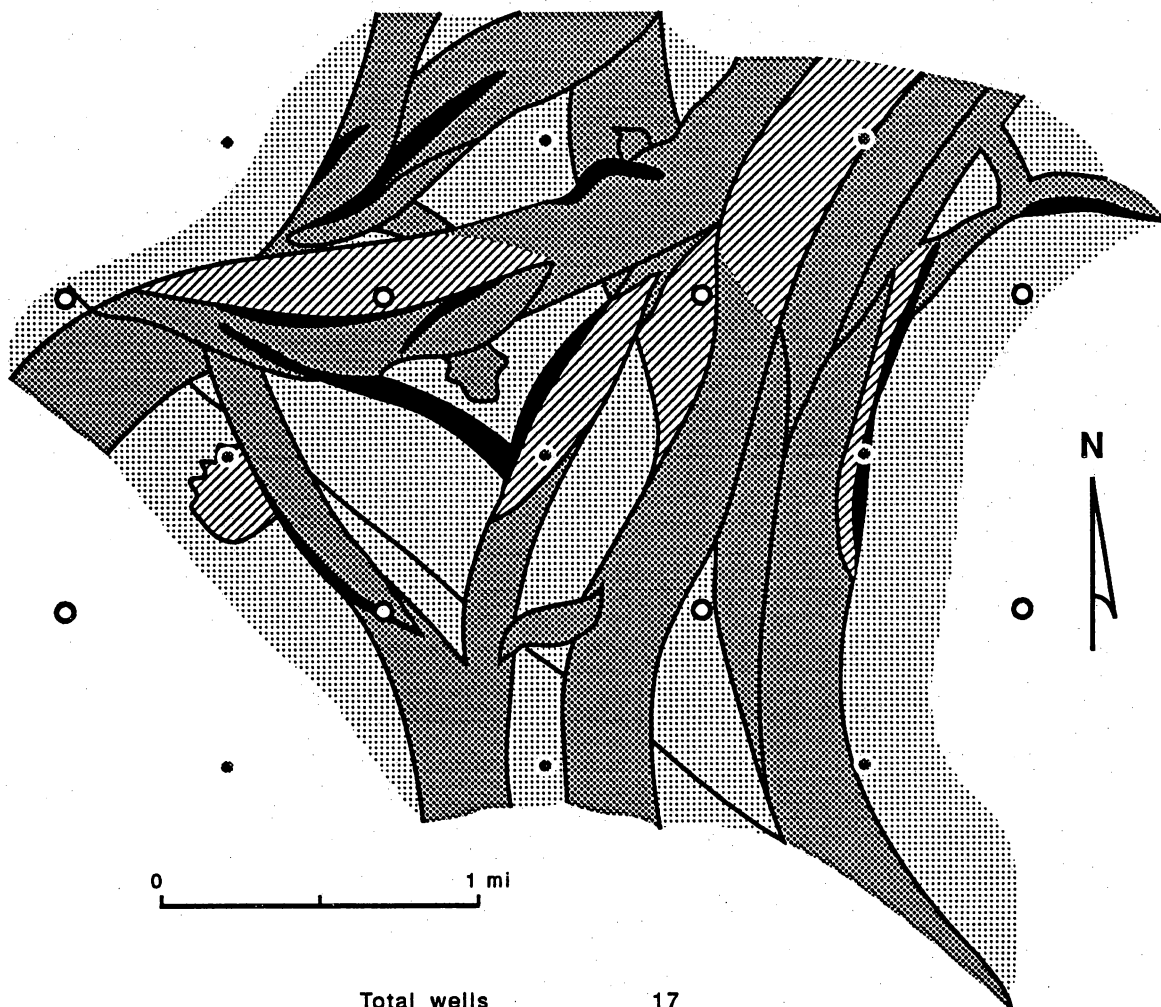
Assuming burial and gas migration into the Ferron reservoir analog and using this hypothetical reservoir to evaluate the degree of contact in a conventional infill drilling program, we undertook an analysis of infill drilling effectiveness. Drilling at 640-acre spacing (fig. 44) requires eight wells and produces two successful wells in the channel complex, four marginal wells in the delta-front complex, and two dry holes. Only 8.4 percent of the most productive reservoir (distributary-channel sandstones) area is contacted. Drilling at 320-acre spacing (fig. 45) requires an additional nine wells and adds only two successful completions in distributary-channel sandstones. The total productive reservoir area contacted is increased to 20.3 percent. Infill drilling at 160-acre spacing (fig. 46) adds 16 new wells, of which 7 are successful, 7 are marginal, and 2 miss the mapped fluvial-deltaic complex. After drilling at 160-acre spacing, only 40.6 percent of the productive reservoir target has been contacted.

This exercise demonstrates that landward-stepping fluvial-deltaic sandstones are difficult targets for infill drilling unless there are means to image the distributary-channel distributions. The facies tract is significantly compressed, delta-front sandstones have low permeability, and distributary channels, the primary locus of reservoir-quality sandstones, are laterally complex and poorly interconnected. Additional exploration tools such as cross-well tomography or three-dimensional seismic surveys, integrated with geologic and facies architectural modeling, would probably be cost efficient in such geologic settings and would reduce the expense of drilling additional wells at conventional spacings.



QAa950c

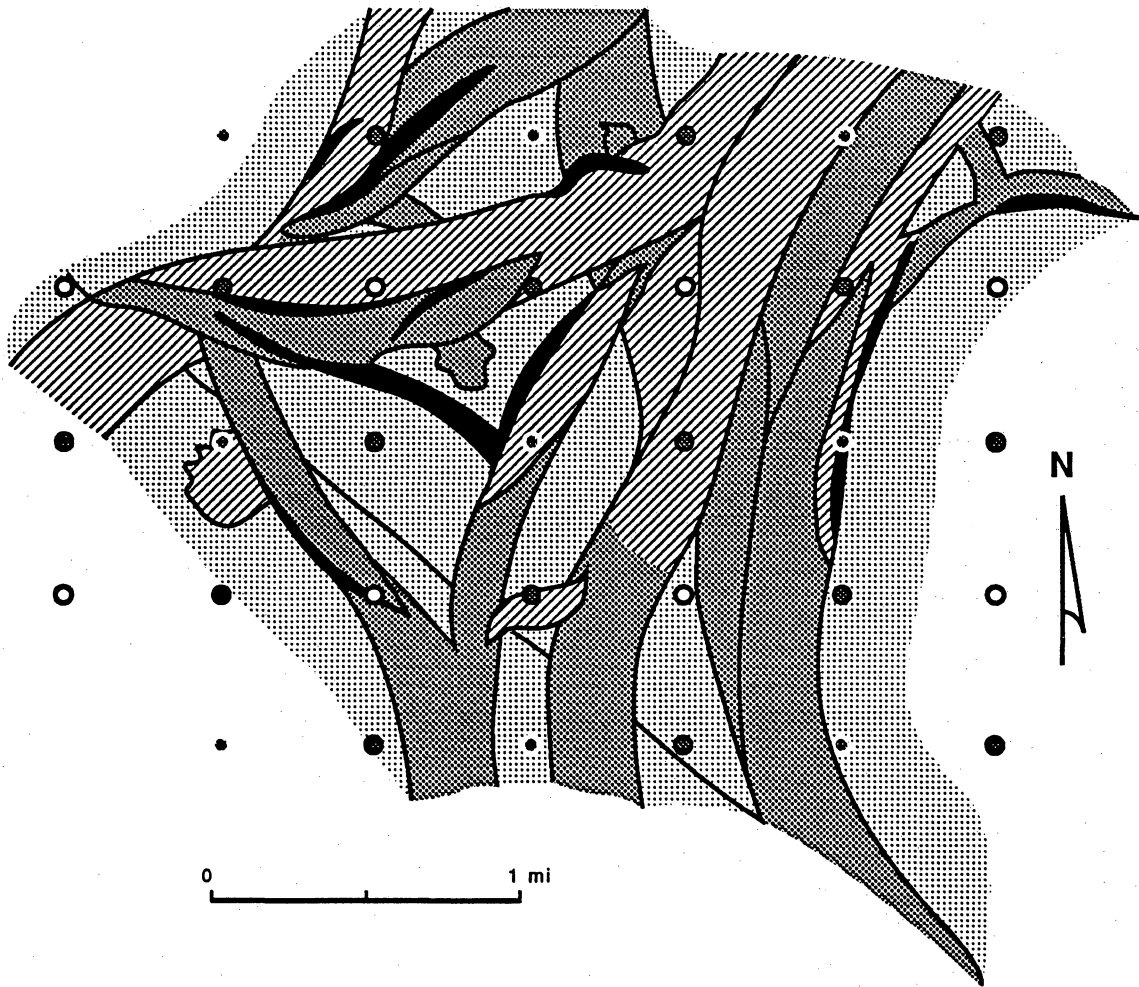
Figure 44. Map of distributary-channel and interdistributary strata in Ferron GS 5 from the landward extent near Muddy Creek to the seaward limit near Cedar Ridge showing the effects of conventional infill drilling. Drilling Ferron GS 5 at 640-acre spacing produces two wells in the distributary-channel complex, two wells in interdistributary muds, and four wells in the delta-front sandstones.



Total wells	17
New wells drilled	9
Dry holes	2
Marginal wells	5
Successful wells	2
Incremental contact	11.9%
Total reservoir contacted	20.3%

QAa951c

Figure 45. Map of distributary-channel and interdistributary strata in Ferron GS 5 from the landward extent near Muddy Creek to the seaward limit near Cedar Ridge showing the effects of conventional infill drilling. Drilling Ferron GS 5 at 320-acre spacing produces an additional two wells in the distributary-channel complex.



Total wells	33
New wells drilled	16
Dry holes	2
Marginal wells	7
Successful wells	7
Incremental contact	20.3%
Total reservoir contacted	40.6%

QAa952c

Figure 46. Map of distributary-channel and interdistributary strata in Ferron GS 5 from the landward extent near Muddy Creek to the seaward limit near Cedar Ridge showing the effects of conventional infill drilling. Drilling Ferron GS 5 at 160-acre spacing adds 16 new wells, of which 7 contact the distributary-channel complex.

SUMMARY AND CONCLUSIONS

We conducted a comprehensive, integrated outcrop characterization of the Ferron Sandstone in central Utah to better understand the complexity of sandstone reservoirs and to improve the efficiency of natural gas recovery from known reservoirs, fields, and plays. The Ferron Sandstone is ideal for such an outcrop study because it was deposited in environments similar to those of sandstone reservoirs in the Texas Gulf Coast, it is well exposed both parallel and perpendicular to sediment transport direction by a series of bifurcating canyons, and it has a well-documented sequence stratigraphic setting.

Our study combined quantification of sandstone, mudstone, and shale geometry of strata exposed near the landward limit, central position, and seaward limit of fluvial-deltaic sediments with field measurements of permeability, petrographic and petrophysical characterization, and geostatistical analysis of permeability relations. This report summarizes findings for architectural, petrographic, and permeability investigations of the landward-stepping Ferron GS 5 sandstone. Results of equivalent studies of the seaward-stepping Ferron GS 2 and of the petrophysical investigations are presented in separate documents.

Major conclusions of this study are the following:

1. The landward-stepping, wave-modified deltaic facies tract is laterally compressed, extending less than 4 mi from the landward limit of delta-front deposits to the seaward limit of distributary-channel influence.
2. In landward-stepping (wave-modified) Ferron GS 5, the delta-front facies consists of a series of offlapping sand bodies that dip gently seaward and are highly vertically compartmentalized. Offlapping sigmoidally shaped sand bodies are poorly connected to each other but are well integrated internally. Lateral and vertical continuity is disrupted by overlying fine-grained bounding surfaces and by distributary-channel deposits that locally erode deeply into the delta-front sandstones. Both mean permeability and permeability variability of the delta front are significantly lower than they are in

distributary-channel sandstones. Because most of the sand in the landward-stepping genetic sequence resides in the distributary-channel system, and because permeability is generally higher in the channels, our study of the Ferron GS 5 as a reservoir analog focused on the distributary-channel sandstones.

3. Detailed facies analysis indicates three stages of channel development. The early stage of channel-belt evolution reflects channel incision into delta-front and shoreface deposits, the middle stage is characterized by lateral expansion, and the late stage records aggradation. In turn, each stage of channel development is characterized by a distinctive geometry, lateral extent, internal architecture, and predictable position within the facies tract. Early-stage channels are thin and narrow in the landward portion of the facies tract, becoming thicker and much wider near the seaward limit of the facies tract. Middle-stage channel deposits have approximately the same width-to-thickness ratio from landward to seaward extent of the facies tract. Late-stage channel deposits are both wide and thick; however, they are isolated from each other and from middle-stage channels by low-permeability overbank and delta-plain mudstones and shales. As a result of this orderly arrangement of distributary-channel types, facies architecture and permeability patterns are predictable both laterally and vertically within the genetic sequence.
4. Middle-stage distributary-channel belts, the volumetrically most important type in Ferron GS 5, overlap and crosscut each other. Because of the common presence of mud chips and mudstones along bounding surfaces within and between individual channel deposits, middle-stage distributary-channel sandstones are separated from each other and are internally segmented by low-permeability bounding elements. This architecture will result in a complex reservoir structure. Large reservoir compartments in late-stage distributary channels will exist in close proximity to smaller isolated compartments of the middle-stage distributary-channel complex. Reservoir flow units will have a range of volumes, a multicompartment response, and significant support volume.

5. A strong and predictable relation exists between permeability, macroforms, and sedimentary facies type. Facies and lithofacies define distinctive permeability characteristics and correlation structure. Our study demonstrates that lithofacies and macroforms are the fundamental building blocks of both sandstones and sandstone reservoir models. Permeability relations within lithofacies and macroforms are consistent throughout the facies tract. However, syndepositional erosion and truncation of earlier deposits greatly modifies both preservation of lithofacies and macroforms and the resulting permeability structure.
6. Permeability characteristics and structure are scale dependent. Changes in the variance, distribution type, and correlation structure closely reflect geologic scales of heterogeneity. Statistical tests show that stratal types or lithofacies display the highest degree of permeability stationarity. Consequently, permeability variation and patterns at higher levels of stratal organization reflect variation in the proportion and arrangement of lithofacies or stratal types.
7. Permeability characteristics are transferable between locality within the facies tract but not between sequences; that is, permeability characteristics of trough cross-stratified sandstones in GS 5 are not directly comparable to trough cross-stratified sandstones in GS 4. These results indicate that although depositional process are the primary control at the flow unit scale, diagenetic processes are important at the pore and field-to-reservoir scale (that is, within lithofacies and between genetic sequences). Furthermore, these results demonstrate that in a comparable field situation, reservoir properties should be calibrated to rock type for each genetic sequence.
8. Although the Ferron Sandstone complex was buried to depths of approximately 10,000 ft, it was never subjected to temperatures greater than about 65° to 80°C. Consequently, the diagenetic overprint is mild and both detrital and diagenetic mineralogy correlate well with depositional facies. Furthermore, mineralogy correlates predictably with permeability variations from landward to seaward positions in the depositional system.

9. The distribution of distributary-channel types, the degree of internal sandstone organization, the segregation of mud from sand within and between channel macroforms, the sandstone mineralogy, and the permeability structure of landward-stepping distributary-channel sandstones are sufficiently different from those of seaward-stepping sandstones that landward-stepping systems can be identified on the basis of well logs and other conventional exploration tools.
10. A good correlation in permeability characteristics exists between the outcrop and nearby core samples. Thus, surface weathering has not severely altered the permeability characteristics, and Ferron outcrops are suitable reservoir analogs for investigating permeability relations. Using the Ferron GS 5 sandstone as a model for field-scale infill drilling shows that only about 40.6 percent of the total potential reservoir rock would be contacted at 160-acre spacing. Conventional infill drilling patterns yield only poor incremental reservoir contact. For this reason, landward-stepping fluvial-deltaic reservoirs are excellent candidates for targeted infill drilling. A drilling program based on the architectural and permeability relations reported here and complemented by three-dimensional seismic surveys could provide substantial reserve growth from mature Gulf Coast Tertiary natural gas reservoirs.

In summary, this investigation shows that outcrop characterization studies conducted within a sequence stratigraphic framework are a simple and powerful tool for understanding sandstone reservoir heterogeneity. Fundamental properties of natural gas reservoirs, such as sand body dimensions and internal complexity, mineralogy, permeability mean and distribution type, and arrangement of low-permeability strata, vary systematically from landward to seaward extent of the depositional system.

ACKNOWLEDGMENTS

This study was funded by the Gas Research Institute, contract number 5089-260-1902, and cofunded by the Department of Energy, contract number DE-FG22-89BC-14403. We thank GRI Project Manager Anthony Gorody for his support and guidance throughout the project.

Summer field assistants Todd Muelhoeser, Chuck Cluck, and Sam Epstein helped with mapping and minipermeameter measurements. Field assistant Ted Angle contributed significantly to all aspects of the research throughout the three-year project. Discussions with Mike Gardner, Rex Cole, Rob Finley, Larry Lake, Mark Miller, Jon Holder, Dennis Nielson, and Lee Allison improved our understanding of the Ferron Sandstone, geostatistics, and petrophysics. We greatly appreciate the hospitality of the residents of Castle Valley, Utah.

Others contributing to the publication of this report were Bobby Duncan, editing, Susan Lloyd, word processing, and Jamie Coggin and Margaret Evans, design and pasteup. Kerza Prewitt and Joel Lardon drafted the figures under the supervision of Dick Dillon. Diane Spinney, Rick Edson, Rodney Heathcott, and Joseph Yeh helped with the various computer applications.

REFERENCES

- Allen, J. R. L., 1965, A review of the origin and characteristics of recent alluvial sediments: *Sedimentology*, v. 5, p. 89-191.
- Allen, J. R. L., 1966, On bed forms and paleocurrents: *Sedimentology*, v. 6, p. 153-190.
- Allen, J. R. L., and Banks, N. L., 1972, An interpretation and analysis of recumbent-folded deformed cross-bedding: *Sedimentology*, v. 19, p. 257-283.
- Allen, P. A., and Underhill, J. R., 1989, Swaley cross-stratification produced by unidirectional flows, Bencliff Grit (U. Jurassic), Dorset, U.K.: *Journal of the Geological Society of London*, v. 146, p. 241-252.
- Almendinger, R. W., Sharp, J. W., Tish, D. V., Serpa, L., Brown, L., Kaufman, S., Oliver, J., and Jordan, T. E., 1983, Cenozoic and Mesozoic structure of the eastern Basin and Range province, Utah, from COCORP seismic-reflection data: *Geology*, v. 1, p. 532-536.
- Armstrong, R. L., 1968, Sevier orogenic belt in Nevada and Utah: *Geological Society of America Bulletin*, v. 79, 429-458.
- Brown, L. F., Jr., Solis-Iriarte, R. F., and Johns, D. A., 1990, Regional depositional systems tracts, paleogeography, and sequence stratigraphy, upper Pennsylvanian and lower Permian strata, north- and west-central Texas: The University of Texas at Austin, Bureau of Economic Geology Report of Investigations No. 197, 116 p.
- Chandler, M. A., Kocurek, G. A., Goggin, D. J., and Lake, L. W., 1989, Effects of stratigraphic heterogeneity on permeability in eolian sandstone sequence, Page Sandstone, Northern Arizona: *American Association of Petroleum Geologists Bulletin*, v. 5, p. 658-668.
- Clifton, H. E., 1969, Beach lamination—nature and origin: *Marine Geology*, v. 7, p. 553-559.
- Cotter, E., 1975, Deltaic deposits in the Upper Cretaceous Ferron Sandstone, Utah, in Broussard, M. L. S., ed., *Deltas, models for exploration*: Houston Geological Society, p. 471-484.
- Davis, L. J., 1954, Stratigraphy of the Ferron Sandstone: *Intermountain Association of Petroleum Geology Fifth Annual Field Guidebook*, p. 55-58.
- Davis, R. A., Jr., 1983, *Depositional systems: a genetic approach to sedimentary geology*: Englewood Cliffs, New Jersey, Prentice-Hall, 669 p.
- Doelling, H. H., 1972, Central Utah coal fields, Sevier-Sanpete, Wasatch Plateau, Book Cliffs, and Emery: *Utah Geological and Mineralogical Survey, Monograph Series No. 3*, p. 571.
- Dott, R. H., Jr., and Bourgeois, J., 1982, Hummocky stratification: significance of its variable bedding sequences: *Geological Society of America Bulletin*, v. 93, p. 663-680.
- Dreyer, T. A., Scheie, A., and Walderhaug, O., 1990, Minipermeameter-based study of permeability trends in channel sand bodies: *American Association of Petroleum Geologists Bulletin*, v. 74, no. 4, p. 359-374.
- Fisher, R. S., Tyler, Noel, Barton, M. D., Miller, M. A., Sepehrnoori, Kamy, Holder, Jon, and Gray, K. E., 1992, Quantification of flow unit and bounding elements properties and geometries, Ferron Sandstone, Utah: implications for heterogeneity in Gulf Coast Tertiary deltaic sandstones: The University of Texas at Austin, Bureau of Economic Geology, annual report prepared for the Gas Research Institute (GRI-92/0072), 160 p.

- Folk, R. L., 1974, Petrology of sedimentary rocks: Austin, Texas, Hemphill Publishing Company, 182 p.
- Friend, P. F., 1983, Towards a field classification of alluvial architecture or sequence: *Sedimentology*, v. 6, p. 345-354.
- Gardner, M. H., 1991, Sequence stratigraphy of the Ferron Sandstone, east-central Utah, *in* Tyler, Noel, Barton, M. D., and Fisher, R. S., eds., Architecture and permeability structure of fluvial-deltaic sandstones: a field guide to selected outcrops of the Ferron Sandstone, east-central Utah: The University of Texas at Austin, Bureau of Economic Geology, guidebook prepared for 1991 field trips, p. 4-55.
- Gardner, M. H., 1993, Sequence stratigraphy of mid-Cretaceous strata, central Utah: Golden, Colorado, Colorado School of Mines, Ph.D. dissertation.
- Goggin, D. J., 1988, Geologically-sensible modeling of the spatial distribution of permeability in eolian deposits, Page Sandstone (Jurassic), northern Arizona: The University of Texas at Austin, Ph.D. dissertation, 418 p.
- Hale, L. A., 1972, Depositional history of the Ferron Formation, central Utah, *in* Plateau-Basin and Range transition zone: Utah Geological Association, p. 29-40.
- Hale, L. A., and Van De Graaf, F. R., 1964, Cretaceous stratigraphy and facies patterns—northeastern Utah and adjacent areas: Intermountain Association of Petroleum Geologists Thirteenth Annual Field Guidebook, p. 115-138.
- Hamblin, A. P., and Walker, R. G., 1979, Storm-dominated shelf deposits: the Fernie-Kootenay (Jurassic) transition, southern Rocky Mountains: *Canadian Journal of Earth Sciences*, v. 16, p. 1673-1690.
- Harms, J. C., Southard, J. B., Spearing, D. R., and Walker, R. G., 1975, Depositional environments as interpreted from primary sedimentary structures and stratification sequences: SEPM Short Course No. 2.
- Hayes, M. O., 1967, Hurricanes as geological agents: case studies of Hurricanes Carla, 1961, and Cindy, 1963: The University of Texas at Austin, Bureau of Economic Geology Report of Investigations No. 61, 56 p.
- Hintze, L. F., 1988, Geologic History of Utah: Provo, Utah, Brigham Young University Geology Studies, Special Publication 7, 202 p.
- Jackson, R. G., II, 1976, Depositional model of point bars in the lower Wabash River: *Journal of Sedimentary Geology*, v. 46, p. 579-594.
- Jensen, J. L., Lake, L. W., and Hinkley, D. V., 1986, A statistical study of reservoir permeability: Distributions, correlations, and averages: Society of Petroleum Engineers, SPE paper no. 14270, presented at the 60th Annual Technical Conference and Exhibition, Las Vegas, Nevada, September 22-25, 1985.
- Jones, J. R., Scott, A., and Lake, L. W., 1987, The geological aspects of reservoir characterization for numerical simulation, Mesaverde meanderbelt sandstone, northwestern Colorado: Society of Petroleum Engineers Formation Evaluation, March, p. 97-107.
- Katich, P. J., Jr., 1954, Cretaceous and early Tertiary stratigraphy of central and south-central Utah with emphasis on the Wasatch Plateau area: Intermountain Association of Petroleum Geologists Fifth Annual Field Guidebook, p. 42-54.

- Kittredge, M. G., 1988, Analysis of permeability variation—San Andres Formation (Guadalupian) Algrita Escarpment, Otera County, New Mexico: The University of Texas at Austin, Master's thesis, 361 p.
- Lawton, T. F., 1985, Style and timing of frontal thrust structures, thrust belt, central Utah: American Association of Petroleum Geologists Bulletin, v. 69, p. 1145–1159.
- Miall, A. D., 1985, Architectural-element analysis, a new method of facies analysis applied to fluvial deposits: Earth-Science Reviews, v. 222, p. 261–308.
- Miall, A. D., 1990, Principles of sedimentary basin analysis (2d ed.): New York, Springer-Verlag, 668 p.
- Miller, Mark A., Holder, Jon, and Gray, K. E., in preparation, Petrophysical property measurements and scale-up transforms, Ferron Sandstones, Central Utah.
- Mitchum, R. M., 1977, Seismic stratigraphy and global changes of sea level, part 1: glossary of terms used in seismic stratigraphy, *in* Payton, C. E., ed., Seismic stratigraphy—applications to hydrocarbon exploration: American Association of Petroleum Geologists Memoir 26, p. 205–212.
- Nadeau, P. H., and Reynolds, R. C., Jr., 1981, Burial and contact metamorphism in the Mancos Shale: Clays and Clay Minerals, v. 29, p. 249–259.
- Penland, S., Ramsey, K. E., McBride, R. A., Mestayer, J. T., and Westphal, K. A., 1988, Relative sea-level rise and delta-plain development in the Terrebonne Parish region: Louisiana Geological Survey, Coastal Geology Technical Report No. 4, 122 p.
- Ryer, T. A., 1981a, Deltaic coals of the Ferron Sandstone Member of the Mancos Shale predictive model for Cretaceous coal-bearing strata of the western interior: American Association of Petroleum Geologists Bulletin, v. 65, no. 11, p. 2323–2340.
- _____ 1981b, The Muddy and Quitcupah projects: a project report with descriptions of cores of the I, J, and C coals beds from the Emery coal field, central Utah: U.S. Geological Survey Open-File Report 81-460, 34 p.
- _____ 1982, Possible eustatic control on the location of Utah Cretaceous coal fields: Utah Geological and Mineralogical Survey, Bulletin 118, Proceedings, 5th ROMOCO Symposium, p. 89–93.
- _____ 1983, Transgressive-regressive cycles and the occurrence of coal in some Upper Cretaceous strata of Utah: Geology, v. 111, p. 207–210.
- Schmidt, Volkmar, and MacDonald, D. A., 1979, Texture and recognition of secondary porosity in sandstones, *in* Scholle, P. A., and Schluger, P. R., eds., Aspects of diagenesis: SEPM Special Publication No. 26, p. 209–226.
- Stalkup, F. I., and Ebanks, W. J., Jr., 1986, Permeability variation in a sandstone barrier island-tidal delta complex, Ferron Sandstone (Lower Cretaceous), central Utah: Society of Petroleum Engineers, SPE paper no. 15532, p. 1–8.
- van Veen, F. R., 1977, Prediction of permeability trends for water injection in a channel-type reservoir, Lake Maracaibo, Venezuela: Society of Petroleum Engineers, SPE paper no. 6703, presented at the 52nd Annual Fall Technical Conference, Denver, October 9–12.

- Van Wagoner, J. C., Mitchum, R. M., Campion, K. M., and Rahmanian, V. D., 1990, Siliciclastic sequence stratigraphy in well logs, core, and outcrops: Tulsa, Oklahoma, American Association of Petroleum Geologists, Methods in Exploration Series, No. 7, 55 p.
- Walker, R. G., 1981, Shelf sedimentation in the Cretaceous seaway of western Canada: Geological Society of Australia, 5th Geological Convention Abstracts, p. 55-56.
- Weber, K. J., 1982, Influence of common sedimentary structures on fluid flow in reservoir models: *Journal of Petroleum Technology*, March, p. 665-672.
- _____ 1986, How heterogeneity affects oil recovery, *in* Lake, L. W., and Carroll, H. B., eds., *Reservoir characterization*: Orlando, Academic Press, p. 487-544.